Evaluation and Design of Polymer Systems for Enhanced Microwave Heating

by
John Ludman

Thesis Submitted to the Faculty of the
Virginia Polytechnic Institute and State University
in partial fulfillment of the requirements for the degree of
Master of Science
in
Mechanical Engineering

APPROVED:

Dr. Curtis H. Stern, Chairman

Dr. Elaine P. Scott

Dr. William C. Thomas

March 18, 1994
Blacksburg, Virginia

Evaluation and Design of Polymer Systems for Enhanced Microwave Heating

by

John Ludman

Dr. Curtis H. Stern, Chairman

Mechanical Engineering

(ABSTRACT)

Microwave heating of different polymer systems (epoxy-amine, polypropylene-iron, carbon-black-filled perfluoroelastomer) was evaluated using dielectric testing and monitored processing in a multimode microwave cavity. Dielectric measurements were made using a field perturbation technique and a transmission/reflection technique. The electric loss factor of the epoxy system continuously decreased during cure. Results for the microwave heating of the polypropylene-iron composites show that heating is enhanced with increased iron concentration and smaller iron particle size, although the penetration depth of the microwaves is decreased, especially after the onset of percolation. A novel solid-state processing technique for thermoset systems was also evaluated. By milling the reactants to a fine powder, and mixing them completely, the extent to which diffusion limited the process was significantly reduced: increased milling resulted in higher activation energies. In addition to the inherent advantages of solid-state processing, it is possible that processing times for solid-state processing could approach processing times for traditional melt processing.

Acknowledgements

Several people have helped make the preparation of this thesis a productive and enjoyable learning experience. I would especially like to thank the following people:

Dr. Curtis H. Stern, for creating a very enjoyable working environment. His willingness to discuss problems, and give technical guidance at any time has been greatly appreciated.

Mitch Jackson, for providing instruction and information regarding dielectric measurements and microwave processing.

Dr. W.C. Thomas and Dr. E.P. Scott for evaluating and editing this document, and serving as members of my committee. Dr. Ronald Kander for his technical support in evaluating the solid-state processing technique, and allowing us the use of many laboratory items. Dr. Alex Aning, and his student Raymond Barber for their help in milling the polypropylene-iron composites. Dr. W. Davis, electrical engineering, for providing training on the network analyzer. To Dr. J. Graybeal, chemistry department, for allowing us to use the network analyzer. To Carl Musser for helping in the preparation and testing of samples during the summer.

Virginia Institute of Material Systems (VIMS) for funding this research. Shell for supplying the different epoxy systems.

Jimmy D. for playing the blues on the guitar when times were tough. Zoubeir Saad for his patience in answering any question, good or bad. Debbie Moncman for editing help, and the rest of the labmates of 100-V Randolph, for being a great bunch of friends.

My parents Frederick G. and Lois B. Ludman for giving me the tools needed to produce this work. Their infinite love and support has been extremely valuable.

Angela Spinelli, my best friend, for her love, encouragement, and willingness to listen to all my concerns throughout the duration of this work.

Table of Contents

List of Figures vi

List of Tables xi

List of Nomenclature xii

1. Introduction 1

2 Theoretical 5
2.1 Background 5
2.2 Permittivity 9
2.3 Permeability 14

3. Literature Review 17
3.1 Metal Filled Polymers 17
3.1.1 Microwave Processing of Metal-Filled Polymers 19
3.1.2 Percolation Analysis 23
3.1.3 Dielectric Measurements of Metal-Filled Polymers 32
3.2 Microwave Cure of Polymers 36
3.2.1 Dielectric Properties 39
3.2.2 Microwave Curing of Thermoset Polymers 42
3.2.3 Solid State Processing of Thermoset Polymers 44

4. Procedures and Results 46
4.1 Procedures and Results for Polypropylene-Iron Composites . . . 46
4.1.1 Sample Preparation 47
4.1.2 Resistivity Testing 49
4.1.3 Dielectric Testing 54
4.1.3.1 Uncertainties in Dielectric and Magnetic Measurements 58
4.1.3.2 Results of Dielectric and Magnetic Testing 61
4.1.4 Microwave Heating of Polypropylene-Iron Composites . . 65
4.1.4.1 Description of Multimode Microwave Processing System 65
4.1.4.2 Results of Heating in a Multimode Oven 67
4.2 Procedures and Results of Epoxy Systems 70
4.2.1 Solid State Processing of an Epoxy System 71
4.2.2 Microwave Curing of an Epoxy System 79
4.2.2.1 Sample Preparation 79
4.2.2.2 Dielectric Testing 80

4.2.2.2.1 Perturbation Technique Background . 81
4.2.2.2.2 Experimental Set-up for Perturbation Technique 83
4.2.2.2.3 Calibration 85
4.2.2.2.4 Test Procedure 86
4.2.2.2.5 Results 87
4.2.2.3 Microwave Processing of Epoxy in a Multimode Cavity 90
4.3 Procedures and Results for a Carbon-Black-Loaded Perfluoroelastomer 93
4.3.1 Description of Material 94
4.3.2 Dielectric Testing 95
4.3.3 Microwave Heating in Multimode Cavity 97

5. Conclusions 99

6. Recommendations 104

References 107

Tables and Figures 113

Appendix A 182

Appendix B 185

Vita 191

List of Figures

Figure		Page
1	Mechanisms of Polarization by an electric field (Von Hippel, 1954).	117
2	Dielectric properties of a typical polymer in the frequency domain (Metaxas and Meredith, 1983).	118
3	Dielectric properties of a typical polymer at microwave frequencies as a function of temperature (Frosini & Butta, 1967).	119
4	Variation of the dielectric properties of an epoxy system during cure (Delmotte, 1991).	120
5	Steel mold used for pressing polypropylene-iron test specimens.	121
6	Percolation curve for a representative metal-filled polymer system (Gurland, 1966).	122
7	Resistivity of hot pressed and cold pressed polypropylene-iron composites.	123
8	Photomicrographs of polypropylene-iron composites (40% iron by volume), milled for various times.	124
9	Resistivity measurements of polypropylene-iron composites for three milling times.	125
10	Photomicrographs of polypropylene-iron composites milled for 2 hours at various filler concentrations (% by volume).	126
11	Photomicrographs of polypropylene-iron composites milled for 4 hours at various filler concentrations (% by volume).	127
12	Photomicrographs of polypropylene-iron composites milled for 20 hours at various filler concentrations (% by volume).	128
13	Schematic of the dielectric property measurement system using an HP 8510B network analyzer (HP Product Note 10).	129
14	Uncertainty analysis for transmission/reflection	

technique for a) high loss (loss factor) and b) low loss (dielectric constant) materials (Jarvis, 1990). 130

15 Dielectric constant of polypropylene-iron (10% iron by volume) composite over the frequency range 2-10 GHz. 131

16 Electric loss factor of polypropylene-iron (10% iron by volume) composite over the frequency range 2-10 GHz. 132

17 Permeability of polypropylene-iron (10% iron by volume) composite over the frequency range 2-10 GHz. 133

18 Magnetic loss factor of polypropylene-iron (10% iron by volume) composite over the frequency range 2-10 GHz. 134

19 Dielectric constant of polypropylene-iron (30% iron by volume) composite over the frequency range 2-10 GHz. 135

20 Electric loss factor of polypropylene-iron (30% iron by volume) composite over the frequency range 2-10 GHz. 136

21 Permeability of polypropylene-iron (30% iron by volume) composite over the frequency range 2-10 GHz. 137

22 Magnetic loss factor of polypropylene-iron (30% iron by volume) composite over the frequency range 2-10 GHz. 138

23 Dielectric constant at 2400 MHz for polypropylene-iron composites milled for 2 hours. 139

24 Electric loss factor at 2400 MHz for polypropylene-iron composites milled for 2 hours. 140

25 Permeability at 2400 MHz for polypropylene-iron composites milled for 2 hours. 141

26 Magnetic loss factor at 2400 MHz for polypropylene-iron composites milled for 2 hours. 142

27 Dielectric constant at 2400 MHz for polypropylene-iron composites milled for 4 hours. 143

28 Electric loss factor at 2400 MHz for polypropylene-iron composites milled for 4 hours. 144

29 Permeability at 2400 MHz for polypropylene-iron

composites milled for 4 hours. 145

30 Magnetic loss factor at 2400 MHz for polypropylene-iron composites milled for 4 hours. 146

31 Dielectric constant at 2400 MHz for polypropylene-iron composites milled for 20 hours. 147

32 Electric loss factor at 2400 MHz for polypropylene-iron composites milled for 20 hours. 148

33 Permeability at 2400 MHz for polypropylene-iron composites milled for 20 hours. 149

34 Magnetic loss factor at 2400 MHz for polypropylene-iron composites milled for 20 hours. 150

35 Dielectric constant for three milling times at 2400 MHz for polypropylene-iron composites. 151

36 Electric loss factor for three milling times at 2400 MHz for polypropylene-iron composites. 152

37 Permeability for three millings time at 2400 MHz for polypropylene-iron composites. 153

38 Magnetic loss factor for three milling times at 2400 MHz for polypropylene-iron composites. 154

39 Penetration depth for three milling times at 2400 MHz for polypropylene-iron composites. 155

40 Schematic of microwave processing test set-up 156

41 Microwave heating of cold pressed polypropylene-iron composites (milled 2 hours) with a nominal power of 58 watts. 157

42 Microwave heating of cold pressed polypropylene-iron composites (milled 4 hours) with a nominal power of 58 watts. 158

43 Microwave heating of cold pressed polypropylene-iron composites (milled 20 hours) with a nominal power of 58 watts. . . . 159

44 Schematic of cryogenic milling set-up. 160

45 DSC plot of 1071/1061M epoxy cryogenically milled for

1/2 hour. 161

46 DSC plot of 1071/1061M epoxy cryogenically milled for 1 hour. 162

47 DSC plot of 1071/1061M epoxy cryogenically milled for 1-1/2 hours. 163

48 DSC plot of 1071/1061M epoxy cryogenically milled for 2 hours. 164

49 DSC plot of 2004/P101 epoxy milled for 15, 30, and 60 minutes. 165

50 DSC plot of 2004/P101 epoxy milled for 2.5, 10, and 20 hours. 166

51 Activation energies of 2004/P101 epoxy system milled for 15 minutes, 20 hours, and 40 hours where R=8.314 J/mol*K. . . 167

52 Experimental set-up for perturbation technique. 168

53 Dielectric constant of 1071/1061M epoxy system at 2.5 GHz as a function of degree of cure. 169

54 Electric loss factor of 1071/1061M epoxy system at 2.5 GHz as a function of degree of cure. 170

55 Dielectric constant of 1071/1061M epoxy system at 9 GHz as a function of degree of cure. 171

56 Electric loss factor of 1071/1061M epoxy system at 9 GHz as a function of degree of cure. 172

57 Electric loss factor of 1071/1061M epoxy system at 2.45 and 9 GHz as a function of degree of cure. 173

58 Teflon mold used for microwave heating of epoxy. 174

59 Microwave heating profile of 1071-1061M epoxy system in a multimode oven at a nominal power of 385 watts. 175

60 Microwave heating profile of 1071-1061M epoxy system in a multimode oven at a nominal power of 320 watts. 176

61 Microwave heating profile of 1071-1061M epoxy system

in a multimode oven at a nominal power of 255 watts. 177

62 Dielectric constant of perfluoroelastomer compounds at room temperature using the transmission/reflection and perturbation technique. 178

63 Electric loss factor of perfluoroelastomer compounds at room temperature using the transmission/reflection and perturbation technique. 179

64 Microwave heating of carbon-black-filled perfluoroelastomer sheet in a multimode oven at a nominal power of 125 watts. 180

65 Microwave heating of carbon-black-filled perfluoroelastomer sheet in a multimode oven at a nominal power of 650 watts. 181

List of Tables

Table		Page
1	Complex permittivity and complex permeability of polypropylene-iron composites at 2.4 GHz using the transmission/reflection technique at room temperature.	113
2	Maximum temperatures during heating in a multimode cavity for polypropylene-iron composites (milled 2, 4, 20 hours).	114
3	Dielectric properties of 1071/1061M epoxy-amine system at 2.5 and 9 GHz using the perturbation technique at room temperature.	115
4	Dielectric properties of various carbon-black-filled perfluoroelastomers at 2.5 GHz using both the perturbation and transmission/reflection techniques at room temperature.	116

List of Nomenclature

A	Cross-sectional area
$\mathbf{B}$	Magnetic flux density vector
C	Capacitance of dielectric
C_0	Capacitance of free space
C_n	Coordination number
d	Length of resonant cavity
$\mathbf{D}$	Total electric flux density vector
$\mathbf{D}_0$	Electric charge density of free space
D_p	Penetration depth
e	Eccentricity of spheroid
e_p	Eccentricity of prolate spheroid
e_o	Eccentricity of oblate spheroid
$\mathbf{E}$	Electric field vector
$\mathbf{E}_{mean}$	Mean electric field
$\mathbf{E}_{eff}$	Effective electric field
$\mathbf{E}_{cond}$	Electric field in conducting inclusion
$\mathbf{E}_{ins}$	Electric field in insulating medium
$\mathbf{E}_{rms}$	Root mean square value of electric field
f	Linear frequency
f_r	Resonant frequency
f_c	Resonant frequency of empty cavity

f_d	Resonant frequency of cavity with test sample
f_{rct}	Fraction of epoxy reacted
Δf	Frequency bandwidth
F	Depolarization factor
$\mathbf{H}$	Magnetic field vector
$\mathbf{H}_{rms}$	Root mean square value of magnetic field
J_c	Conduction current density vector
J_d	Displacement current density vector
J_t	Total current density vector
L	Thickness of sample
N	Number of half waves
$\mathbf{P}^{\bullet}$	Polarization field vector
P_{elec}	Power dissipated by electric field
P_{mag}	Power dissipated by magnetic field
P	Power dissipated
P_c	Critical probability
q	Charge
Q_a	Activation energy
Q_c	Quality factor of empty resonant cavity
Q_d	Quality factor of cavity with sample
Q	Cavity quality factor
r	Ratio of primary axes
R	Ratio of particles participating in network

R'	Rate of reaction
R_g	Universal gas constant
R_p	Radius of polymer particle
R_m	Radius of metal particle
R_v	Volumetric Resistance
t	Thickness
v_{cond}	Volume fraction of conducting particle
v_{ins}	Volume fraction of insulating material
V	Voltage
V_0	Volume
V_c	Volume of resonant cavity
V_d	Volume of test sample
W	Width
x	Charge separation distance
α	Wave attenuation constant
$\tan \delta$	Dielectric loss tangent
ε^*	Complex permittivity
$[\varepsilon^*]$	Complex permittivity tensor
ε_0	Free space permittivity
ε_s	Dielectric constant in a dc field
ε_{inf}	Dielectric constant at very high frequencies
ε_{mtl}	Dielectric constant of a specific material
ε'_{eff}	Effective dielectric constant

ε'	Dielectric constant
ε''	Electric loss factor
ε_d''	Dielectric loss due to dipole relaxation
ε''_{cond}	Dielectric loss due to electronic conduction
ε''_{eff}	Effective relative electric loss factor
λ	Wavelength
λ_m	Wavelength of radiation in material
η	Packing factor
λ_0	Wavelength in free space
μ^*	Complex permeability
μ''_{eff}	Effective magnetic loss factor
μ'	Real part of complex permeability
μ''	Imaginary part of complex permeability
μ_0	Free space permeability
μ_d	Dipole moment
ω	Circular frequency
Φ	Matter fraction
ϕ_{crit}	Critical volume fraction
σ	DC conductivity
σ_{eff}	Total effective conductivity
σ_{cond}	Conductivity of conductive inclusions
θ	Time

Chapter 1

Introduction

Microwave processing of materials offers several advantages over conventional techniques including faster processing times, reduced energy consumption and the flexibility of selective heating. However, some materials are not inherently processable with microwaves. Therefore, it is necessary to alter the material composition or structure to enable internal conversion of electromagnetic energy to thermal energy. The addition of electrically conductive particles is one technique used to enhance this microwave coupling. This modification leads to resistive heating on the surface of the conductive particle. The focus of this research is to better understand microwave heating mechanisms so materials can be designed specifically for microwave processing.

Thermoplastic and thermoset polymers are used for many industrial, military, and consumer applications. In order to improve their cost and reliability, it is necessary to develop more efficient processing techniques. Thermoplastic polymers must be melted before they are formed, and thermoset polymers must undergo a cure reaction in which the monomers are converted into a three-dimensional molecular network. Traditionally the energy used for these processes has been provided by conductive or convective heating techniques. However, these

methods can be time consuming and typically require large thermal gradients, especially since polymers have relatively low thermal diffusivities. The large thermal gradients can lead to uneven curing and undesirable mechanical properties in polymers (Mijovic and Wijaya, 1990).

Microwave processing presents an alternative to traditional processing techniques, and is already being used in the food processing industry, the rubber industry, and the foundry industry (Kachmar, 1992; Chabinsky, 1983; Osepchuk, 1984). Microwave heating differs from conductive or convective heating because the electromagnetic energy is dissipated as heat within the material. This volumetric heating can result in faster, more energy efficient processing (Lewis et al., 1992; Strand, 1980).

Understanding the mechanisms by which microwave energy is converted to heat is essential for evaluating a material's microwave processability and for designing materials specifically for microwave processing. Materials which propagate and absorb electromagnetic waves are called dielectrics. The primary heating mechanisms within a dielectric material subjected to high frequency radiation are dipole polarization, and resistive heating (Metaxas, 1983). Dipole polarization occurs when charges within a dielectric material attempt to align with an alternating electric field, leading to molecular friction which causes the material to heat (Strand, 1980). Resistive heating results when free charges, such as ions or electrons, flow in conductive paths throughout the medium, leading to ohmic heating.

The properties which determine the material response to electromagnetic fields are the complex permittivity and the complex permeability. The real part of the permittivity, ε', known as the dielectric constant, indicates a material's ability to store electric energy. The imaginary part of the permittivity, ε'', known as the electric loss factor, indicates to what extent electrical energy is converted to heat in the material. Similarly, the real part of the permeability μ' represents storage of the incident magnetic energy, while the imaginary term μ'' indicates a magnetic loss. Measurements of these properties at microwave frequencies were performed in this work with a network analyzer.

The polymer systems investigated included an epoxy system EPON HPT Resin 1071/1061-M (Shell), and a series of polypropylene-iron composites with iron volume fractions from 0.0-0.40. In addition, a carbon-black-filled perfluoroelastomer was characterized in order to assess its potential for microwave processing.

The 1071/1061M system permitted investigation of the cure characteristics of thermoset polymers using microwave energy, including an investigation of how the dielectric properties vary during cure. Similar studies have been done by several researchers using other systems (Smith, 1987; Baker et al, 1992; Jordan et al., 1992). In addition, the epoxy system was processed using a novel solid-state technique which may allow the polymer system to react without first melting. Another epoxy system (EPON 2004/P101) was also chosen for the solid-state processing technique. The processing consists of mechanically milling the epoxy system with a SPEX 8000 ball mill to a fine powder, allowing intimate contact

between the reacting species so that diffusion through the mixture is no longer the limiting factor. The potential advantages of this processing technique include reducing harmful volatiles, reducing voids, and the ability to produce more complex shapes since the powder may retain its pressed geometry (Kander et al., 1993).

The polypropylene-iron composite system served as a representative polymer composite specifically designed for improved microwave heating. Polypropylene has a very low electric loss factor, making it difficult to heat with electromagnetic energy. The lossiness of the polypropylene can be enhanced through the addition of a conductive material like iron. Iron provides heating primarily from the electron conduction on the surface of the metal particles. Researchers have tested this idea previously and demonstrated enhanced processing (Bouazzi and Gourdenne, 1987; Raj, 1987; Raj and Gourdenne, 1986; Gourdenne, 1992; Baziard and Gourdenne, 1988; Baziard and Gourdenne, 1988). However, many questions remain about the heating mechanisms and their impact on material design.

The main goal of this research was to provide a better understanding of some promising mechanisms by which polymers can be heated with microwave energy. Several polymer systems were tested and evaluated to determine their processability. The results of this and subsequent studies will ultimately lead to improved design of polymer systems for microwave processing.

Chapter 2

Theoretical

2.1 Background

Microwave energy can be used in many ways in the processing of polymers. The energy can be used in drying the polymer or reacting chemical species, or it can be used to heat the material. In the case of thermoplastic polymers, the heat can be used to melt the polymer so that it can be formed to desired shapes. For thermoset polymers the heat can be used to initiate a cross-linking reaction.

The focus of this research was on the processing of polymers at microwave frequencies. A major advantage of microwave processing is that energy conversion occurs throughout the material. In conventional heating methods, the heat is applied from an external source and must diffuse through the media. For low thermal diffusivity materials, this process can be slow. Therefore microwave processing can potentially reduce the time and energy requirements for processing polymers. However, not all polymers can be heated effectively by high frequency electromagnetic energy. The constitutive properties which describe the ability of a material to propagate and dissipate electromagnetic energy are the complex permittivity and complex permeability. The complex permittivity and permeability are normally reported as relative quantities (normalized with the permittivity or permeability of free space), hence the term relative is often omitted, but implied.

Bur (1983) and Von Hippel (1954) have acquired and compiled dielectric properties for some polymers, but dielectric property measurements for most polymers are limited or non-existent. This scarcity of data is due to the difficulties encountered in performing dielectric tests at microwave frequencies.

Knowledge of the dielectric and magnetic properties of a material is necessary for processing with microwaves. These properties govern how much power is dissipated in the material, and how far the microwaves will penetrate into the material. The electromagnetic power dissipated in a material due to conductive, dielectric and magnetic losses can be derived from Poynting's theorem. Poynting's theorem is a power balance equation for electromagnetic fields, and can be derived from Maxwell's equations. Poynting's theorem states that the power delivered by an external source is equal to the sum of the power transmitted through the surface, the power dissipated in the volume via magnetic and electric losses, and the reactive energy stored in the volume (Pozar 1990). Poynting's theorem can be written as

$$-\int_s (E\times H)\cdot ds = \sigma\int_V E^2 dV$$

$$+\omega\int_V (\varepsilon_0\varepsilon_r'' E^2 + \mu_0\mu_r'' H^2)dV + j\omega\int_V (\mu_0\mu_r' H^2 - \varepsilon_0\varepsilon_r' E^2)\,dV \qquad (2.1)$$

The surface integral represents the electromagnetic power flow through the surface. The first integral on the right hand side of Equation (2.1) gives the dissipation of electric energy via electronic conduction, where σ is the dc

conductivity of the volume, V. The second integral on the right hand side represents the electromagnetic power dissipated by both dielectric and magnetic loss mechanisms, where ε_0 is the permittivity of free space and μ_0 is the free space permeability. The last integral represents the electromagnetic energy stored in the volume, where ω is the circular frequency of the electromagnetic radiation.

Conductive and dielectric losses occur in a material through which an electric field is propagated. The average power dissipated in an isotropic material in a uniform electric field is given by

$$P_{elec} = \omega \varepsilon_0 \varepsilon''_{eff} E^2_{rms} V_0 \tag{2.2}$$

where ε''_{eff} is the effective relative loss factor which accounts for both conductive and dielectric losses, E_{rms} is the root mean squared value of the electric field, and V_0 is the volume of the material.

Power can also be dissipated in some materials (ferromagnetic, ferrimagnetic) due to the magnetic field. The average power dissipated in an isotropic material due to a uniform magnetic field is

$$P_{mag} = \omega \mu_0 \mu''_{eff} H^2_{rms} V_0 \tag{2.3}$$

where H_{rms} is the root mean square value of the magnetic field strength, and μ''_{eff} is the effective magnetic loss factor. For an electrically and magnetically lossy material, the total power dissipated in an isotropic material due to uniform electromagnetic radiation is given by the sum of the magnetic and electric losses.

In addition to determining the power dissipation in the material, the dielectric and magnetic properties also determine how far the electromagnetic radiation will penetrate into the material as given by the penetration depth D_p. The penetration depth is defined as the distance from the surface that the electromagnetic power drops to 0.367 (e^{-1}) of its original strength. The penetration depth of a plane wave in an electrically and magnetically lossy material is given by

$$D_p = \frac{\lambda_0}{2\sqrt{2(\mu'\varepsilon' - \mu''\varepsilon'')}} \left(\left(1 + \left(\frac{\mu'\varepsilon'' + \mu''\varepsilon'}{\mu'\varepsilon' - \mu''\varepsilon'} \right)^2 \right)^{0.5} - 1 \right)^{-0.5} \tag{2.4}$$

where μ', μ'', ε', and ε'' are the real and imaginary parts of the relative permeability and permittivity respectively, and λ_0 is the free space wavelength of the incident electromagnetic radiation. As the loss factors increase, the penetration depth decreases. For a material to be processable with microwaves, it must be sufficiently lossy to produce adequate volumetric heating, but not so lossy that the electromagnetic fields cannot penetrate the width of the material.

Now that the importance of the dielectric and magnetic properties has been established, the mechanisms by which electromagnetic energy is both stored and dissipated in a material are described.

2.2 Permittivity

The complex permittivity describes how a material responds to an alternating electric field. Materials contain free and bound charge carriers which become polarized in the presence of an electric field. Polarization results in a net charge separation which leads to a dipole moment

$$\mu_d = q\,x \tag{2.5}$$

where x is the charge separation distance, and q is the net charge. This charge separation arises from either induced polarization which occurs when charges are displaced from their equilibrium position, or from the inherent charge imbalance present in polar molecules. When an electric field is applied, these polarized charges align with the electric field, storing a portion of the incident electromagnetic energy. The amount of storage is quantified by the real part of the relative permittivity, or dielectric constant, which can be thought of as the ratio of the capacitance of the material to that of free space, and is given by

$$\frac{C}{C_0} = \frac{\varepsilon'_{mtl}}{\varepsilon'_0} = \varepsilon'_r \tag{2.6}$$

As mentioned earlier, the permittivity and permeability are normally reported as relative quantities; therefore, the subscript r will be omitted (but implied) in this document.

Von Hippel (1954) describes the primary mechanisms by which charges can be polarized in a dielectric. The physical mechanisms are illustrated in Figure 1. The four main types of polarization are electronic, atomic, dipole, and space charge polarization. Electronic polarization occurs when the applied electric field displaces the electrons relative to the nuclei leading to a net dipole moment. Atomic or molecular polarization occurs in materials containing ions with different charge values such as NaCl. The electric field causes a deflection of the ions from their equilibrium position inducing a dipole moment. Both electronic and atomic polarization are considered induced polarization since the electrons or molecules are being displaced from their equilibrium positions. Dipole polarization occurs when an inherent asymmetric charge distribution of the molecules is oriented by an electric field, leading to a net charge displacement in the material. Finally, space charge polarization occurs when free charges accumulated or trapped at interfaces within the material become polarized by the applied electric field.

The sum of these polarization effects leads to a charge density in the dielectric described by the net polarization field vector $\boldsymbol{P}^*$. In free space the electric charge density is given by

$$\boldsymbol{D}_0 = \varepsilon_0 \boldsymbol{E} \tag{2.7}$$

where ε_0 is the free space permittivity, and $\boldsymbol{E}$ is the applied electric field vector. For a dielectric undergoing polarization effects, the total electric charge density is given by

$$D = \varepsilon_0 E + P^* \tag{2.8}$$

where P^* is the polarization field vector. The total electric charge density vector is related to the electric field vector via the following constitutive equation for a general material

$$D = \varepsilon_0 [\varepsilon^*] E \tag{2.9}$$

where $[\varepsilon^*]$ is the complex permittivity tensor, and ε_0 is the free space permittivity. The polarization vector can then be related to the electric field by substituting Equation (2.9) into Equation (2.8), giving

$$P^* = ([\varepsilon^*] - [1])\, \varepsilon_0 E \tag{2.10}$$

The polarization vector and the electric field vector are related by a complex property (permittivity) which accounts for losses that result when the dipoles are unable to fully orient with the alternating electric field, due to the frictional resistance of the material.

Metaxas and Meredith (1983) describe how molecular dipoles react in the presence of an alternating electric field in the frequency domain. They note that at lower frequencies, the dipoles have time to reorient with the electric field resulting in maximum energy storage. As the frequency of the electric field increases, the polarization of the molecular dipoles begins to lag the electric field, resulting in decreased energy storage. This decreased energy storage results in a

decrease in the dielectric constant as shown in Figure 2. Some of the energy which was being stored by the dipoles at lower frequencies is now being dissipated in the medium as heat due to frictional resistance to dipole motion. The frequencies required to induce losses depend on the type of polarization. Dipole polarization losses occur at radio and microwave frequencies. Atomic and electronic polarizations occur in the visible light frequency range, and therefore, play no role in microwave heating.

The frequency at which the dipole rotation begins to lag the alternating electric field is a function of the relaxation time of the dipole. The relaxation time is a measure of the time required for the dipole to align with the electric field. As discussed in Section 3.2, the relaxation time in polymers is dependent on many factors including the physical state of the polymer, the crystallinity of the polymer, and the size of the polymer chains (Bur, 1983).

The product of the complex permittivity and operating frequency relate the electric field vector to the current density in the electric field. When an alternating electric field is propagated through a lossless medium (vacuum), a charging current is set up that leads the voltage by 90 degrees, hence no power is dissipated. However, in a dielectric, there is a component of current in phase with the voltage, resulting in power dissipation. Since in general the current is composed of a component in phase with the charging voltage and a component 90 degrees out of phase with the charging voltage, the two effects can be combined into a complex quantity known as the complex permittivity. The total current density induced by a given alternating electric field is comprised of a conduction

current density in phase with the charging voltage and a displacement current density caused by the polarization of charges which can have a component both in phase and 90 degrees out of phase with the charging voltage. The conduction current density is related to the electric field by

$$J_c = \sigma E \tag{2.11}$$

where σ is the electrical conductivity of the material. The displacement current density, caused by the polarization, is related to the electric field by

$$J_d = j\omega\varepsilon_0(\varepsilon'_d - j\varepsilon''_d)E \tag{2.12}$$

where ε_d' is the relative dielectric constant indicating storage of the electric field by the charges, and ε_d'' is the relative loss factor. This loss factor characterizes the amount of electrical energy lost as heat generated by frictional dissipation of rotating dipoles. Adding the two current densities together yields

$$J_t = J_c + J_d \tag{2.13}$$

Substituting Equations (2.11) and (2.12) into Equation (2.13) yields

$$J_t = j\omega\varepsilon_0(\varepsilon'_d - j(\varepsilon''_d + \frac{\sigma}{\omega\varepsilon_0}))E \tag{2.14}$$

This equation can also be written as

$$J_t = j\omega\varepsilon_0(\varepsilon'_{eff} - j\varepsilon''_{eff})E \tag{2.15}$$

where ε'_{eff} is the effective relative dielectric constant and ε''_{eff} is the effective relative loss factor. Equation (2.15) describes how a material will interact in an electric field without regard to the physical mechanisms involved. The effective complex permittivity accounts for electrical energy storage and loss caused by both direct conduction effects and all polarization effects. This latter form is convenient since techniques of measuring the complex permittivity typically yield only effective values. At microwave frequencies, the loss factor ε'' is a result of conductive losses and/or losses due to dipole or space charge polarization.

For polymers, the value of the complex permittivity over a range of temperatures and frequencies will determine if the polymer can be considered for processing with microwave power. However, for a polymer filled with magnetic particles, such as iron, the complex permeability is also important.

2.3 Permeability

The complex permeability describes the influence of a magnetic field on a material. Similar to the complex permittivity which relates the electric field to the electric charge density, the complex permeability relates the magnetic field vector $\boldsymbol{H}$ to the magnetic flux density, and is given by

$$B = \mu_0 \mu^* H \tag{2.16}$$

where μ_0 is the permeability of free space, and μ^* is the complex relative permeability. The permeabilities of most dielectric materials, including

diamagnetic, paramagnetic, and antiferromagnetic materials are the same as that of free space. However, ferromagnetic materials have relative permeabilities greater than one. Ferromagnetic materials not only store magnetic energy, but are also magnetically lossy making the permeability a complex quantity (Balanis, 1989). Iron is a ferromagnetic material, therefore consideration of the complex permeability is an important factor in determining how the polypropylene-iron composites couple with the electromagnetic field.

Ferromagnetic materials store and dissipate magnetic energy because of inherent magnetic moments. These strong magnetic moments are caused by electron spin moments that align with one another, yielding a larger magnetic moment in the atom. Normally the magnetic moments of more than one atom become grouped into regions called domains which have an even larger effective magnetic moment. Although each domain may have a large magnetic moment, macroscopically the material is made up of several of these domains. These domains are randomly oriented in the absence of a magnetic field, hence there is no resultant magnetization. When a magnetic field is applied to the material, the magnetic moments of the domains align, increasing the magnetic field strength. This ability of the domains to be oriented with the applied magnetic field results in storage of magnetic energy, and is described by the real part of the permeability μ'. In addition to storing magnetic energy, ferromagnetic materials also dissipate magnetic energy. The losses are due to domain wall and electron spin resonances in the material. Clarricoats (1961) describes these loss mechanisms in detail.

A summary of research related to microwave processing is given in the next chapter. Research on metal-filled polymers is first described, including work related to microwave processing, percolation analysis, and dielectric measurements at microwave frequencies. Then, work related to the cure of thermoset resins using microwave energy is described.

Chapter 3

Literature Review

3.1 Metal-Filled Polymers

Processing polymers using microwave energy requires the conversion of electromagnetic energy to thermal energy within the polymer. Although some polymers are able to convert enough electromagnetic energy to be processed, many others must be modified in order to get sufficient heating. One method of improving the microwave processability of "low loss" polymers is through the addition of a conductive powder. This method was investigated experimentally with a representative system of polypropylene and iron powder. The concentration and particle size of the iron powder was varied to study the effects on microwave processability.

For neat polymers the primary mechanism responsible for converting microwave energy to heat is dipole polarization which induces a frictional heating effect in the polymer. Heating induced by the polarization of bound molecular dipoles in an alternating electric field is referred to as dielectric heating. Dielectric heating is possible at both radio and microwave frequencies. The amount of dipole polarization depends on the molecular polarity, crystallinity, molecular weight, branching, end group content, and presence of polar impurities (Bur,1985). Low crystallinity and molecular weight, high polarity, and the presence of branching

end groups and polar impurities enhance the polarization. Polypropylene is a slightly polar, high molecular weight thermoplastic polymer. Consequently, dielectric heating of polypropylene is minimal. However, dielectric heating can be enhanced by the addition of a conductive filler like iron, which introduces conductive losses in the composite material. Heating is also enhanced by magnetic losses induced because the iron is ferromagnetic. These magnetic losses are due to electron spin and domain wall resonances which occur at radio and microwave frequencies.

The extent of heating in the polypropylene-iron composite is dependent on the size, shape, and concentration of the iron particles. Results of this research have shown the heating to be enhanced with increasing iron content until percolation occurs. Percolation is the marked transition of the composite from an insulator to a conductor. After the percolation threshold is reached, the penetration distance of the electromagnetic energy into the sample (penetration depth) is reduced significantly, leading to reduced bulk heating. The penetration depth is determined from measured values of the dielectric and magnetic properties of the composite.

A commercially available carbon-black-filled perfluoroelastomer was also investigated in this research. The unfilled elastomer has a low loss factor, and would not be a candidate for microwave heating without the carbon-black. Although the carbon-black was not added specifically for microwave heating, its presence is shown to produce sufficient heating for microwave processing. Some samples contained a very fine carbon-black, and others a coarse carbon-black.

Results show that the finer carbon-black produces substantially better heating.

Literature related to the use of conductive fillers to enhance microwave processing is grouped here into three different areas: microwave processing of various metal-filled polymer systems, dielectric measurements of polymer-metal systems at radio and microwave frequencies, and analyses of the percolation phenomena in materials with conductive inclusions.

3.1.1 Microwave Processing of Metal-Filled Polymers

Microwave processing of polymers can be enhanced by the addition of a conductive inclusion. Carbon-black in rubber is a well known example. The primary function of the carbon-black is the improvement of tensile strength. However, the carbon-black also makes microwave heating of the rubber possible (Krieger, 1992). Similar effects have also been demonstrated experimentally for different epoxy systems filled with various metals including iron, copper, and aluminum (Raj and Gourdenne, 1986; Raj, 1987; Baziard and Gourdenne, 1988). Their results indicate that the time required for complete polymerization can be greatly reduced with judicious additions of these metals. Although these examples demonstrate the potential benefits of adding conductive fillers, specific guidelines regarding the recommended amount, shape, and size of filler are not provided. Gourdenne (1992) mentions that, currently, an empirical approach is used to fabricate metal-filled polymers for microwave processing. This approach has led

to limited success, suggesting that a better understanding of the physical mechanisms that cause the heating is needed.

Raj and Gourdenne (1986) investigated how the metal particle size influences the absorption of microwaves. They added different size copper particles (10, 40, and 63 microns in diameter) to epoxy and measured the power absorbed by the composite in a waveguide propagating in the TE_{01} mode. They concluded that the larger particles increased power absorption. In addition they varied the weight percent of copper (20, 40 and 60%). They found that increasing the copper concentration from 20% to 40% led to greater power absorption, but a similar jump in concentration from 40% to 60% led to slightly decreased power absorption. Although no physical explanation is given for these results, the percolation phenomena could be an important factor.

A different conclusion was reached by Krieger (1992) regarding the influence of particle size. Krieger looked at the microwave heating of rubbers loaded with different carbon-blacks (25% by weight) and found that the finer carbon-blacks produced better heating than the coarser carbon-black. Bouazzi and Gourdenne (1988) describe the mechanisms by which a small dispersion (5% by weight) of carbon-black in epoxy leads to enhanced microwave absorption. The first mechanism is by electronic conduction at the level of the carbon-black aggregates; and the second is the result of multiple reflections of electromagnetic waves within the epoxy matrix increasing the effective distance travelled in the material.

Raj (1987) examined the influence of introducing iron particles (10 microns in diameter) into epoxy. He varied the concentration of the iron powder (0 - 60%

by weight), and determined that above 40% iron there was a sudden jump in the amount of power absorbed in the composite. Raj explained that at lower concentrations the composite consists of randomly distributed iron particles segregated from one another; but at higher concentrations the number of particle contacts increases, eventually leading to the formation of conductive chains. The formation of these conductive chains is described and predicted by percolation analyses.

Similar research is described by Baziard and Gourdenne (1988) using aluminum as the filler. The curing of epoxy with the addition of aluminum powders (20 and 50% by weight) was investigated. They concluded that the 50% aluminum loading led to better heating and faster curing of the epoxy than the 20% loading. The heating was attributed to electronic conduction on the surface of the metal, and to multiple reflections which increased the effective distance travelled by the electromagnetic energy through the epoxy. However, from photo-micrographs it was noted that aggregation of the metal particles was occurring in the 50% loading. The influence of aggregation was to "hide" some of the metal filler because of the small penetration depth of the microwaves in the metal. A wider range of aluminum powder loadings (0-70% by weight) was then investigated. As expected, the microwave heating increased with the addition of aluminum powder up to a 40% loading, then decreased with the addition of more aluminum powder. Optical microscopy showed that aluminum particles were isolated and uniformly distributed up to a 30% loading of aluminum. However, the 40%-70% loadings of aluminum showed significant aggregation.

Consequently, aggregation could explain the decrease in power absorption above the 40% loading.

Another important application for metal-filled polymers has been described by Kumar (1989). Kumar mentions that the radar cross-section of targets can be reduced by coating surfaces with radar-absorbent materials. He considered the absorption of radiowaves and microwaves in fiber-glass composites embedded with iron-oxide particles. Kumar presents dielectric data for the fiber-glass composite with a 60% loading of iron-oxide. He notes that it was hard to compare his data to other work since very little dielectric data exists for mixtures of conducting particles in a dielectric. Kumar suggests that by varying the volume fraction, shape, size, and distribution of conductive particles, optimal microwave absorbing properties can be obtained.

The addition of conducting particles to a polymer for improved microwave processing is still largely empirical. Research studies described in this section are an important start in the scientific understanding of how conducting particles can be used for heating polymers in a microwave field. Although the influence of particle size and content have been researched, contradictory results and vague explanations raise many questions. The work described herein addresses many of the questions raised in the previous works including: the influence of particle size, the influence of metal content, and the influence of the onset of percolation on the microwave processability of metal filled polymers.

3.1.2 Percolation Analysis

Electronic percolation is a phenomena that occurs in metal-filled polymers. Percolation is characterized by a sudden decrease in electrical resistivity after a critical concentration of metal has been added to the metal-polymer composite. The necessary concentration is dependent on many factors including size, morphology, and distribution of the particles. An understanding of how these factors influence percolation is useful for designing metal-filled polymers for microwave processing. Metal-polymer composites that have reached the percolation threshold are not good candidates for microwave heating since the penetration depth is greatly reduced, eliminating the volumetric heating effect. Researchers have used empirical, numerical, and theoretical treatments to model the percolation phenomena, and a review of the various research studies is now presented.

The addition of conductive inclusions to low loss dielectric (non-conducting) materials allows these materials to be heated with microwaves. However, the quantity and morphology of the conductive inclusions strongly influence the extent of heating. The primary electric loss mechanism in metal-filled systems is a conductive loss mechanism approximated by

$$\varepsilon''_{cond} = \frac{\sigma}{\varepsilon_o \omega} \tag{3.1}$$

where ε''_{cond} is the loss factor due to conductive mechanisms. Note that the loss factor is proportional to the dc conductivity, σ, of the material. Since the loss factor is proportional to the conductivity, it is important to understand how the addition of conductive particles affects the conductivity.

Janzen (1975) noted that the addition of conductive inclusions to an insulating matrix causes a precipitous drop in electrical resistivity commencing at a threshold volume fraction ϕ_{crit}, which depends on filler particle form and spatial distribution. Typically, spherical or irregularly shaped metal fillers of 100 microns or less in diameter are used. However, these particle shapes require relatively high loadings to achieve the drop in resistivity. Therefore, more fibers, flakes, and ribbon forms are now being used because lower concentrations of these are required (Bigg, 1986). Carbon-black is the main additive used in polymers to alter electrical conductivity, although metal powders are also used (Kusy, 1986).

Many researchers have focused on predicting the onset of percolation. Physically, the onset of percolation can be thought of as the incipient formation of a continuous network of the conductive phase. This continuous network allows transport of electrons through the medium. Several different techniques have been used to predict this transition from insulator to conductor. The predictive models are primarily based on either effective medium theory, numerical methods, or empirical formulations.

Hsu (1983) describes an effective medium formulation which can be used to predict the onset of percolation in insulator-conductor composites, with

conductor physical structures ranging from lamellar to fibrillar. The effective medium formulation determines the conductivity of an insulator-conductor composite as a function of the volume fraction of conductor, and a shape dependent depolarization factor. This relationship was determined by letting the effective electric field of the composite be equal to the sum of the electric field in the insulating and conducting material. It was assumed that the direction of the electric field was along the axes of revolution of the spheroids. Hsu developed the following relationship for the dc conductivity

$$\sigma_{eff}=\sigma_{cond}\frac{(v_{cond}-F)}{1-F} \qquad 1\geq v_{cond}\geq F \tag{3.2}$$

$$\sigma_{eff}=0 \quad 0\leq v_{cond}\leq F \tag{3.3}$$

where F is the shape dependent depolarization factor, and v_{cond} is the volume fraction of the conductor. Hsu's model predicts that the onset of percolation occurs when the volume fraction of the conductor is equal to the shape dependent depolarization factor. The depolarization factor is dependent on the eccentricity of the spheroid. Spheres have an eccentricity of 1, and a corresponding depolarization factor of .33. Depolarization factors for other spheroids can be determined depending on their axis ratio; the ratio of major to minor axis. Prolate (needle) spheroids have an axis ratio of less than one, while oblate (plate) spheroids have an axis ratio greater than one. For prolate (needle) spheroids (axis ratio less than one), the depolarization factor is given by

$$F(e) = \frac{1-e^2}{2e^3}\left(\ln\left(\frac{1+e}{1-e}\right) - 2e\right) \tag{3.4}$$

and for oblate (plate) spheroids (axis ratio greater than one)

$$F(e) = \frac{1}{e^2}\left(1 - \left(\frac{(1-e^2)^{1/2}}{e}\right) atan\left(\frac{e}{(1-e^2)^{1/2}}\right)\right) \tag{3.5}$$

where e is the eccentricity of the spheroid. For oblate spheroids the eccentricity is given by

$$e_o = \left((1/r)^2 - 1\right)^{1/2} \tag{3.6}$$

and for prolate spheroids by

$$e_p = \left(1 - (1/r)^2\right)^{1/2} \tag{3.7}$$

where r is the axis ratio. Therefore, the depolarization factors are a quantitative measure of the volume fractions of different shaped conductors necessary to form a continuous network of particles. For example, spherical shaped inclusions have a depolarization factor of .33, which according to Hsu's effective medium analysis, results in a transition from insulating to conducting behavior at a volume loading of 33%. Contrast this to a medium filled with prolate (needle) spheroids with an

axis ratio of 0.1, where the percolative transition is predicted with a volume loading of 0.01 or 1.0%.

Hsu's effective medium formulation is fairly accurate except close to the percolation threshold. The predicted volume fraction of conducting inclusions required to reach percolation is usually greater than that found experimentally. This discrepancy is due to clustering of inclusions that occur as loadings approach the percolation threshold, reducing the loading necessary for percolation. Clustering is not accounted for in Hsu's formulation since the depolarization factor used is for a single isolated spheroid.

Granqvist and Hunderi (1978) introduced an improved effective medium theory to account for the clustering effect. They noted that in the original effective medium treatment the local electric field effects between conducting inclusions were ignored. These local field effects, such as dipole-dipole interactions become important as clustering becomes prevalent. Granqvist and Hunderi accounted for these interactions by replacing the depolarization factors with empirically determined effective depolarization factors for loadings approaching percolation. The effective depolarization factors depend on the specific clustering geometry. However, Granqvist and Hunderi have determined values for two common clustering shapes: chains and clusters. The effective depolarization factors reduce the critical volume fraction of conducting inclusions necessary to reach percolation. For chains, the percolation threshold occurs at a volume fraction of 0.271; while for clusters, the threshold volume fraction is 0.156. The Granqvist

and Hunderi Effective Medium Model gives better agreement with experimental results than the original effective medium theory.

Other researchers have developed statistical techniques to predict the percolation concentration (Kirkpatrick, 1973; Bernasconi and Wiesman, 1976; Janzen, 1975; Bueche, 1972; Webman et al., 1975). Bueche (1975) used the theory of infinite chains to determine the variation of conductivity with particle concentration. This technique assumes a certain packing fraction of conducting particles and then relates it statistically to the fraction of conductive particles that are involved in the continuous network. This fraction can then be used to determine the resistivity of the composite by assuming that the conducting network chains act as parallel conductors through the sample. This technique predicts a broad spectrum of percolation thresholds depending on the packing fraction assumed. For close-packed particles a precipitous drop in resistivity is predicted to occur at a volume fraction of 0.07. However Bueche suggested that most of the experimental data exhibits percolation at higher volume fractions since the packing is imperfect.

Janzen (1975) assumed a functional relationship between the critical volume fraction associated with percolation ϕ_{crit}, and the mean number of contacts that the conductive inclusion makes with its neighbors. Using a heuristic approach Janzen developed the following equation

$$\phi_{crit} = \left(1+(C_n/1.5)\frac{(1-\Phi)}{\Phi}\right)^{-1} \qquad (3.8)$$

where C_n is the coordination number, and Φ is the matter fraction. Janzen noted that high accuracy cannot be expected using this result, but that it serves as a good rule of thumb.

Conductivity of metal-filled insulator composites has also been analyzed using resistor network models (Kirkpatrick, 1973; Webman et al., 1975). The resistor network models assume that the medium of interest is comprised of a cubic network of resistors, representing either sites or bonds in the network of conducting particles. After the network is established, the resistors are assigned values of conductance. For percolation analysis certain sites or bonds are removed from the lattice by assigning them a conductance value of zero. Once the conductances of the sites are assigned, a constant voltage is applied to each of the nodes on one side of the medium, and the voltages on the other side of the medium are set to zero. A finite difference technique is then used to solve for the current flow between the two sides of the medium, to determine if percolation has occurred. This would be evidenced by a non-zero current value throughout the medium. Depending on the specific resistor network model used, the predicted percolation threshold is calculated to be between 0.15-0.27. It should be noted that the resistor network models can also be solved using Monte Carlo, and analytical techniques (Kirkpatrick, 1973).

In addition to the analytical and numerical studies already described, empirical work relating particle morphology to the onset of percolation has also been done. Aharoni (1972) developed a model showing that the conductivity of metal-filled insulators was directly proportional to the surface area of the metal.

Aharoni considered the onset of percolation physically as the point where the average number of contacts per metal particle was equal to one, and the probability of infinite chains forming is non-zero. Aharoni claimed that the resistivity of the composite will decrease monotonically over many orders of magnitude after this point until the number of contacts per particle was equal to two. After this point, only a slight decrease in resistivity occurs with increasing volume fraction. Aharoni noted that the number of contacts per particle is directly dependent on the surface area of the conducting particles available. He predicted that the sudden drop in resistivity would occur at some volume fraction, and it would continue until the volume fraction doubled. Aharoni tested his empirical model using a polymer-iron system and found that his simple model accurately predicted a monotonic decrease in resistivity, and was fairly close in predicting the range of volume fractions over which this decrease occurred. His iron-polymer system started to decrease in resistivity at 7% iron by volume and continued to decrease monotonically until about 20% iron was added, compared to a value of 14% iron predicted by his model.

Mallaris and Turner (1971) looked at the influence of particle size on the resistivity of polymer-metal composites. They compared the critical composition of metal-polymer composites for a range of particle size ratios (R_p/R_m from 1 to 16), where R_p and R_m are the radii of the polymer and metal particles, respectively. They assumed percolation would occur due to the formation of infinitely long chains of metallic contacts in a single layer of polymer particles. They predicted that percolation could occur when the probability of infinitely long chains becomes

non-zero. When the volume fraction of metal particles is 0.33, the probability of infinite chain formation is unity. The probability of chain formation becomes non-zero at some lower volume fraction, depending on the packing arrangement. The volume fraction corresponding to a non-zero probability of chain formation is quantified by assigning a critical probability P_c for various packing arrangements (square, triangle, hexagonal, etc.). This critical probability is the probability of incipient chain formation for a full planar lattice. The critical volume loading of conducting particles was shown to be a function of the particle size ratio, and the critical probability as shown below

$$\phi_{crit} = 50P_c\left(1+(\frac{\eta}{4})(\frac{R_p}{R_m})\right)^{-1} \tag{3.9}$$

where η is the packing factor for the desired lattice. They concluded that the critical composition of metal decreases as the ratio R_p/R_m increases, or as the size of the metal particles decrease. However, the model underestimates the critical composition by a factor of two to three due to the poor packing of the metal particles.

Kusy (1977) attempted to improve the model proposed by Mallarais and Turner. Kusy also investigated the effects of particle size ratio, but made a distinction between different microstructures that can form depending on the particle size ratio and the continuity of the dispersed phase. He identifies four basic microstructure: random and isolated, random but continuous, segregated

but isolated, and segregated and continuous, where the first word refers to the geometry in terms of the particle size ratio and the second word refers to the continuity of the dispersed phase in terms of the critical volume fraction. Kusy chose these microstructures to account for the non-uniform accumulation of dispersed phase in interstitial spaces at all volume fractions. His model accounts for these different microstructures by defining a particle ratio R. This particle ratio gives the ratio of the total dispersed particles participating in the conducting network to those not participating depending on the type of microstructure and the packing factor. The critical volume fraction of conducting particles is given by

$$\phi_c = 100\left(\frac{1+R}{1+R+\left(\frac{\eta}{2X_c}\right)\left(\frac{R_p}{R_m}\right)}\right) \tag{3.10}$$

where η is a packing factor, and X_c is the critical fraction of the primary particle covered by the dispersed phase. Kusy presents a table comparing experimental results to his model for a series of particle size ratios, and finds good agreement especially for large particle size ratios (R_p/R_m).

3.1.3 Dielectric Measurements of Metal-Filled Polymers

Dielectric properties of metal-filled polymers at microwave frequencies are not readily available in the literature. This is due to the difficulty encountered in

making these measurements, and the proprietary nature of some of the existing data. Metal-filled polymers have been used by the military to reduce the radar cross-section of aircraft (Kumar, 1989). Dielectric measurement techniques suitable for metal-filled polymers have been established, and the data for some systems have been reported.

Weir (1974) used a microwave vector network analyzer (Hewlett Packard Model 8540), similar to the one used in this study, to measure the complex permittivity and permeability. The network analyzer sends a small amplitude electromagnetic signal to the DUT (device under test) to measure the transmission and reflection coefficients. From these reflection and transmission coefficients the real and imaginary parts of the permittivity and permeability are determined. The solution technique described by Weir was used in this work, and more detail is given in the results section. Weir presents results for a silicone rubber system loaded with an unknown quantity of lossy magnetic particles over a frequency range of 8-12 GHz. A relatively high value of 14 was measured for the dielectric constant, but a low loss factor (less than one). In addition the material was found to be magnetically lossy with a permeability of about 2, and a magnetic loss factor greater than one. The relatively low electric loss factor is probably due to a low loading of magnetic particles.

Erhu et al. (1988) used Weir's solution technique to measure the dielectric properties of several high-loss solid materials. However, they used a microwave interferometric system to measure the reflection and transmission coefficients. Their results include measurements of an unknown dielectric matrix filled with

different loadings of ferrite, carbonyl iron, and carbon-black at 10 GHz. Their results showed that both the real and imaginary terms of the electric and magnetic properties increased with increased loading. The electric loss factor for 50% carbonyl iron by weight was about 0.5, but at 80% carbonyl iron by weight the loss factor jumped to about 13, indicating that the percolation threshold had probably been reached between 50% and 80% carbonyl iron by weight.

Ueno et al. (1980) performed dielectric and magnetic testing on ferrite impregnated plastics at 9.4 GHz using a cavity perturbation technique, and over a range of frequencies (1-6 GHz) using a short-circuited coaxial-specimen mount. Their results showed that the ferrite-plastic composites were magnetically and electrically lossy. The complex permittivity decreased with increasing frequency, while the complex permeability had a resonant loss in this frequency range. Lagarkov et al. (1992) measured the dielectric properties of silicone filled with carbon or aluminum fibers over a range of frequencies (2-25 GHz). Their data showed that two resonance peaks existed over this frequency range. They conclude that by properly choosing the amount and type of filling agent a material can be designed to have selected dielectric properties.

Baziard et al. (1988) did some dielectric measurements on epoxy composites filled with aluminum powder and copper powder. They measured the dielectric properties of these composites at different concentrations of metal powder (0-80% by weight) using a vector network analyzer operating between 1 Hz and 800 kHz. Their results show that the loss factor increased with increasing metal content. Their results indicate the existence of two loss mechanisms in the measured

frequency range. The first loss mechanism at 1 kHz was attributed to interfacial polarization brought about by charges accumulating at the polymer-metal interface. The second loss mechanism occurred at 200 kHz and was due to the dipole polarization of the hydroxyl side groups in the epoxy matrix. Although these data are below microwave frequencies, they show the relative increase of the loss factor with increasing metal volume fraction.

The research described in this section has provided only limited information necessary to use metal particles to aid microwave processing of polymers. Hence, further study is needed. Questions pertaining to the amount, shape, and size of the metal filler still need to be answered. The study described herein focussed on how the metal volume fraction and particle morphology influence the dielectric properties of metal-filled polymers. This information is necessary to assess the potential for designing metal-filled polymers specifically for microwave processing.

3.2 Microwave Cure of Polymers

Processing of thermoset polymers using microwave energy has received much attention recently. This interest stems from the potential advantages microwave processing has over conventional processing including: more uniform heating, faster processing times, efficient heating, and selective heating. The primary difference between microwave and conventional processing (curing) of thermoset polymers is how the heat needed to initiate the reaction is provided. Conventional heating of thermoset polymers requires that the heat be transferred from an external source and diffused through the volume. For large, low thermal conductivity parts, large thermal gradients may be required to keep process times reasonable. With microwave heating the electromagnetic energy is converted to heat throughout the volume of the material, making it theoretically possible to achieve a more uniform temperature profile.

The principle mechanism by which thermoset polymers convert microwave energy into heat is through the orientation and relaxation of molecular dipoles. Molecular dipoles result from an unequal charge distribution in molecules. Hydroxyl, amino, and cyanate are three common dipole groups found in thermoset polymers (Lewis and Shaw, 1993). Normally the dipoles are randomly oriented, but in the presence of an electromagnetic field they become ordered as they align themselves with the alternating field. At low frequencies the dipoles are able to follow the oscillating electric field. Under these conditions the applied electric

energy is being stored in the oriented dipoles. At higher frequencies (radio and microwave), the dipole reorientation begins to lag behind the alternating electric field due to molecular friction within the material, leading to dissipation of electromagnetic energy as heat. As the frequency of the electromagnetic radiation increases further, the dipoles are unable to orient with the field and the effect of dipole orientation diminishes. The ability of a molecular dipole to store and dissipate electromagnetic energy is quantified by the dielectric properties.

A simple model for the behavior of the dielectric properties was developed by Debye. Debye considered a dielectric material undergoing dipole reorientation in an alternating electric field. He related the dielectric properties of the dielectric to the frequency of the incident field and the relaxation time of the dipoles. The relationship is given by

$$\varepsilon^* = \varepsilon'_\infty + \frac{\varepsilon'_s - \varepsilon'_\infty}{1 + j\omega\tau} \tag{3.11}$$

where ε'_s and ε'_∞ are the dielectric constants of the dielectric at dc and very high frequencies, respectively, and τ is the relaxation time of the polarized dipole. The relaxation time is a quantitative measure of the time it takes for the dipole to become reoriented in an alternating electric field. Equation (3.11) can be separated into its real and imaginary parts as follows

$$\varepsilon' = \varepsilon'_\infty + \frac{\varepsilon'_s - \varepsilon'_\infty}{1 + \omega^2\tau^2} \tag{3.12}$$

$$\varepsilon''_d = \frac{(\varepsilon'_s - \varepsilon'_\infty)\omega\tau}{1+\omega^2\tau^2} \tag{3.13}$$

where ε_d" is the loss factor due to dipole polarization losses only. Equation (3.13) shows that the loss factor is a maximum when the frequency of the applied electric field is equal to the reciprocal of the relaxation time. This frequency, known as the molecular resonant frequency, varies with material properties and processing conditions. The relaxation times of many molecular dipole groups correspond to resonant frequencies at or near microwave frequencies (Jow et al., 1987). The dependence of the dielectric properties of a typical polymer on frequency is shown in Figure 2. The frequencies of the dielectric loss peaks caused by dipole reorientation are also functions of temperature. Increasing the temperature generally shifts the dispersion (loss peak) to higher frequencies, since the relaxation time decreases with increasing temperature.

The mobility of the molecular dipoles strongly influences their relaxation time. Bur (1985) notes that this mobility is dependent on material properties such as the extent of crystallinity, molecular weight, end group content, and the presence of polar impurities. High crystallinity, high molecular weight, few end groups, and low polar impurity content leads to decreased mobility. The molecular location of the dipole is also important. Lewis and Shaw (1993) note that a dipole group dangling from the main chain will couple more strongly than a less mobile group in the main chain.

In addition to these material properties, the physical state of the polymer also influences how well the microwaves will couple with dipoles present in the polymer. At microwave frequencies there is a substantial increase in the amount of electromagnetic energy absorbed by the polymer when the polymer moves from the solid state through its glass transition (for an amorphous polymer) or melting point (for a semi-crystalline polymer) as shown in Figure 3. Lewis and Shaw (1993) note that the microwave absorption increases rapidly in the rubbery phase; this is a potential problem when processing polymers since the degradation temperature of most polymers is close to the process temperature. The molecular structure of the polymer also changes during the processing of thermoset polymers. Cross-linking of the polymer reduces the mobility of the dipoles, reducing the amount of microwave energy that is dissipated as heat.

Research related to the cross-linking of thermoset polymers with microwaves has focused on measuring the dielectric properties and evaluating different microwave processing techniques. A review of this research follows.

3.2.1 Dielectric Properties

Dielectric properties of several polymer materials at microwave frequencies have been measured and tabulated (Bur, 1985; Von Hippel, 1957; Frosini and Butta, 1967). Bur (1985) gives dielectric data for a broad range of polymers including: epoxy resin, conducting polymers, low loss polymers (polypropylene, teflon, etc.), and higher loss polymers such as PVC. Bur presents data over a

broad range of frequencies (100 MHz - 100 GHz), and over a range of temperatures depending on the polymer. Frosini and Butta (1967) measured the dielectric properties of several polymers at 9 GHz over a range of temperatures (-150 - 200° C).

Investigation of the effect of curing on dielectric properties has also been performed. Delmotte et al. (1991) measured how the cross-linking reaction in epoxy systems effects the dielectric properties. Delmotte looked at one epoxy resin, diglycidylether of bis-phenol-A (DGEBA) with three different curing agents: 4,4'-diaminodiphenylmethane (DDM), 4,4'-diaminodiphenylsulfone (DDS), and 4,4'-diaminodiphenylether (DDE). Processing of the different epoxy systems was done in a resonant cavity that also allowed measurement of the dielectric properties. The experiment consisted of a sequence of dielectric measurements which lasted approximately 0.05 - 0.1 seconds followed by microwave heating at 2.45 GHz for 1-4 seconds. The dielectric measurements were made by measuring the resonant frequency and the transmission coefficients in the cavity. At 2.45 GHz, the DGEBA resin had a relatively high loss factor ($\varepsilon''=1$) at room temperature, while the loss factors of the pure amino hardeners were very low ($\varepsilon''<0.01$) at room temperature. The DGEBA resin had its maximum loss at 50° C. The loss factor for the DDM curing agent reached a maximum at 100° C, the DDS curing agent had a sharp increase above 150° C, while the DDE curing agent remained lossless in the temperature range studied. Dielectric measurements were also made of the epoxy-hardener mixtures during processing. As expected the dielectric properties increased initially due to the increased mobility caused by melting, but as cross-

linking occurred the values of the dielectric constant and loss factor decreased as shown in Figure 4.

Baker et al. (1992) also studied how the dielectric properties of a DGEBA-DDS epoxy system varied during cure. They used the cavity perturbation technique described in Section 4.2 to measure the dielectric properties of the epoxy system undergoing both thermal and microwave cure. Baker used WR430 rectangular waveguide operating in the TE_{103} mode at 2.45 GHz for the resonant cavity. The test signal was processed by an HP8510 Network Analyzer, which allowed on-line measurement of the dielectric properties during thermal cure, as well as during microwave cure when the nitrogen gas was replaced by a microwave power generator. Results using the hot nitrogen gas showed that the dielectric loss of the DGEBA epoxy was greater than the DDS hardener at temperatures below 150° C (Marand et al., 1990). The loss factor of the DDS hardener jumped after it melted at 170° C. The dielectric properties of the mixture decreased rapidly as it cured.

Jow et al. (1987) combined the on-line measurement of the dielectric properties with microwave processing. They successfully processed a DGEBA-DDS epoxy system using a single mode (TM_{012}) resonant cavity while simultaneously measuring the dielectric properties. This on-line information makes it possible to automatically control the microwave processing.

Measurement of a polymer's dielectric properties is required if microwave heating is to be considered. Research has shown the dielectric properties of different polymers to be dependent on temperature, frequency, physical state, and

extent of cure. The study described herein includes measurement of the dielectric properties of an EPON 1071/1061M epoxy system as a function of frequency and extent of cure using the perturbation technique. No published dielectric data exists for this epoxy system.

3.2.2 Microwave Curing of Thermoset Polymers

Researchers have also studied the kinetics of microwave curing for various thermoset systems. Lewis et al. (1987) compared the rate at which an epoxy system (Shell Epon 828 - DDS) cured using both microwave and thermal energy. They found that the microwaves significantly accelerated the curing of the epoxy resin. Le Van and Gourdenne (1987) identified stages in the curing reaction for a DGEBA-DDM epoxy system undergoing microwave irradiation. The temperatures during microwave heating were found to be similar to those during conventional heating. The heating can be separated into three stages. The first stage is the initial heating period in which the DGEBA resin is generating heat via dipole reorientation. The next stage, characterized by a decrease in the amount of heating via reorientation polarization, is due to the exothermic reaction (conversion of the epoxide groups). The final stage is evidenced by a temperature drop since heat loss to the surroundings is the primary energy transfer. Le Van and Gourdenne also studied the effects of varying the intensity of the microwave power on the cure kinetics. As expected, when the power was increased, the rate of reaction increased. Teffal and Gourdenne (1983) did a similar study with 2-

hydroxyethylmethacrylate (HEMA). They also concluded that as the incident power increased, the rate of cure increased.

Beldjoudi et al. (1981) investigated the effect of curing an epoxy system (DGEBA-DDM) with pulsed microwave power. They processed samples in a waveguide using a 2.45 GHz microwave generator. The microwave generator was connected to a pulse generator that allowed the incident radiation to be pulsed on and off at different frequencies, and different pulse times. They compared continuous microwave irradiation with various pulsed irradiation patterns. The average power for all cases was the same. They found that improved heating was achieved by pulsing the microwaves. This improved heating was attributed to the relaxation of segments of epoxide chains at low frequencies (200 Hz), in addition to the relaxation of the dipoles occurring at 2.45 GHz; the relaxation times of the chains being substantially longer than that of individual dipoles. The larger relaxation times correspond to much lower maximum-dielectric-loss frequencies as given by the Debye equation (Equation 3.13).

Jullien and Valot (1985) investigated the use of pulsed microwave power to process polyurethane. They measured the hardness of the polyurethane to determine if microwave radiation could improve the mechanical properties of the polyurethane. They concluded that the hardness of the polyurethane processed with microwaves depended on the particular pulse regime used, but that the microwave cured polyurethane was always much harder than the oven cured samples. However, they were unable to determine if this difference was due to a more complete reaction of the system, or if a different structure was formed in the

polymer. Their research also investigated the kinetics and stages of microwave curing.

Previous research has shown that microwave curing of thermoset polymers has the potential to reduce process times, and possibly improve mechanical properties. In the research described herein, the curing kinetics of an epoxy system heated in a multimode microwave oven was investigated. This information is important in evaluating the relative advantages of microwave heating. It is also needed if controlled microwave processing is to be achieved, since the dielectric properties change during processing.

3.2.3 Solid State Processing of Thermoset Polymers

In addition to the investigation of the microwave processability of an epoxy system, a novel solid-state processing technique for thermoset polymers was evaluated. Solid-state processing consists of mechanically milling and mixing the reacting species (epoxy and curing agent) at a sub-micron level so that intimate contact between the reacting species can be achieved. This process may allow the species to be reacted completely in the solid-state, eliminating the need to melt the mix. Potential benefits of this technique include: reduction or elimination of harmful vapors, the ability to form more complex parts, and the ability to process the reactants at lower temperatures.

Although the idea of reacting thermoset polymers in the solid state is new, the mechanical alloying process used to mill and mix the reactants is not.

Benjamin (1970) developed the mechanical alloying process to produce oxide-dispersion-strengthened superalloys. Kander (1993) notes that mechanical alloying has been primarily used for microstructural control of metals. Kander has tested this technique for processing thermoplastic polymer-based systems because it has the potential to reduce the production costs and improve the mechanical properties of certain polymer blends. In addition, the process enables the alloying of some polymers which cannot be alloyed with traditional processing techniques.

Mechanical alloying can also be used to produce thermoset polymers for solid-state processing. Investigation of this idea is described in this thesis. No similar work has been found in the literature. Results of this work are given in Section 4.2.1.

Chapter 4

Procedures and Results

This chapter describes the experimental procedures and results for the polypropylene-iron composites and the epoxy systems. In addition, the results of the dielectric testing and heating of a carbon-black-filled perfluoroelastomer are summarized.

4.1 Procedures and Results for Polypropylene-Iron Composites

In this section the enhancement of the microwave processability of "low loss" ($\varepsilon''<0.01$) polymers with conductive powders is considered. Polypropylene was used as a representative low loss polymer, and iron was the conductive powder. In a microwave field, currents are set up on the surface of the iron particles resulting in ohmic heating, which can be used to process the polymer. The objective of the research was to investigate how the amount and particle size of the conductive powder influenced the microwave heatability of the metal-filled polymer.

The influence of metal powder concentration was investigated by looking at a series of iron-polypropylene mixtures ranging from 5% iron to 40% iron by volume. The iron particle size was altered by ball-milling the polypropylene and

iron powders for different lengths of time: two, four, and twenty hours. The influence of these variables on the microwave heatability was evaluated by measuring the resistivity and dielectric properties, and by measuring temperature histories during heating in a multimode microwave cavity. The resistivity tests were performed to predict the percolation threshold of the composite. The percolation threshold is the volume fraction of metal powder at which a sudden transition from an electrical insulator to conductor occurs. Since the dielectric loss factor of the composite is proportional to the conductivity, the percolation threshold strongly influences microwave heating.

The dielectric properties describe how much microwave power can be dissipated within the material. The dielectric properties also determine the penetration depth of the microwaves into the material, which is critical when processing higher loss materials or large parts. The following sections will describe the polypropylene-iron sample preparation, the procedure and results of the property measurements, and the relationship between these properties and the microwave heating of metal-filled polymer composites.

4.1.1 Sample Preparation

The polypropylene-iron composites were formed by ball-milling iron powder and polypropylene pellets to the sub micron level, and then pressing the resulting powder mix under pressure at room temperature (cold pressed) or at an elevated temperature (hot pressed). Preparation of the samples was done with the help of

Raymond Barber, a student working in Dr. Alex Aning's metal processing laboratory. This section describes how the polypropylene-iron composites were produced.

The first step was to combine the polypropylene with different amounts of iron. The mixtures investigated were polypropylene with 5,10,15,20,25,30,35, and 40 percent iron by volume. The broad range of iron loadings was chosen to ensure that the percolation threshold could be identified. The volume fractions for each sample were prepared gravimetrically before milling or pressing of the powders. The appropriate mass fractions were determined from the desired volume fractions using the component bulk densities of the polypropylene and iron: 0.91 g/cc and 7.87 g/cc, respectively. All test results are reported using this equivalent volume fraction, which actually varied as samples were pressed. The next step was to mill the particles to the sub micron level. A SPEX 8000 mixer/mill was used to perform this task. The mill rapidly shakes tungsten-carbide balls contained inside a tungsten-carbide vial to mechanically alter materials in the vial. The powder particles are deformed and fractured by collisions with the balls and the vial. Four 1/2" diameter tungsten-carbide balls with a total mass of approximately 66 grams were used in the vial. The tungsten carbide balls lose some weight during milling. In order to keep processing conditions consistent, a constant charge ratio (ratio of ball mass to sample mass) of four was used. The mass of the balls was measured before every run, and the mass of sample adjusted accordingly.

The polypropylene-iron powder was milled for two, four, or twenty hours. Longer milling times produced finer powders. Milled mixtures were stored in an

Argon-filled container to prevent oxidation of the iron. The powders were then cold or hot pressed for resistivity testing and microwave heating. Cold pressed samples were made by pressing the powder under 3000 pounds of load at room temperature in a half-inch diameter dye for five minutes using a Carver Model C Laboratory Press. Hot pressed polypropylene-iron samples were made by placing the powder mix in a 2" X 1" rectangular mold and pressing the mix under 6600 pounds of load at a temperature of 204°C (400° F) for five minutes.

Dielectric test samples were also made from the various polypropylene-iron powder mixtures. The dielectric testing (detailed in section 4.1.3) required an annular test piece that fit snugly into a coaxial transmission line with an outside diameter of 7 mm and an inside diameter of 3.04 mm. In order to make these test samples, a steel mold (shown in Figure 5) was designed and fabricated. Samples were hot pressed at 149°C (300° F) using this mold.

4.1.2 Resistivity Testing

The dielectric loss factor due to conductive losses can be approximated by

$$\varepsilon''_{cond} = \frac{\sigma}{\varepsilon_0 \omega} \tag{4.1}$$

where σ is the dc volume conductivity of the material. The dc conductivities of most polymers are very low; they are usually considered insulators. For example, polypropylene has a conductivity value of approximately 1×10^{-17} ohm-cm. A

polymer sample can be made conductive by adding enough conductive filler so that a continuous network of conductive particles is formed. This transition from an insulating medium to a conductive medium is known as electronic percolation, and the associated volume fraction of conductive powder is given by the critical volume fraction, ϕ_{crit}. Figure 6 shows the transition from insulator to conductor for a representative metal-filled polymer system (note that resistivity is the inverse of conductivity).

Knowing the conductivity of the metal-filled polymer as a function of metal content and particle size is invaluable for designing materials for microwave processing. For example, if an electric loss factor of 0.1 is desired at a microwave frequency of 2.45 GHz, Equation (4.1) indicates that the resistivity of the sample should be approximately 7200 ohm-cm, if only conductive losses are considered. Percolation analysis can establish the metal concentration which produces this resistivity. Although it may not be possible to produce a metal-filled polymer with a precise resistivity, percolation analysis can establish the acceptable range of metal volume fractions for microwave processing (heating). Inadequate penetration of the microwaves, and poorly distributed heating could result when the conductivity is too high, while negligible heating would result if the conductivity is too low. Figure 6 shows how difficult it may be to establish an intermediate value of resistivity (like 7200 ohm-cm), since the resistivity is extremely sensitive to small changes in the volume fraction. However this transition may not be as sharp for some conductive fillers such as certain carbon-blacks.

Resistivity testing of the polypropylene-iron system was performed to identify the range of iron loadings which would enable microwave processing. The resistivities were measured as a function of iron concentration (volume percentage), particle size, and pressing method. The resistivity tests were performed in the Electrical Engineering Department by Fred Barlow, and in accordance with ASTM standard D257-91 (ASTM 1991). Silver paint was applied to both sides of the test sample to reduce contact resistance between the sample and the meter leads. The resistances of the samples with higher loadings of iron were measurable with a hand-held ohm-meter. However, the samples with lower loadings of iron required the use of a high voltage (1500 V) dc power supply in combination with a precision electrometer to measure the current. The resistance, R_v, was computed by taking the ratio of the applied voltage to the measured current. The resistivity is then

$$\rho_v = \frac{A}{t} R_v \tag{4.2}$$

where A is the cross-sectional area of the test piece, and t is its thickness.

Results of the resistivity testing clearly indicate a percolative transition in each set of samples tested. Figure 7 shows the resistivity of hot pressed and cold pressed polypropylene-iron samples as a function of iron concentration. The two pressing techniques were compared to determine if hot pressing the samples would reduce voids, minimizing the resistance between iron particles. A decrease in resistance could make microwave processing of metal-filled systems more

practical, since it would reduce the metal content necessary to form a conductive composite. In Figure 7, it is evident that the hot pressed samples become conductive at a lower volume fraction of iron than the cold pressed samples. The resistivity of the hot pressed samples drops between 10% and 20% iron by volume, while the resistivity of the cold pressed samples drops between 25% and 35% iron. However, this is probably more a result of non-uniform iron distribution than of void reduction, although it was impossible to quantitatively differentiate between the two effects. The hot pressing caused the polypropylene to flow to the outside of the mold, leaving the middle rich in iron. The resistivity measurements shown in Figure 7 are for bulk resistivity, and assume that the material is homogeneous. The higher iron content in the center of the test sample certainly biased the results, and had the effect of decreasing the value of the measured resistance. This problem was not encountered with the cold pressed sample since the powders were never melted, preventing the iron particles from flowing.

Resistivity measurements were also made to determine the effect of iron particle size. Particle size was altered by milling the iron and polypropylene powders for three different lengths of time: two, four, and twenty hours. Although this results in a wide range of particle sizes for each milling time, in general the iron particle size decreases with increased milling time as shown in Figure 8. The pictures in Figure 8 were taken using an Olympus BH-2 optical microscope at a magnification of 177. The figure shows composites cold pressed from a 40% iron-polypropylene mix milled at two, four, and twenty hours. The iron particles appear to be roughly spherical. The iron has an average diameter of

approximately 0.5 microns for the twenty hour milling, 1-5 microns for the four hour milling, and 5-10 microns for the two hour milling. The unmilled iron particles have a median diameter of 57 microns. In addition to reducing the particle size, the longer milling times resulted in more uniform particle size (Figure 8). For a given milling time, the average size of the particles also decreased with increasing iron concentration.

The resistivity testing showed that longer milling times decreased the iron concentration necessary to reach percolation (Figure 9). The onset of percolation occurred at approximately 20% iron for the twenty hour milling case, 30% iron for the four hour milling case, and 35% iron for the two hour milling case. This difference can be attributed to the size and distribution of the iron particles. Smaller particles have more surface area for a given volume fraction, allowing more contacts to form between neighboring iron particles. As a result, the incipient formation of a continuous network of conductive phase occurs at a smaller volume fraction. The decrease in the critical volume fraction with decreased particle size was also observed by Mallaris and Turner (1971) and Aharoni (1972).

Photographs were taken for the entire series (5-40% iron) of polypropylene-iron samples for each milling time to determine if the formation of a continuous network could be identified. Figures 10-12 show these series for two, four, and twenty hours, respectively. The pictures seem to correlate well with the resistivity measurements. At lower concentrations of iron (0-15% by volume) a continuous network of iron is not visible in all the cases. It is also clear that a continuous

network of iron seems to form at a lower iron concentration for the twenty hour milling case, which is in agreement with the resistivity testing.

In summary, the resistivity testing verified the presence of a percolative transition in the polypropylene-iron composites. The resistivity testing also showed that smaller particle size reduces the volume fraction of iron needed to reach the percolation threshold. This information, coupled with Equation (4.1), can be used as a first step in designing metal-filled polymers for microwave processing.

4.1.3 Dielectric Testing

Knowledge of the electric (permittivity) and magnetic (permeability) properties of a material at microwave frequencies is important for microwave processing. This section will describe how these properties were measured, and how these properties varied with iron concentration. The complex permittivity ε^* and complex permeability μ^* of the polypropylene-iron composites were measured using an automated network analyzer (Hewlett Packard 8510). Network analyzers measure the magnitude and phase response of linear networks by comparing the incident signal with the signal transmitted or reflected by the device. The magnitude and phase response of the system are measured in terms of S-parameters which can be given as a linear magnitude ratio and relative phase angle of the transmitted or reflected signal to the input signal. The HP 8510 network analyzer is a two port system which measures two sets of S-parameters.

To prevent confusion the notation $S_{out,in}$ is used, where out represents the port where the incident signal was measured, and in represents the port from which the incident signal was sent. By using an automated network analyzer, the S-parameters of the network can be measured for a range of frequencies at up to 801 frequency points (depending on calibration), instead of at a single frequency. From the measured S-parameter data the complex permittivity and permeability can be computed as first shown by Nicolson and Ross (1970) using the transmission/reflection method. This technique relates the measured S-parameters to the transmission and reflection coefficients, which are then related to the complex permittivity and permeability. The equations used to calculate the complex permittivity and permeability from the S-parameter data are given in Appendix A.

Figure 13 shows the measurement system which includes the network analyzer which processes the S-parameters, an HP 8340 synthesized frequency sweeper for generating test signals over a range of frequencies (30 MHz- 26.5 GHz), and an S-parameter test set which provides signal separation. An HP Model 9000 Series 320 computer processor was used to control the network analyzer, acquire data, and compute the dielectric and magnetic properties from the S-parameters. The test signals were sent from the S-parameter test set to the device under test (DUT) via flexible coaxial transmission lines with APC-7 connectors (manufactured by Gore). The DUT was placed in a 5-cm-long coaxial sample holder connected to the transmission lines. The material being tested was placed in the annular space between the inner and outer conductor of a coaxial sample holder having an

outside diameter of 7 mm, and an inside diameter of 3.04 mm. The solution technique of Nicolson and Ross assumes that the entire annular area is filled with the material being tested. As described in Section 4.1.1, test samples were made by pressing the polypropylene-iron powders into annular rings to fit into the coaxial sample holder.

Before measurements were performed, the network analyzer was calibrated. Calibration is required to account for systematic effects that can effect measurement results such as leakage, test port mismatch, and resonances. These systematic effects are quantified by measuring and comparing the measured response with different standards. Calibration can be performed either with or without the sample holder in place, although calibration with the sample holder in place is recommended since it will correct for errors brought about by transmission through the sample holder. However, some residual systematic effects remain even after calibration due to imperfect calibration standards. The HP 8510 has eight different calibration routines included with the instrument. A Thru-Reflect-Delay (TRL) two port calibration was used for the measurements of the polypropylene-iron composites. The TRL 2-port calibration was chosen since it is accurate and relatively simple to perform: only different lengths of transmission line are used as standards, instead of a variety of impedance standards.

Before starting the TRL calibration, the frequency range and number of measurement points in this frequency range must be input to the network analyzer. The frequency range that can be measured is a function of the type of

transmission line being used to hold the test sample. Coaxial air lines and rectangular waveguide are two devices that can be used as sample holders. Waveguides have the advantage of being rectangular, which makes samples easier to manufacture. However rectangular waveguide has a limited range of operating frequencies. For example WR-90 waveguide can only support a test signal in the frequency range 8.2-12.4 GHz. However, 7 mm coaxial air lines can operate in a much wider frequency range: 45 MHz - 18 GHz, although a low band correction must be performed during calibration to get accurate measurements at the low end of this frequency range. The drawback to using coaxial air lines is that precisely dimensioned test samples are required.

Coaxial air line was used as the sample holder for the polypropylene-iron composite measurements. The input measurement frequency range was 2-10 GHz, with a total of 401 measurement points at discrete frequencies in this range. The TRL calibration technique consisted of three steps. The first was to measure a reference throughput. This step consisted of directly connecting the APC-7 connectors of Port 1 and Port 2. The next step was to place a highly reflective short at the termination of each port to define the calibration plane. The calibration plane is assumed by the network analyzer to be the measurement plane. If the measurement plane is not the same as the calibration plane, a reference plane rotation must be performed to account for the phase shift in measured S-parameter data (HP Product Note 3). Finally, the line part of the calibration was performed by placing a piece of line of known length between the two ports, and measuring the resulting signal. It is important to note that the

length of line for the throughput reference and the line reference must be different. After these steps were performed, the calibration was saved and measurements performed. A step by step description of the procedure used to perform the TRL 2-port calibration is listed in Appendix B.

Measurements were controlled through an existing program on the HP 9000 Series computer. The program prompts the user to pick a stored calibration set for the measurement, and then measures the S-parameters using this calibration. The S-parameters are then stored in a data file. The program then calculates the complex permittivity and complex permeability from the S-parameter data.

4.1.3.1 Uncertainties in Dielectric and Magnetic Measurements

There were several potential sources of error in the measurements using the transmission/reflection technique. However, the magnitude of the error for each measurement depended on the sample being measured. Jarvis et al. (1990) have done a comprehensive uncertainty analysis for the transmission/reflection technique using an HP 8510B network analyzer. One of the error sources is uncertainty in the measured length of the sample. Since the length was measured to within one percent and the error in the permittivity and permeability is proportional to the error in the measured length, the resulting uncertainty in the measurements is small. Gaps between the sample holder and the sample are another source of error. The solution technique assumes that the entire cross-sectional area of the sample holder is filled with the material being tested. This

error is very hard to quantify because it is difficult to measure these gaps. Based on visual inspection, it was assumed that no gaps existed for the polypropylene-iron samples measured. There was also some uncertainty in the location of the measurement planes. This uncertainty is caused by movement of the test sample when the sample holder and coaxial transmission lines are being connected. Once again this error was not quantifiable since the displacement was not visible after the connection was made.

Instrumentation error also contributes to uncertainty in the measurements of the permittivity and permeability. This systematic uncertainty comes from the uncertainty in the measured S-parameter values (S_{11} and S_{21}). The error in the S-parameters depends on their magnitudes. The magnitude and phase errors in the S_{11} parameter increase as it approaches 0, and decrease as it approaches 1. The magnitude and phase errors for the S_{21} parameters are small and do not depend strongly on the magnitude of S_{21} when it is greater then 0.1, which was the case for all of the measurements made in this work. Therefore the minimum instrumentation error occurs as S_{11} is maximized (Hewlett Packard Note 8510-3). Hewlett Packard gives the uncertainties in the S-parameters due to instrumentation error over the range 0-1. Jarvis et al. (1990) performed a differential uncertainty analysis of the complex permittivity based on the uncertainty of the S-parameters for both high loss and low loss materials. The analysis is presented in Figures 14a and 14b with the uncertainty shown as a function of L/λ_m, where L is the length of the sample and λ_m is the wavelength of the radiation in the sample given by

$$\lambda_m = Re\left(\frac{\lambda_0}{\sqrt{\varepsilon^* \mu^*}}\right) \tag{4.3}$$

These plots (Figures 14a and 14b) were used to determine the approximate uncertainties of the complex permittivity. First the approximate values for L/λ_m were calculated for each measurement. Using this value the approximate uncertainty was found by using the appropriate figure. Figure 14b gives the uncertainty in the measured value of the dielectric constant for materials with low loss factors (lower iron loadings), while Figure 14a gives the uncertainty in the electric loss factor for materials with high loss factors (higher iron loadings). From these figures, the uncertainty in the dielectric constant due to instrumentation error for the lower iron concentrations was estimated to be less than 5%, while the uncertainty in the electric loss factor for the higher iron concentrations was between 8 and 20%. The uncertainty in the electric loss factor for low loss factor materials was not given because the loss tangent (ratio of electric loss factor to dielectric constant) must be greater than one for reasonable accuracy (Hewlett Packard Note 8510-3). The uncertainty in the dielectric constant for the higher iron concentrations was between 4 and 8%, although this plot is not shown in Figure 14. It is important to remember that this error is only the systematic error due to error in the measurement of the S-parameter, and does not include error due to reference plane position and gaps in the sample holder. In addition, errors caused by nonuniformities within the sample are not included. These errors result

from sample preparation, and include particle size distributions and non-uniform particle size concentration. While these uncertainties were not quantified, they are probably significant.

4.1.3.2 Results of Dielectric and Magnetic Testing

The complex permittivity and permeability of the polypropylene-iron composites were measured as a function of frequency, iron concentration, and milling time. Two samples of different thicknesses were tested for each iron concentration and milling time to improve accuracy. A total of 401 measurements were made for each sample over the frequency range 2000 - 10000 MHz.

Plots of the complex permittivity and permeability over this frequency range are shown in Figures 15-22 for representative low (10%) and high (30%) loadings of iron (measurements of loadings of 5, 15, 20, 25, 35, and 40% iron showed the same trends as these representative figures). The plots show that the real part of the permeability did not vary much over this frequency range (Figures 17 and 21). However, there is a small decrease in the magnetic loss factor (Figures 18 and 22). The dielectric constant of the polypropylene-iron composites varied very little with frequency at the lower volume fractions of iron (Figure 15), but at higher volume fractions of iron the dielectric constant decreased with frequency (Figure 19). The electric loss factor increased slightly with frequency at low loadings (Figure 16), but decreased by 50% in the 30% iron loading. This decrease is expected since

the electric loss factor of the conductive loading is inversely proportional to the incident frequency (Equation 3.1).

Plots of the complex permittivity and permeability at 2400 MHz as a function of iron concentration for each milling time are shown in Figs. 23-34. Each figure shows the measurements of both samples and the average of these two measurements. The same average data are shown in Figures 35-38 and Table 1 to highlight the effect of milling time on the average permittivity and permeability.

Measurement of the dielectric constant at different iron volume fractions (Figure 35) revealed that at milling times of 2 and 20 hours the dielectric constant consistently increased with increasing iron content up to 40% iron. However, for the 4 hour milling case the dielectric constant dropped off above 35% iron. The decrease in dielectric constant could be due to a decrease in charge accumulation at the interfaces of the polypropylene and iron, resulting in a decrease in the amount of interfacial charge polarization. The charge at the interfaces decrease because the conducting network which has formed in the medium draws the charges away. This drop in dielectric constant was also experimentally found by Chung (1982) for carbon-black-PVC composites. Although continuous networks have formed in the other two cases (2 and 20 hour milling) at high iron volume fractions there are probably local regions in the medium where the charge storage may be locally high, resulting in a large dielectric constant. However, the drop in the dielectric constant at 40% iron could also be attributed to an abnormally high measured value at 35% iron. This is a strong possibility since an abnormally high

value for the electric loss factor was also measured for the 35% iron sample milled for 4 hours. The measured values are sensitive to the iron concentration and particle size distribution, especially near percolation where small discrepancies in the iron loading cause large differences in the measured dielectric constant and loss factor. The effect of milling time on the dielectric constant is fairly clear in Figure 35 at volume fractions below the percolation thresholds (below approximately 25%). The longer milling times increase the dielectric constant by creating more surface area which allows more charge storage (capacitance), resulting in a larger dielectric constant.

The electric loss factor dramatically increases after the onset of percolation (Figure 36). This is due to the creation of a continuous network of conductive particles which substantially increases ohmic losses and the electric loss factor. Comparison of the three milling times in Figure 36 shows that samples milled for twenty hours had a higher loss factor up to the percolation threshold than the two and four hour milling times. However, after the onset of percolation was reached in the twenty hour samples (approximately 25% iron), it was found that the two and four hour milled samples had higher loss factors. This probably was a result of the reduced penetration of incident radiation in the twenty hour samples since greater conductivity results in more reflection of the radiation.

Figures 37 and 38 show the permeability and magnetic loss factor of the polypropylene-iron composite for three milling times as a function of iron concentration. Measurements reveal that for each milling time (2,4, and 20 hours) the real and imaginary parts of the permeability steadily increase with increased

iron concentration. In addition, the results show that the real and imaginary parts of the permeability both increased with increased milling time at a given iron concentration. This is due to an increase in the number of magnetic domains that results from increased iron concentration and decreased particle size. The magnetic domains interact with the applied magnetic field to both store and dissipate magnetic energy.

The penetration depth is the distance from the surface that the incident electromagnetic radiation drops to 0.367 (e^{-1}) of its original strength. The penetration depth of the polypropylene-iron composites was calculated and found to be less than 12 cm even for low loadings of iron (approximately 5%). Figure 39 shows that the penetration depth decreases as the percolation threshold is approached and drops to near zero after percolation. The penetration depth is an important parameter when considering microwave processing since it limits the size of the specimen which can be heated volumetrically by microwaves.

The measured values of the complex permittivity and permeability give an indication of how well the polypropylene-iron composites heat in a microwave field. To further evaluate microwave heating, the composites were heated in a multimode oven and the heating histories correlated with the electric and magnetic properties. A description of the multimode oven and the results of the processing are given in the next section.

4.1.4 Microwave Heating of Polypropylene-Iron Composites

4.1.4.1 Description of Multimode Microwave Processing System

The polypropylene-iron composites were heated in a Microwave Materials Technologies (MMT) multimode microwave oven capable of delivering up to 1300 watts of power. Heating was monitored with a Luxtron Model 790 fluoroptic thermometer with the fiber-optic temperature sensor placed at the surface of the polypropylene-iron samples. The fiber optic probes are virtually invisible to the microwaves and therefore do not concentrate the electric field. Temperature was manually recorded at 30 second intervals. The entire processing set-up including the MMT microwave furnace controller is shown in Figure 40.

Before going into the details of how the polypropylene-iron samples were heated, a brief description of how a multimode microwave oven operates is given. A more detailed description is given in Chapter 6 of Metaxas and Meredith (1983). Microwave radiation is generated by a magnetron and transmitted to an applicator which contains the material being processed. There are several different types of applicators including single mode cavities, multimode cavities, and travelling wave applicators. The primary function of the applicator is to focus the microwaves into the material being processed. Travelling wave applicators use transmission lines to propagate the electromagnetic energy continuously, while single mode and multimode cavities use one or more resonant modes to deliver the microwave energy. Single mode cavity applicators can produce high field strengths but only

over a small fraction of the cavity, which is typically less than a wavelength in size. Therefore, only parts of limited diameter can be processed uniformly.

Multimode ovens are designed to produce many modes in the cavity at a given excitation frequency. However, since the microwave energy is now divided among many modes the field strengths are lower in a multimode cavity than in low mode cavities. Each resonant mode in a multimode cavity has a distinct resonant frequency and frequency bandwidth. A measure of the frequency bandwidth is the quality factor, Q, defined as

$$Q = \frac{f_r}{\Delta f} \tag{4.4}$$

where f_r is the resonant frequency, and Δf is the half power bandwidth. A high Q signifies a narrow bandwidth, and a low Q signifies a broad bandwidth. Low Q's are desirable in multimode cavities because the resonant modes are broad and their frequencies overlap, resulting in good coupling with the dielectric material in the cavity in the operating bandwidth of the magnetron. Although the intensity of each mode is reduced, the number of modes present at the operating frequency has increased, leading to more efficient and more uniform heating. A high Q occurs when the cavity is empty, lightly loaded, or loaded with a low loss material. Therefore, in order to lower the Q the cavity should have a sufficient heating load. Although the uniformity of the electric field is improved by reducing the Q factor, the microwave cavity will still exhibit "hot spots" where the field strength is relatively high (owing to the sinusoidal nature of the modes). Steps can be taken

to offset this non-uniform field distribution. A standard method, which is used in the MMT multimode cavity, is the use of mode stirrers that continuously change the mode patterns within the cavity.

4.1.4.2 Results of Heating in a Multimode Oven

A series of polypropylene-iron composites was heated in the multimode oven. The temperature histories of these composites were recorded to determine the relative heatability of the various composites. The effect of milling time was examined by heating the polypropylene-iron samples with 58 watts (nominal) power. This power is nominal since some of the incident power is not absorbed in the sample due to losses incurred in the cavity.

The results for cold pressed samples milled for two, four, and twenty hours are shown in Figures 41-43. The heating results were consistent with the resistivity and dielectric measurements previously described. The percolation threshold can be identified on these plots by a marked jump in the temperatures when comparing a concentration below percolation to one above. In the twenty hour milling case (Figure 43), there is a shift upward at 25% iron; in the four hour milling case (Figure 42), there is a shift upward at 35% iron; while for the two hour milling case (Figure 41), the jump occurs 40% iron. This correlates very well with the resistivity measurements: the resistivity of the samples milled for twenty hours started to drop at 25% iron, at four hours the drop occurred at 35% iron, while samples milled for two hours did not drop until 40% iron.

The temperature history results generally follow the electric and magnetic loss factor results. The heating was found to be greater for composites with higher loss factors except when the penetration depth was a factor. The effect of diminishing penetration depth can be observed in Figure 43 where the 40% iron sample temperatures are below those for the 35% iron sample.

Table 2 shows the maximum temperature reached for each sample during heating in the multimode cavity. The table also indicates the lowest iron concentration above percolation for each milling time (2,4 and 20 hours). For concentrations up to 35% iron, the highest temperatures occurred with the composites milled for 20 hours with the exception of the 15% iron loading (Table 2). At 35% iron the sample milled for 4 hours reached the highest temperature and at 40% iron the 2 hour sample reached the highest temperature gave the best heating. For these cases the penetration depth has probably decreased the total power dissipation in the sample volume.

A description of how the results for the polypropylene-iron system could be used for a microwave heating application is useful. If volumetric heating is desired, it is best to avoid polypropylene-iron composites with iron loadings at or near the percolation threshold (25-40% iron), where loss factors are high and penetration depths small. The conductivity and electric loss factor of the composites are very sensitive to small deviations in particle size and concentration at these loadings, which would make the fabrication of these composites difficult. The appropriate concentration of iron is largely a function of part size and desired heating time. For example, the 20% iron-polypropylene composite milled for 20

hours has a relatively high electric loss factor of 2.42 and a magnetic loss factor of 0.77, but a penetration depth of only 1 cm. This would limit volumetric heating to parts of thicknesses not much greater than 1 cm. A penetration depth of 12 cm is possible with the 5% iron-polypropylene composite milled for 20 hours, but the loss factors are only 0.02 for the electric loss factor and 0.09 for the magnetic loss factor. Hence the necessary increase in penetration depth would result in a much reduced heating rate.

The results clearly show that metal-filled polymers can be designed specifically for microwave heating. By varying the type, shape, and concentration of conductive filler added to a low loss polymer, the dielectric properties can be tailored to match the heating requirements.

4.2 Procedures and Results for Epoxy Systems

Two distinct methods of enhancing the processability of an epoxy-amine system were investigated: using microwave energy to cure the epoxy system, and using a novel solid-state processing technique which may enable the epoxy system to react without melting. Microwave processing has potential advantages over conventional processing including more uniform heating and faster curing. The advantages of solid-state processing over conventional melt processing include reduction or elimination of harmful vapors, and the potential to produce complex parts easily since the powder will retain its pressed shape.

This chapter will describe how these processing techniques were investigated, and what conclusions can be drawn regarding microwave curing and solid-state processing of epoxy systems. Chapter 4.2 includes two sections. The first section, 4.2.1, discusses how the epoxy system was prepared specifically for solid-state processing. The proof-of-concept experiments used to determine if solid-state processing is feasible are described, and interpretation of the results is given. The data are primarily DSC plots which show that the curing of epoxy systems in the powder form is a diffusion limited process, and that the diffusion limitation can be reduced by mechanical milling of the epoxy-amine system.

The second section of the chapter, 4.2.2, looks at the microwave curing of epoxy. A description of the experimental procedure and results of the dielectric testing are given, followed by a description of how the epoxy-amine system was cured in the multimode microwave cavity. The section concludes with a

description of how the Differential Scanning Calorimeter (DSC) was used to determine the degree of cure of the dielectric measurement samples and of the microwave processed samples.

4.2.1 Solid State Processing of an Epoxy System

Curing of an epoxy system in the solid-state was examined. The basic idea of solid-state processing is to reduce the reacting species to their thermodynamic minimum size (through ball milling) and to thoroughly mix them so that the reaction will only be limited by kinetics, not diffusion. Currently, reacting species are melt-mixed so that contact between reacting species can occur by rapid diffusion in the liquid. By eliminating or reducing the need for diffusion, it may be possible to react thermoset polymer systems without melting either component. A description of the experimental steps taken to test this idea, and results of these experiments are now given.

Two different epoxy systems were chosen as candidates for solid-state processing. The first was an EPON HPT 1071 epoxy resin with an aromatic diamine curing agent 1061M, and the second was an EPON 2004 epoxy resin with a curing agent P101. Both epoxy systems were donated by Shell. The 1071/1061M epoxy system was chosen because both the epoxy and amine are solids at room temperature. The curing agent was supplied in the form of a finely ground powder with a melting temperature of 161°C, while the epoxy came as a dark solid with a melting temperature of 50°C, but a glass transition temperature

of 23°C. It was important that the epoxy and amine be solids at room temperature in order for them to be ball milled in a SPEX 9000 mixer/mill. Ball milling causes the powders to be fractured into smaller pieces through collisions with the tungsten carbide balls and the vial walls. However, if the material being milled is not in a solid, glassy state, the material may not be brittle enough to fracture (as was discovered with the 1071/1061M epoxy system).

The following steps were used for milling the 1071/1061M epoxy system. A stoichiometric ratio of the epoxy and hardener was placed in the vial and milled with two tungsten carbide balls. The stoichiometric mass ratio of amine hardener to epoxy resin was determined by dividing the approximate equivalent weight of the active hydrogen group in the amine curing agent (86) by the average weight per epoxide (160). The stoichiometric ratio makes it theoretically possible to have each epoxide group react with an amine group. After the first milling run, it was determined that the glass transition temperature of the epoxy was not high enough (the epoxy was not brittle enough) since the epoxy flowed into a blob, instead of fracturing, during room temperature milling.

In order to achieve the necessary fracturing during milling, the temperature of the epoxy had to be lowered by cooling the vial with liquid nitrogen. Cryogenic milling (milling in the liquid nitrogen environment) was achieved by adapting the existing mixer/mill. The only modification to the mixer/mill was a hole drilled into the side of the casing to allow insertion of a 1/4" copper tube. As shown in Figure 44 the copper tube was connected to a 50 gallon liquid nitrogen supply tank. The

nitrogen was dripped from the tank through the copper tube onto the vial, which was being vigorously shaken by the mill.

Initial results using cryogenic milling were promising. The temperature of the epoxy was reduced so that it was brittle enough to fracture on impact. Several runs were made to produce milled mixtures of epoxy and hardener. Milling times of up to two hours were achieved. However, the milling process had to be constantly monitored because the supply of nitrogen fluctuated and moisture from the dripping nitrogen often caused the belts to start slipping, which limited the runs to two hours. After the powders were milled, a DSC was used to determine if milling affected the rate of reaction. The powder mixtures of the 1071/1061M epoxy system produced from the cryogenic milling were also used for dielectric measurement samples and processing in the multimode microwave oven.

A DSC was used to determine if the milling process was causing any significant change in the rate of reaction of the epoxide with the amine curing agent. The DSC measures heat given off by a chemical reaction. An increased rate of reaction with increased milling time would suggest that the reaction was becoming less diffusion limited, due to more intimate contact between reacting species. Samples for the DSC were made by cold pressing milled powders of 1071/1061M into a sheet and cutting off small (5-10 mg) pieces of the sheet. Powder mixtures that had been milled for a half hour, one hour, one and a half hours, and two hours were made into samples. The samples were placed into small aluminum crucibles that were placed on heat flux sensors in the furnace unit of the DSC.

Enhancement of the reaction rate of the epoxy system due to milling was tested by ramping temperature in the DSC. The epoxy system was ramped from 50 to 300° C at a rate of 10°C/minute. The sample completely reacts during this ramping and the heat released by chemical reaction is recorded. An increase in the rate of reaction would be evidenced by a shorter reaction time. However, as shown in Figs. 45-48, there does not appear to be any shift in the reaction rate since all four milling times have fairly identical reaction profiles. The exothermic reaction is seen on the plots as an increase in heat flow. The temperature axis also represents time since the temperature was ramped at a constant rate. Although there was no indication of improved reaction rate for the milling times investigated, it seemed worthwhile to try longer milling times. However, due to difficulties with cryogenic milling (including the cost of liquid nitrogen), and mechanical difficulties from excessive condensation, the 1071/1061M epoxy system was abandoned for a newly identified epoxy system that could be milled at room temperature.

The second epoxy system tested was an EPON 2004 epoxy resin with a P101 curing agent. The epoxy and curing agent were solids up to temperatures above 100° C and sufficiently brittle at room temperature for effective milling. The procedure for milling the 2004/P101 system was the same as the 1071/1061M system except that liquid nitrogen cooling was not used. Therefore, longer milling times were achievable. Milling times of fifteen minutes, thirty minutes, one hour, two and a half hours, ten hours, twenty hours, and forty hours were tested. Approximately ten grams of the epoxy system was milled for each milling time,

with the exception of the forty hour milling in which the mass of epoxy system was reduced to five grams. The effect of placing less mass in the vial is to increase the amount of milling for a given time, since the number of collisions per particle will increase. The epoxy-amine mixtures were combined at a mass ratio of 100 parts epoxy per 3 parts amine. After the 2004/P101 epoxy system was milled, samples of the milled powder were then ramped with the DSC from 50 - 200° C at 10° C/minute.

The initial DSC results showed that milling had enhanced the rate of reaction. Figure 49 shows the heat flow plots for epoxy samples milled for fifteen minutes, thirty minutes, and one hour. The powder milled for one hour reacted faster and at a lower temperature than the epoxy mixtures milled for fifteen and thirty minutes. This is evidenced by a shift in the exothermic peak to lower temperatures (or shorter times since the temperature is being ramped at a constant rate). It should be noted that the relative vertical position of each curve has no physical significance, and is due only to drift in the instrument. Figure 50 is a similar plot for epoxy mixtures milled for two and a half, ten, and twenty hours. The samples milled for ten and twenty hours reacted faster and at lower temperatures than the sample milled for two and a half hours.

In order to quantify the effect of milling time on the reaction of the epoxy-amine powders, the activation energies of the epoxy mixtures were determined. The activation energy is a measure of how sensitive the extent of reaction is to a change in temperature. Higher activation energies correspond to reactions which are more sensitive to temperature change: higher temperatures lead to increased

total reaction. Therefore higher activation energies lead to faster reaction rates than do low activation energies at temperatures near the glass transition temperature. The rate of reaction R′ is related to the absolute temperature T, and activation energy Q_a by

$$R' = R_0 \exp\left(\frac{-Q_a}{R_g T}\right) \tag{4.5}$$

where R_0 is a constant, and R_g is the universal gas constant.

The time dependence of Equation (4.5) can be integrated out by considering a system that has been allowed to react for a given amount of time. The integrated rate of reaction is the extent of reaction (or cure) for a given amount of time

$$f_{rct} = A \exp\left(-\frac{Q_a}{R_g T}\right) \tag{4.6}$$

where f_{rct} is the fraction of the total reaction that took place for the given period of time and temperature, and A is a constant. The fraction f_{rct} can also be expressed as percent cure by multiplying by 100. Therefore, Equation (4.6) relates the extent of cure for a given time to the temperature and activation energy. Equation 4.6 can be rewritten as

$$\ln(f_{rct}) = -A' \frac{Q_a}{T} \tag{4.7}$$

where A' is a constant. Hence, the activation energy Q_a is proportional to the slope of the line generated by plotting $\ln(f_{rct})$ versus $1/T$. In this way the activation energy can be determined experimentally.

Using this analysis, the activation energies of the epoxy-amine mixtures were experimentally determined for different milling times. Isothermal cures of one hour duration at different temperatures were performed. The extent of cure was then determined using a DSC. The percent cure for each milling condition was normalized with the total heat of reaction for epoxy powders milled for the same time. This was done to account for any effects longer milling times had on the epoxy. The longer milling times caused the total heat of reaction to decrease. This could have been due to curing taking place during milling, or because some of the cure sites had been damaged. The natural log of f_{rct} and the reciprocal of the isotherm temperature were then plotted and a linear regression using a least squares analysis was used to determine the activation energy. Epoxy mixtures milled for fifteen minutes, twenty hours, and forty hours were measured at isothermal cure temperatures of 80, 90, and 100° C. The isothermal cure involved placing the sample in a vacuum oven for one hour. Three different samples were cured for each isotherm and milling condition. The standard deviations of the three-sample-average values from the regression fits at the same milling time were 3.2% for the 15 minute case, 8.8% for the 20 hour case, and 43% for the 40 hour case.

Figure 51 shows that longer milling times clearly increased the activation energy. The epoxy-amine powder milled for forty hours has an activation energy

of 12479*R_g J/mol (100,150 J/mol), the powder milled for twenty hours has an activation energy of 3677*R_g J/mol (30,571 J/mol), and the powder milled for fifteen minutes has an activation energy of 3032*R_g J/mol (25,210 J/mol). The increase in activation energy with increased milling time indicates that the reaction between the epoxides and amines is diffusion limited, since milling reduces the distance between reactive sites (by reducing particle size). By milling the powders to even smaller sizes it may be possible to further reduce or even eliminate the diffusion limitation of the reaction process (reaction kinetics would then become the limiter). The need to melt the reactants to increase reaction rates is thus eliminated, making solid state processing of the epoxy system an alternative.

The work described herein is part of experiments designed to test the feasibility of solid-state processing of thermoset polymers. The initial testing shows promising results: the reaction rates are faster and the activation energies are increased with increased milling times. However, additional work is necessary. First, the limit on the increase in activation energy with further milling should be established. This limit would establish that the reaction is only kinetically limited: diffusion is no longer limiting the reaction. In addition, mechanical testing should be performed to determine if the mechanical properties are affected by reacting the components as solid powders.

4.2.2 Microwave Curing of an Epoxy System

Microwave curing of an epoxy system was also investigated. The procedures and results of the dielectric testing and microwave processing of a 1071/1061M epoxy-amine system are given in this section. Descriptions of how the test samples were prepared and how the DSC was used to determine degree of cure are also given.

4.2.2.1 Sample Preparation

A tetrafunctional epoxy resin EPON HPT 1071 with an aromatic diamine curing agent 1061-M (both donated by Shell) was investigated. This epoxy system was chosen because it came in solid form at room temperature, which enabled the investigation of both microwave processing and solid state processing at room temperature. However, as discussed in the previous section the investigation of the solid state processing was complicated by the low glass transition temperature of the 1071 epoxy resin. Although a second epoxy system proved to be a better choice for the solid-state processing work, the 1071/1061M epoxy system was used for investigating the microwave processability.

The cryogenic milling procedure used to mix the 1071/1061M epoxy system is described in Section 4.2.1.1. After the epoxy and curing agent were milled, the powders were stored in a freezer to prevent appreciable curing until samples were needed. For processing in the multimode microwave cavity, the epoxy-amine

powder mix was placed in a teflon mold and heated. Dielectric properties of the epoxy-amine powder were also measured using a perturbation technique. The perturbation technique required a relatively small diameter test sample with lengths of approximately 2 1/4" for dielectric testing at 2.5 GHz and 1" for testing at 9 GHz, depending on the height of the waveguide. These test samples were made by placing the mixed epoxy and amine powders into a quartz glass tube designed for Nuclear Magnetic Resonance (NMR) samples. The NMR tubes were chosen because they are very thin walled, and quartz is a low loss material (hence it is nearly transparent to microwaves). After the NMR tubes were filled with the epoxy and amine powders they were placed in a vacuum oven and allowed to cure for various lengths of time. They were cured under vacuum to remove entrapped air which would lead to error in the dielectric measurement.

4.2.2.2 Dielectric Testing

Dielectric testing was performed on the EPON 1071/1061M (Shell) epoxy system using an HP network analyzer. However, due to difficulties in manufacturing annular test samples, the transmission/reflection measurement technique used for the polypropylene-iron measurements could not be used. Instead, a field perturbation technique was used for these measurements. Unlike the transmission/reflection technique, the perturbation technique does not require test pieces with tight tolerances. The test pieces must be of known volume, and isotropic with respect to the electric field. Measurements using the perturbation

technique are made at a single frequency, which depends on the type of resonant cavity used. (The transmission/reflection technique allowed broad frequency band measurement of dielectric properties.)

This section first briefly describes the theory behind the perturbation technique, including relevant equations. Next, the calibration and measurement procedures are reviewed. Finally, results of the dielectric testing and interpretation of these results are given.

4.2.2.2.1 Perturbation Technique Background

The perturbation technique is a method of measuring the dielectric properties of relatively low loss materials. The technique uses resonant microwave cavities with high Q factors to determine the complex permittivity of materials at the resonant frequency of the cavity. The measurement frequency is dependent on the type of resonant cavity used and the modes available. Two different rectangular waveguides were used as resonant cavities. During measurement, both cavities were resonant in a TE_{103} mode, where TE stands for transverse electric, and the subscript includes indices which correspond to the number of half wavelengths in each direction of the waveguide. The first index is the number of half wavelengths across the width of the waveguide, the second index is the number of half waves across the height of the waveguide, and the third index is the number of half waves along the length of the waveguide. The TE_{103} mode was used so that the electric field would be symmetric in the cavity with and without

the test sample. The material being tested is inserted through holes at the center of the waveguide where the electric field is maximum. For rectangular waveguide the resonant frequency (GHz) of an empty cavity is given by

$$f_r = 15[(1/W)^2+(N/d)^2]^{0.5} \tag{4.8}$$

where W is the width of the cavity in cm, d is the length of the cavity in cm, and N is the number of half waves along the waveguide where N is odd (ASTM D2520-86).

The Q value indicates the bandwidth of the resonant frequency. A high Q value refers to a sharp frequency peak, which results from low electrical and magnetic loss in the cavity. The cavity Q is the reciprocal of the electric loss tangent. In order to attain high Q values, resonant cavities are usually made of highly conductive and polished metals. For rectangular microwave cavities Q values of over 2000 are recommended (ASTM D2520-86).

When a dielectric material is present in a resonant microwave cavity the resonant frequency and cavity Q factor are decreased. Jackson (1993) notes that the frequency shift is due to the increased energy storage caused by the insertion of the dielectric, while the decrease in Q factor is due to power dissipation caused by the dielectric. Using perturbation theory, the electric storage and loss properties of the dielectric can be related to the changes in the resonant frequency and cavity Q factor. Although only the results will be repeated here, the full derivation can be found in Jackson (1993) or Altschuler (1963). The dielectric constant (storage term) is given by

$$\varepsilon' = \frac{V_c}{2V_d}\frac{(f_c - f_d)}{f_c} + 1 \tag{4.9}$$

where V_c and V_d are the volumes of the empty cavity and dielectric, respectively, and f_c and f_d are the resonant frequencies of the cavity without and with the dielectric test sample, respectively. The electric loss factor is given by

$$\varepsilon'' = \frac{V_c}{4V_d}\left(\frac{1}{Q_d} - \frac{1}{Q_c}\right) \tag{4.10}$$

where Q_c and Q_d are the Q factors without and with the dielectric test sample in place, respectively. The perturbation technique can only be used for test specimens that are either small enough or low loss enough that the resonant condition in the cavity is maintained, and the shift in resonant frequency is small. For example, conductive test samples cannot be measured using this technique.

4.2.2.2.2 Experimental Set-up for Perturbation Technique

The experimental system used to perform the perturbation technique was similar to the set-up used with the transmission/reflection technique. The main difference is that the DUT in the perturbation method is a single port cavity, whereas in the transmission/reflection technique the DUT was a section of coaxial transmission line with two ports (Section 4.1.3). The HP 8510B network analyzer

monitors responses from the DUT via the HP8515A S-parameter test set which is connected to the DUT via flexible coaxial cables with APC-7 connectors. An HP 8340 microwave frequency signal generator was used to generate the input test signal. The signal generator can sweep through the range of microwave frequencies necessary for the network analyzer to determine the resonant frequency and the Q factor of the cavity.

The DUT is a single port resonant cavity constructed from rectangular waveguide. Figure 52 shows the experimental set-up used to perform the perturbation technique, including the resonant cavity operating in the TE_{103} mode. The resonant frequency of the empty waveguide cavity is determined from its geometry. Since measurements at two different frequencies were desired, two different waveguide cavities were used. (Liao (1985) lists available standard waveguide, and the modes and frequencies that the each will support.)

At 2.5 GHz, WR-430 waveguide was operated in the TE_{103} mode; WR-90 waveguide was used at 9.0 GHz. The resonant waveguide is connected through an adapter flange by APC-7 connections to a coaxial line from the network analyzer. An inductive iris between the waveguide and the adapter flange couples the input signal into the cavity. The circular iris in the WR-430 waveguide has a diameter of 1.02" and is 0.0056" thick, while the iris for the WR-90 waveguide is 0.267" in diameter and 0.0056" thick. The 8" straight section of WR-430 waveguide and the APC7-101M coax to WR-430 waveguide adapter flange were manufactured by Struthers Electronics. The WR-430 waveguide included an adjustable shorting plate which allowed fine tuning of the resonant cavity. The

2.6" straight section of WR-90 waveguide was manufactured at Oak Ridge National Laboratories. The X209D2 coax to WR-90 waveguide adapter flange was manufactured by Maury Microwave Corporation. Both straight sections of waveguide had holes on the top and bottom to allow insertion of the dielectric materials to be tested.

4.2.2.2.3 Calibration

Calibration of the measurement system was performed by measuring known standards and correcting for any differences. The same 2-port TRL (Thru-Reflect-Line) calibration method used for the transmission/reflection technique was used for the perturbation method. The TRL calibration relies only on transmission line and reflection standards. Transmission line standards are advantageous since they are relatively easy to manufacture, and their impedances are easy to determine (HP Product Note 8). The 2-port TRL calibration is a built-in calibration option for the HP network analyzer. The procedure used to calibrate the network analyzer was basically the same as that described previously for the transmission/reflection technique (Section 4.1.3). The only difference is the type of transmission line used in the calibration. For the transmission/reflection technique coaxial transmission line is used, and for the perturbation technique waveguide transmission line is used. An outline of the calibration procedure is given in Appendix B.

4.2.2.2.4 Test Procedure

The network analyzer was interfaced with an HP 9000 series 300 computer which allowed the measurements to be controlled from a computer keyboard. An existing program, CAVPERT, was used to interface with the network analyzer. Since the epoxy-amine sample was inside an NMR tube, the diameter was assumed to be the inside diameter of the NMR tube (4mm). The diameter of the test specimen and the frequency range (around the resonant frequency of the cavity) were entered into the program. Although the resonant frequency drops when the test sample is placed in the cavity, the relative frequency change is small, on the order of 0.001 (Rzepecka, 1973). For the WR-430 waveguide, a frequency band of 2400-2500 MHz was used, for the WR-90 waveguide a frequency band of 8500-9500 MHz was used. The network analyzer detects at which frequency resonance occurs in the cavity. The network analyzer also determines the bandwidth of the resonant frequency for calibration of the Q factor.

The resonant frequency and Q factor of the empty resonant cavity are measured before inserting a sample. Since the epoxy-amine mixtures being tested were cured inside of NMR tubes, the tubes were permanently part of the test sample. Although the quartz tube did not significantly perturb the electric fields in the cavity, any bias they might introduce was removed by inserting an empty NMR tube into the resonant cavity in the "empty" state. The sample being tested was carefully inserted directly in the center of the access hole to maintain the symmetry of the electric field in the cavity. After the resonant frequency and Q

factors of the "empty" and loaded cavity were measured by the network analyzer, the program determined the relative complex permittivity using Equations 4.9 and 4.10. All testing was done at room temperature. The procedure for both waveguides was the same, the only difference being the measurement frequency range, and waveguide dimensions.

The perturbation technique has several potential sources of error. The primary source of error occurs because the solution technique assumes that a symmetric electric field exists in the cavity. If the test sample is not placed exactly in the center of the cavity or if the test sample is not homogeneous, the field is no longer symmetric. The measurement of the sample dimensions involved a small uncertainty (probably less than 1%). Uncertainty could also have resulted from entrained air in the samples. It is important to remember that this solution technique is only accurate for low loss samples that cause a frequency shift of less than 0.001 (0.1%). This criterion was met for all of the epoxy-amine samples measured. An uncertainty of just 1-2% for the dielectric constant, and 5% for the loss factor is possible using this technique for a rod specimen in an axial field (ASTM D2520-86).

4.2.2.2.5 Results

After the dielectric measurements were completed, a DSC was used to determine the degree of cure of the samples in order to correlate the degree of cure with the dielectric properties. The degree of cure was determined by measuring

the heat of reaction of each of the partially cured test samples and dividing this by the heat of reaction for an uncured mixture of epoxy and amine. Table 3 lists the results of the dielectric testing of each sample, and the corresponding percentage cure.

Figures 53-56 show the results of the dielectric testing of the 1071/1061M epoxy samples at 2.5 GHz and 9 GHz using the perturbation technique. In the figures each data point represents a single measurement of a unique sample. Figures 53-54 show the dielectric constant and electric loss factor for the epoxy system at 2.5 GHz as a function of cure. The figures clearly show that both the dielectric constant and electric loss factor decrease as the epoxy cures. Figures 55 and 56 show the same trend (both the dielectric constant and loss factor at 9 GHz decrease) as the percent cure increases. These observations were also made by Delmotte et al. (1991) and Baker et al. (1992) for different epoxy systems. The decrease in the loss factor and dielectric constant with increasing cure is explained by the reduced mobility of the molecular dipoles due to the cross-linking, which forms a rigid network. The formation of the rigid network and the resulting reduction in mobility means that fewer dipoles are able to align with the electric field. With fewer dipoles participating in the dipole reorientation both the storage and loss terms decrease.

The principle mechanism of electric loss and storage in the epoxy-amine system is dipole reorientation, which is dependent upon frequency. Losses due to dipole reorientation reach a maximum when the incident frequency is approximately equal to the reciprocal of the relaxation time of the molecular

dipole. Frequencies above or below this resonant frequency result in lower loss. It is important to know this resonant frequency in order to control the processing. Although the perturbation method did not permit broad frequency band measurement of the dielectric properties, some indication of the relative position of the resonant frequency is apparent in the dielectric properties of the epoxy-amine mixtures at 2.5 and 9 GHz. Figure 57 shows the loss factor of the epoxy-amine mixtures at both 2.5 and 9 GHz. The loss factor at 9 GHz is notably less than the loss factor at 2.5 GHz, which indicates that the frequency corresponding to maximum dielectric loss probably occurs at some frequency below 2.5 GHz at room temperature (since the loss factor has decreased with frequency).

The dielectric properties of the epoxy and amine were also measured independently at 2.5 and 9.0 GHz (Table 3). The dielectric constant and loss factor of the epoxy at both 2.5 and 9.0 GHz were higher than the amine hardener by more than an order of magnitude at room temperature. Therefore, the epoxy is the constituent primarily responsible for heating. Delmotte et al. (1991) found similar results for various epoxy and curing-agent systems.

The results of this section show that at 2.45 and 9.0 GHz the loss factor of an uncured epoxy-amine system is high enough to allow sufficient heating with microwaves to initiate curing. The amount of microwave heating will decrease at the onset of cross-linking due to the reduced mobility of the dipoles.

4.2.2.3 Microwave Processing of Epoxy in a Multimode Cavity

Different aspects of microwave curing were investigated by processing the 1071/1061M epoxy system in a multimode microwave oven, and recording the temperature history. The temperature histories show different stages of microwave cure and how the power level influences the rate of cure.

The experimental set-up was virtually identical to that described in the polypropylene-iron section, except in the way that the sample was placed in the cavity. Since the epoxy melted during processing, it was necessary to design a teflon mold (Figure 58) to contain and insulate the epoxy. Teflon was used because it is a very low loss material. The teflon mold had a hole in the top to allow penetration of an optical temperature probe, which was placed in contact with the epoxy-amine mixture. The optical probe was sheathed with a glass rod for protection. The glass rod containing the temperature sensor penetrated the multimode cavity through an access hole in the top of the cavity.

The amount of power coupled to a material in a microwave cavity is sensitive to the amount and position of the material in the cavity. Therefore, in order to compare the effect of increasing the power level, it was necessary to keep the amount and position of the epoxy-amine mixture fixed. The sample position was consistently fixed at the center of the cavity by a rigid glass rod extending from the top of the cavity. In addition, a fixed weight of 2.5 grams of epoxy-amine sample was used for each run. Due to the possibility of harmful vapors being released during curing, all processing took place in a fume hood.

The epoxy system was processed at nominal power levels of 255, 320, and 385 watts. The power levels are nominal since they are the power leaving the magnetron, and not necessarily the power being absorbed by the epoxy system. The actual power being absorbed is significantly lower. Figure 59 shows the temperature history of the epoxy system heated with a nominal power of 385 watts. The temperature history can be separated into four stages. The first stage which goes from 0-250 seconds, is the initial heating period in which the epoxy resin is generating heat via dipole reorientation. The next stage, which runs from 250-450 seconds, is denoted by a levelling of the temperature. In this stage the epoxide groups are becoming cross-linked. The cross-linking reduces the amount of heat produced by dipole reorientation. However the conversion of the epoxide groups does cause some heat to be released, the third stage. This release of heat starts at about 450 seconds. During the final stage, denoted by a drop in temperature, the heat loss to the surrounding begins to exceed the heat generation. A DSC was used to determine the degree of cure of this sample after microwave heating. The epoxy was found to be approximately fifty percent cured. The cure would have been more complete if the curing temperature could have been maintained longer, either by heating at a higher incident power or by better insulating the sample.

Figure 60 shows the temperature history of the epoxy system processed at a nominal power level of 320 watts. The plot has the same shape as the epoxy system processed at 385 watts. The primary difference is that the cross-linking did not begin as soon (about 350 seconds, compared to 300 seconds). Decreasing

the power apparently increased the time needed to initiate cross-linking. The DSC showed that this piece was 26% cured after microwave processing.

Finally, Figure 61 shows the temperature history of the epoxy system heated with 255 watts of nominal power. Unlike the other temperature histories, only two of the four stages are identifiable. The initial heating of the epoxy due to dipole reorientation is clearly seen in the first 400 seconds, but not enough heat is generated to kick off any significant conversion of the epoxide groups. After microwave heating the epoxy-amine mixture was still liquid, indicating that little or no cross-linking had resulted.

Microwave curing of the 1071/1061M epoxy system has been shown to be feasible. The epoxy is primarily responsible for microwave heat generation according to measurements of the dielectric properties. Dielectric measurements have also shown that the dielectric heating decreases as the epoxy cures. Achieving high degrees of cure has been shown to be highly dependent on the absorbed power level during microwave heating. Careful selection of the heating cycle and conditions (insulation) would be necessary for ensuring product quality.

4.3 Procedures and Results for a Carbon-Black-Loaded Perfluoroelastomer

Although domestic microwave ovens are used extensively, industrial microwave processing of materials is a technology which is largely underutilized. The unwillingness to use microwaves is probably due in part to the technical complexities involved with employing electromagnetic heating (Kachmar, 1992). Currently rubber, food, and ceramics are processed with microwave energy while many other candidate materials are not. One potential candidate is a commercially available perfluoroelastomer loaded with various amounts and types of carbon-black. The perfluoroelastomer is presently processed using thermal energy, and the process is very time consuming. Microwave processing could potentially decrease the processing time. This section outlines the results of a study to assess the feasibility of microwave processing this perfluoroelastomer. The microwave processability was evaluated by dielectric testing at microwave frequencies and heating in a multimode cavity. Some aspects of these results are proprietary, so only key findings are summarized here. The compounds are identified by letter, and the amount, but not the supplier designation, of the carbon-black is given. Only the type and amount of carbon-black in each compound was known; other components (which could effect dielectric properties) may have been present.

4.3.1 Description of Material

Three different neat perfluoroelastomers were investigated (2000,4000, and 5000). They were loaded with varying concentrations (8-14% by volume) of two types of carbon-black: a very fine carbon-black (Type 1) and a coarse carbon-black (Type 2). Table 4 lists the different combinations of perfluoroelastomer and carbon-black. The coarse carbon-black had a mean diameter of about 500 nanometers, while the fine carbon-black had a mean diameter of about 20 nanometers. Currently the carbon-black is used to provide desirable mechanical and aesthetic properties. However, the carbon-blacks are also conductive, which produces resistive heating in a microwave field. This heat could be used to initiate a cross-linking reaction in the perfluoroelastomer. The influence of the type and amount of carbon-black was quantified by dielectric measurements at microwave frequencies and by heating samples in the multimode oven.

Dielectric property measurement of the three neat perfluoroelastomers was done to examine whether dielectric heating via dipole reorientation was possible. Little heating by dipole polarization was expected because the perfluoroelastomer is made up of long chains with very few mobile dipoles. A description of the experimental procedure and results of the dielectric testing follows.

4.3.2 Dielectric Testing

Dielectric testing of the filled and unfilled polymer was performed using the perturbation technique (2.45 GHz) and the transmission/reflection technique (2-10 GHz) as described in Sections 4.1.3 and 4.2.2.2, respectively. The filled perfluoroelastomers were tested using both dielectric measurement techniques, while the unfilled perfluoroelastomers were tested using only the perturbation technique. Samples for the transmission/reflection technique were cut from tubing that was specially extruded to fit the dimensions of the 7 mm coaxial line. Samples for the perturbation technique were cut from sheet pressed from a roll mill. All test samples were dried in a vacuum oven and stored in a container with desiccant to remove water (since water would influence the measured value of the dielectric properties).

Figures 62 and 63 show the measured dielectric constant and loss factor of the filled and unfilled perfluoroelastomers using both measurement techniques at approximately 2.5 GHz. Averages of these results are also included in Table 4. At room temperature the neat perfluoroelastomers are extremely low loss ($\varepsilon'' < 0.004$). This indicates that the unfilled polymer compounds are not good candidates for microwave processing without custom designed applicators. However, the loss factor is greatly increased by the addition of carbon-black.

The relative increase in the value of the loss factor is dependent on the type and amount of carbon-black used. The fine carbon-black (Type 1) increases the loss factor to a greater extent than the coarser carbon-black (Type 2). This is

because the fine carbon-black particles are more than an order of magnitude smaller than those of the coarse carbon-black, greatly increasing the surface area for a given volume fraction of carbon-black. The additional surface area allows more loss-inducing surface currents to be set up throughout the carbon-black-perfluoroelastomer composite. The finer carbon-black also allows more charge storage. This increased charge storage translates into a higher dielectric constant. These results are in agreement with the results from the dielectric testing of the polypropylene-iron composites: at iron loadings below percolation it was found that the dielectric constant and loss factor increased as the iron particle size decreased.

The values of the dielectric properties were also dependent on the amount of each carbon-black used. The results for the fine carbon-black (Type 1 in Table 4) show that the loss factor and dielectric constant both increase with increasing carbon-black content. Once again this is attributed to the additional surface area. From resistivity testing, it was determined that the volume fraction of carbon-black added to the perfluoroelastomer was below the percolation threshold in all cases. The results of the dielectric testing show that microwave heating is possible for all the carbon-black-loaded compounds, and that the extent of heating is enhanced by decreasing the size of the carbon-black and by increasing the amount of carbon-black (up to the percolation threshold).

4.3.3 Microwave Heating in Multimode Cavity

In order to confirm the results of the dielectric testing, each of the carbon-black-loaded compounds were heated in the MMT multimode microwave cavity, and the temperature histories measured. Prior to being heated in the microwave oven, the different compounds were dried in a vacuum oven and stored with desiccant to remove any free water. Samples weighing approximately 5 grams were placed on a sheet of teflon and placed in the middle of the microwave cavity. Temperatures were measured at the surface of the sample using a Luxtron fiber-optic measurement system. Figures 64 and 65 show the temperatures of each compound during heating at nominal power levels of 125 and 650 watts. The relative position of the temperature for each sample follows what is expected from the dielectric testing: the compound with the highest loading of the fine carbon-black (Compound F) heated fastest, while the compound with the coarse carbon-black (Compound G) heated slowest. (Results for Compound H are not plotted, but were essentially the same as those for Compound G, which had the same carbon-black type (Type 2) and concentration (13.7% by volume)). It is uncertain how the other components of these compounds (whose complete compositions are unknown) affected the electric loss factor and microwave heating characteristics.

The tests show that the carbon-black-loaded perfluoroelastomers can be processed with microwaves. The results also show that the microwave heating can

be increased by increasing the concentration of carbon-black, and decreasing the particle size of the carbon-black.

Chapter 5

Conclusions

This research evaluated two methods for enhancing the processing of polymers. Using microwave energy to process polymers was the primary method evaluated. In addition a solid-state processing technique was evaluated.

The following conclusions have been made regarding microwave processing of polymer systems:

1) The microwave heatability of "low loss" polymers such as polypropylene and neat perfluoroelastomers can be enhanced by the addition of conductive inclusions such as carbon-black and iron. The extent to which the heating is enhanced is dependent on factors such as the size and concentration of the conducting particles. The microwave heating is enhanced with decreased particle size and increased concentration of the inclusions up to the percolation threshold.

2) The microwave heatability of the metal-filled polymer composite changed significantly at percolation. Percolation is characterized by a dramatic increase in the conductivity and electric loss factor of the metal-filled polymer over a small range of metal loadings. At

concentrations above percolation the penetration depth of the microwaves into the material decreased, limiting the volumetric heating with microwaves. Therefore, when uniform heating is desired, the volume fraction of metal filler should be below the percolation threshold since the resistivity of the composite becomes very sensitive to small deviations in the size and concentration of filler near percolation.

3) The electric loss factor for the metal-filled polymer composite did not increase as dramatically at percolation as simple models predict. This indicates that the assumed proportionality between dc conductivity and electric loss factor does not hold at microwave frequencies. Although the dc conductivity increased by many orders of magnitude, the increase in loss factor was much more gradual and modest. In addition, the electric loss factor increased well before percolation, even though the conductivity was not increasing, apparently due to local electron conduction on the surface of the metal particles.

4) Iron has drawbacks as a metal filler for composite systems. The iron oxidizes easily, and storage in an oxygen-free environment would be necessary to prevent degradation.

5) The dielectric properties of the 1071/1061M epoxy system are dependent on the extent of cure. The dielectric constant and electric loss factor of the epoxy decrease as the epoxy cures as a result of reduced mobility of the dipole groups.

6) The 1071/1061M epoxy system can be cured with microwave energy, but the extent of cure is dependent on the absorbed power level and processing time.

The following conclusions have been made regarding solid-state processing of thermoset polymer systems:

1) Solid-state processing has been demonstrated by curing an epoxy-amine system below the melt temperatures. By milling the reactants to a fine powder and mixing them completely, the extent to which diffusion limited the process was significantly reduced. Increased milling resulted in higher activation energies. It is possible that processing times for solid-state processing could approach processing times for traditional melt processing, since both processes would only be limited by kinetics.

2) Solid-state processing requires that the polymer being milled be brittle enough to fracture. Therefore, polymers with glass transition

temperatures well above room temperature are desirable since they are in the brittle, glassy state. However, polymers with low glass transition temperatures can still be processed if the temperature of the polymer is kept low enough during milling. In this research cooling of the polymer was successfully achieved by dripping liquid nitrogen on the milling vial.

3) The total heat of reaction of the milled epoxy powders milled for solid-state processing decreased at longer milling times. Although the cause was not determined, it is likely that some pre-curing is occurring in the vial, or that the milling process is damaging cure sites.

In summary, this research has shown that microwave processing of polymers is possible, and can be enhanced by designing the polymer specifically for microwave processing. The addition of a conductive powder is one technique that allows improved processing of polymers. The most important tool in evaluating or designing a polymer for microwave processing is the measurement of the dielectric properties. The dielectric properties indicate how much electromagnetic energy can be dissipated as heat in the material.

This research also showed that solid-state processing of thermoset polymers is a promising technique that could allow thermoset polymers to be cured in the solid-state. Solid-state processing offers several advantages over conventional

methods: 1) It may be possible to eliminate harmful vapors since neither melting the polymer nor forming a solution is necessary, 2) more complex shapes may be formed, and 3) energy requirements may be reduced since parts can be cold pressed and lower processing temperatures are possible.

Chapter 6

Recommendations

This research has investigated new ways of processing polymeric materials. The main focus was on microwave processing of epoxies and metal-filled polymers. A solid-state processing technique for reacting thermoset polymers was also investigated. Recommendations for further study are given in three categories: microwave processing of metal-filled polymers, microwave processing of epoxy systems, and solid-state processing of thermoset polymers.

Microwave Heating of Metal-Filled Polymers:

1) Experimentally study how the shape of the particles affects the microwave heatability of the composite. A complete range of shapes from fibers to plates should be investigated.

2) Heat large metal-filled polymer samples using microwave energy, and monitor the temperature profile within the piece using several optical temperature sensors. This would help quantify how penetration depth affects heating of the sample.

3) Develop a model accurately correlating the electric loss factor with the amount, type, and size of the conductive filler. The simple model traditionally used is not adequate.

Microwave Heating of Epoxies:

1) Perform the dielectric property measurements over a range of temperatures, so that the dielectric properties of the epoxy system during processing can be determined. This is imperative if controlled processing of the epoxy system is desired.

2) Process relatively large test pieces using microwave energy, and then perform mechanical testing to determine if the microwave curing affects mechanical properties.

Solid-State Processing of Thermoset Polymers:

1) Continue milling the epoxy system to finer levels until the activation energy no longer increases. This would indicate that the reaction is no longer diffusion limited and the activation energy is comparable to that for traditional melt processing.

2) Determine if the solid-state processing technique has affected mechanical properties of the cured epoxy by comparative mechanical tests of small samples.

References

Aharoni, S., 1972, "Electrical Resistivity of a Composite of Conducting Particles in an Insulating Matrix," *Journal of Applied Physics*, Vol. 43, No. 5, pp. 2463-2465.

Altschuler, H., 1963, "Dielectric Measurements," *Handbook of Microwave Measurements*, 3rd ed., edited by Sucher and Fox, Polytechnic Press, New York, 495-546.

ASTM 1991 Annual Book of Standards - Electrical Insulation and Electronics, 1991, "D257-91, Standard Test Method for D-C Resistance of Insulating Materials," Vol. 10.01., pp. 111-126.

ASTM 1991 Annual Book of Standards - Electrical Insulation and Electronics, 1986, "D2520-86, Standard Test Method for Complex Permittivity (Dielectric Constant) of Solid Electrical Insulating Materials at Microwave Frequencies and Temperatures to 1650° C," Vol. 10.02., pp. 214-220.

Baker, K., Marand, E., and Graybeal, J., 1992, "Simultaneous Dielectric Constant Measurement and Sample Curing," *Proceedings of American Chemical Society Division of Polymeric Materials; Science and Engineering*, Vol. 66, pp. 474-475.

Beldjoudi, N., Bouazzi, A., Driss, D., and Gourdenne, A., 1988, "Microwave Curing of Epoxy Resins with Diaminodiphenylmethane-Crosslinking Under Continuous or Pulsed Waves," *European Polymer Journal*, Vol. 24, No. 1, pp 49-52.

Balanis, C., 1989, *Advanced Engineering Electromagnetics*, John Wiley & Sons Inc., New York.

Baziard, Y., and Gourdenne, A., 1988, "Crosslinking Under Microwaves (2.45 GHz) Of Aluminum Powder - Epoxy Resin Composites - I. Electrical Power Dependence," *European Polymer Journal*, Vol. 24, No. 9, pp. 873-880.

Baziard, Y., and Gourdenne, A., 1988, "Crosslinking Under Microwaves (2.45 GHz) Of Aluminum Powder - Epoxy Resin Composites - II.

Aluminum Concentration Dependence," *European Polymer Journal*, Vol. 24, No. 9, pp. 881-888.

Baziard, Y., Breton, S., Toutain, S., and Gourdenne A., 1988, "Dielectric Properties of Copper Powder-Epoxy Resin Composites," *European Polymer Journal*, Vol. 24, No. 7, pp. 633-638.

Baziard, Y., Breton, S., Toutain, S., and Gourdenne, A., 1988, "Dielectric Properties of Aluminum Powder-Epoxy Resin Composites," *European Polymer Journal*, Vol. 24, No. 6, pp. 521-526.

Benjamin, J., 1970, "Dispersion Strengthened Superalloys by Mechanical Alloying", *Metallurgical Transactions*, Vol. 1, pp. 2943-2951.

Bernasconi, J., and Wiesmann, H.J., 1976, "Effective Medium Theories for Site-Disordered Resistance Networks," *Physical Review B*, Vol. 13, pp. 1131-1138.

Bigg, D., 1986, "Electrical Properties of Metal-Filled Polymer Composites," *Metal-Filled Polymers*, edited by Bhattacharya, S., Marcel Dekker Inc., New York, NY, pp. 165-223.

Bouazzi, A., and Gourdenne A., 1988, "Interactions Between Carbon-black-Epoxy Resin Composites and Continuous Microwaves I. Electrical Power Dependence of the Rate of Crosslinking Of The Epoxy Matrix," *European Polymer Journal*, Vol. 24, No. 9, pp. 889-893.

Bueche, F., 1972, "Electrical Resistivity of Conducting Particles in an Insulating Matrix," *Journal of Applied Physics*, pp. 4837-4838.

Bur, A., 1985, "Polymer Review - Dielectric Properties of Polymers at Microwave Frequencies: A Review," *Polymer*, Vol. 26, pp. 963-977.

Chabinsky, I.J., 1983, "Practical Applications of Microwave Energy in the Rubber Industry," *Elastomerics*, pp. 17-20.

Chung, K., Sabo, A., and Pica A., 1982, "Electrical Permittivity and Conductivity of Carbon-black-Polyvinyl Chloride Composites," *Journal of Applied Physics*, Vol. 53, No. 10, pp. 6867-6879.

Clarricoats, P.J., 1961, *Microwave Ferrites*, Chapman and Hall, London.

Delmotte, M., Jullien, H., and Ollivon, M., 1991, "Variations of the Dielectric Properties of Epoxy Resins During Microwave Curing," *European Polymer Journal*, Vol 27, No. 4/5, pp. 371-376.

Erhu, N., Weiwei, L., Tiemao, S., and Zhihong, Z., 1988, "Measuring Permittivity and Permeability of High-Loss Solid Materials at Microwave Frequencies," *Proceedings: Second International Conference on the Properties of Applied Dielectric Materials*, Vol. 2, pp. 543-545.

Frosini, V., Butta, E., and Calamia, M., 1967, "Dielectric Behavior of Some Polar High Polymers at Ultra High Frequencies (Microwaves)," *Journal of Applied Polymer Science*, Vol. 11, pp. 527-551.

Granqvist C., and Hunderi O., 1978, "Conductivity of Inhomogeneous Materials: Effective-Medium Theory with Dipole-Dipole Interaction," *Physical Review B*, Vol. 18, No. 4, pp. 1554-1561.

Gourdenne, A, 1992, "Interactions Between Microwaves and Model Composite Materials," *Proceedings of American Chemical Society Division of Polymeric Materials; Science and Engineering*, Vol. 66, pp. 430-431.

Gurland, J., 1966, *Transactions Metallurgical Society (AIME)*, Vol. 236, pp. 642.

Hewlett-Packard Product Note 8510-3, "Measuring Dielectric Constant with the 8510 Network Analyzer," Palo Alto, CA.

Hewlett-Packard Product Note 8510-8, "Applying the HP 8510B TRL Calibration for Non-Coaxial Measurements," Palo Alto, CA.

Hsu, W.Y., 1983, "Morphological Effects on the Physical Properties of Polymer Composites," *Macromolecules*, Vol. 16, No. 12, pp. 1945-1947.

Jackson, M., 1993, "Modeling the Microwave Frequency Permittivity of Thermoplastic Composite Materials," M.S. thesis, Virginia Polytechnic Institute and State University, Blacksburg, VA.

Janzen, J., 1975, "On the Critical Conductive Loading in Antistatic Composites," *Journal of Applied Physics*, Vol. 46, No. 2, pp. 966-969.

Jarvis, J., Vanzura E., and Kissick, W., 1990, "Improved Technique for Determining Complex Permittivity with the Transmission/Reflection Method," *IEEE Transactions on Microwave Theory and Techniques*, Vol. 38, No. 8, pp. 1096-1102.

Jordan, C., Galy, J., and Pascault, J., 1992, "A Comparison of a Standard Thermal Cure and A Microwave Cure of a Bulk Epoxy-Amine Matrix:

Measurement and Mechanical Properties," *Proceedings of American Chemical Society Division of Polymeric Materials; Science and Engineering*, Vol.66, pp. 380-381.

Jow, J., Hawley M., Finzel, M., Asmussen, J., Lin, H., and Manring, B., 1987, "Microwave Processing and Diagnostics of Chemically Reacting Materials in a Single Mode Cavity Applicator," *IEEE Transactions on Microwave theory and Techniques*, Vol. MTT-35, No. 12, pp. 1435-1442.

Jullien, H., and Valot, H., 1985, "Polyurethane Curing by a Pulsed Microwave Field", *Polymer*, Vol. 26, pp. 506-510.

Kachmar, M., 1992, "Microwave Heating: 50 MW and Counting," *Microwaves and RF*, pp. 41-49.

Kander, R., Aning, A., Farrel. M., and Vick, L., 1993, "Nanostructured Polymer Blends and Polymer-Based Nanocomposites formed by Mechanical Alloying," *Proceedings Center for Composite Material Structures - Technical Program Review*, pp. II.E.1-II.E.7.

Kirkpatrick, S., 1973, "Percolation and Conduction," *Review of Modern Physics*, Vol. 45, pp. 574-588.

Krieger, B., 1992, "Vulcanization of Rubber, a Resounding Success For Microwave Processing," *Proceedings of American Chemical Society, Division of Polymeric Materials Science and Engineering*, Vol. 66, pp. 339-340.

Kumar, A., 1989, "Ferrite-Impregnated Fibre-Glass Composites as Microwave Absorbers," *IEEE 1989 Annual Report - Conference on Electrical Insulation and Dielectric Phenomena*, pp. 403-408

Kusy R., 1977, "Influence of Particle Size Ratio on the Continuity of Aggregates," *Journal of Applied Physics*, Vol. 48, No. 12, pp. 5301-5305.

Kusy, R., 1986, "Applications," *Metal Filled Polymers*, Marcel Dekker Inc., edited by Bhattacharya, S., New York, NY, pp. 1-132.

Largarkov, A., and Matitsin, S., 1992, "Microwave Properties of Polymer Materials Containing Conducting Inclusions," *Proceedings of American Chemical Society, Division of Polymeric Materials Science and Engineering*, Vol. 66, pp. 426-427.

LeVan, Q., and Gourdenne, A., 1987, "Microwave Curing of Epoxy Resins with Diaminodiphenylmethane-I. General Features," *European Polymer Journal*, Vol. 23, No. 10, pp. 777-780.

Lewis, D.A., and Shaw, J., 1993, "Recent Developments in the Microwave Processing of Polymers," *MRS Bulletin*, pp. 37-40.

Lewis, D.A., Hedrick, J.C., McGrath, J.E., and Ward, T.C., 1987, "The Accelerated Curing of Epoxy Resins using Microwave Radiation," *Polymer Preprints*, pp. 330-331.

Liao, S., 1985, *Microwave Devices and Circuits*, Prentice Hall Inc., Englewood Cliffs, NJ.

Mallaris, A., and Turner, D., 1971, "Influence of Particle Size on the Electrical Resistivity of Compacted Mixtures of Polymeric and Metallic Powders," *Journal of Applied Physics*, Vol 42, No. 2, pp. 614-618.

Marand, E., Baker, K., and Graybeal, J., 1990, "Dielectric Properties at Microwave Frequencies of Epoxy Undergoing Cure", *Polymer Preprints*, Vol. 31, No. 2, pp. 397-398.

Metaxas, A.C., and Meredith, R.J., 1983, *Industrial Microwave Heating*, Peter Peregrinus Ltd., London, United Kingdom.

Mijovic, J., Wijaya J., 1990, "Review of Cure of Polymers and Composites by Microwave Energy", Polymer Composites, Vol. 11, No. 3, pp. 184-191.

Nicolson, A., and Ross G., 1970, "Measurement of the Intrinsic Properties of Materials by Time Domain Techniques," *IEEE Transactions on Instrumentation and Measurement*, Vol. IM-19, No. 4, pp. 377-382.

Osepchuk, J, 1984, "A History of Microwave Heating Applications," *IEEE Transactions on Microwave Theory and Techniques*, Vol. MTT-32, No. 9, pp. 1200-1223.

Pozar, D., 1990, *Microwave Engineering*, Addison-Wesley Publishing Co., U.S.A.

Raj, R.G., 1986, "Microwave Polymerization of Epoxy - Copper Composites," *Polymeric Materials; Science and Engineering*, Vol. 55, pp 49-51.

Raj, R.G., 1987, "Studies On Microwave Polymerization of Epoxy-Iron Composites," *Polymeric Materials; Science and Engineering*, Vol. 57, pp. 537-539.

Rzepecka, M., 1973, "A Cavity Perturbation Method for Routine Permittivity Measurement," *Journal of Microwave Power*, Vol. 8, No. 1, pp. 3-11.

Smith, V., 1987, "Dielectric Properties of Polymers at Microwave Frequencies," M.S. thesis, Virginia Polytechnic Institute and State University, Blacksburg, VA.

Strand, N., 1980, "Fast Microwave Curing of Microwave Parts," *Modern Plastics*, pp. 64-67.

Teffal, M., and Gourdenne, A., 1983, "Activation of Radical Polymerization by Microwaves-I," *European Polymer Journal*, Vol. 19, No. 6, pp. 543-549.

Ueno, R., Ogasawara, N., and Inui, T., 1980, "Ferrites or Iron Oxide Impregnated Plastics Serving as Radio Wave Scattering Suppressors," *Ferrites: Proceedings of International Conference*, pp. 890-893.

Von Hippel, A., 1954, *Dielectrics and Waves*, M.I.T. Press, Cambridge, Massachusetts.

Von Hippel. A., 1957, *Tables of Dielectric Materials, Technical Report 119, MIT Laboratory for Insulation Research*, Vol. V.

Webman, I., Jortner, J., and Cohen, M., 1975, "Numerical Simulation of Electrical Conductivity in Microscopically Inhomogeneous Materials," *Physical Review B*, pp. 2885-2891.

Weir, W., 1974, "Automatic Measurement of Complex Dielectric Constant and Permeability at Microwave Frequencies," *Proceedings of IEEE*, Vol. 62, No. 1, pp. 33-36.

Table 1. Complex permittivity and complex permeability of polypropylene-iron composites at 2.4 GHz using the transmission/reflection technique at room temperature.

	Polypropylene and iron milled 2 hours				Polypropylene and iron milled 4 hours				Polypropylene and iron milled 20 hours			
% iron volume	Dielectric Constant	Electric Loss Factor	Permeability	Magnetic Loss Factor	Dielectric Constant	Electric Loss Factor	Permeability	Magnetic Loss Factor	Dielectric Constant	Electric Loss Factor	Permeability	Magnetic Loss Factor
0	2.10	0.00	1.00	0.00	2.10	0.00	1.00	0.00	2.10	0.00	1.00	0.00
5	3.08	0.02	0.99	0.09	2.66	0.02	1.06	0.11	3.29	0.02	1.04	0.09
10	4.38	0.15	1.03	0.17	3.94	0.04	1.18	0.15	5.06	0.05	1.24	0.29
15	6.73	0.24	1.11	0.31	7.44	0.25	1.14	0.35	8.17	0.23	1.42	0.54
20	13.44	1.22	1.13	0.51	12.92	0.99	1.28	0.48	17.44	2.42	1.71	0.77
25	20.55	3.92	1.16	0.58	26.25	6.02	1.29	0.74	28.90	8.94	2.20	1.10
30	23.43	7.21	1.37	0.58	37.78	12.82	1.30	0.88	32.26	9.55	2.96	1.67
35	46.66	21.16	1.55	0.99	74.96	59.52	2.46	1.42	37.25	10.11	2.66	1.37
40	79.10	101.29	2.27	1.40	63.90	43.07	2.69	1.89	64.14	50.91	4.06	1.88

Table 2. Maximum temperatures during heating in a multimode microwave cavity for polypropylene-iron composites (milled 2,4, 20 hours).

Iron Concentration (% volume)	Temperature (C) - (Highest temperature denoted with *)			Volume fraction after the percolation threshold is reached
	2 Hours	4 Hours	20 Hours	
5	XXXXXXX	30	36 *	
10	33	34	38 *	
15	38	42 *	39	
20	42	45	46 *	
25	48	48	57 *	Samples milled 20 hours
30	48	51	58 *	
35	56	74 *	64	Samples milled 4 hours
40	93 *	81	60	Samples milled 2 hours

Table 3. Dielectric properties of 1071/1061M epoxy-amine system at 2.5 and 9 GHz using the perturbation technique at room temperature.

	Perturbation Technique (2.5 GHz)		Perturbation Technique (9 GHz)	
% cure	Dielectric Constant	Loss Factor	Dielectric Constant	Loss Factor
Epoxy	3.25	0.254	2.92	0.1565
Amine	2.77	0.009	2.60	0.0095
26.2	2.99	0.108	2.70	0.088
31.9	2.92	0.114	2.76	0.086
34.4	3.28	0.140	2.69	0.074
38.3	3.19	0.143	2.67	0.072
44.6	3.11	0.124	2.69	0.095
58.8	2.87	0.115	2.69	0.092
71.8	2.77	0.108	2.72	0.094
85.5	3.02	0.098	2.62	0.065
88.9	2.68	0.077	2.51	0.066
89.0	2.76	0.078	2.47	0.058
89.7	2.63	0.075	2.62	0.064
89.7	2.86	0.087	2.55	0.066
90.7	2.85	0.086	2.56	0.065
92.2	2.67	0.078	2.66	0.065
93.1	2.64	0.075	2.60	0.064

Table 4. Dielectric properties of various carbon-black-filled perfluoroelastomers, at 2.5 GHz using both the perturbation and transmission/reflection techniques at room temperature.

			Perturbation Technique		Transmission/Reflection Technique	
Compound Name	Carbon Black Type	C.B. Loading (% Volume)	Dielectric Constant	Loss Factor	Dielectric Constant	Loss Factor
2000	Neat	0	2.06	0.00205		
4000	Neat	0	2.01	0.0023		
5000	Neat	0	2.075	0.004		
A	Type 1	8.3	3.745	0.12	3.255	0.1475
B	Type 1	11.7	5.05	0.625	4.77	0.2475
C	Type 1	11.6	4.315	0.2385	4.235	0.191
E	Type 1	11.9	4.985	0.633	4.44	0.453
F	Type 1	11.9	8.945	3.44	4.775	0.1965
G	Type 2	13.7	3.4	0.053	4.115	0.0655
H	Type 2	13.7	3.68	0.1705	3.72	0.177

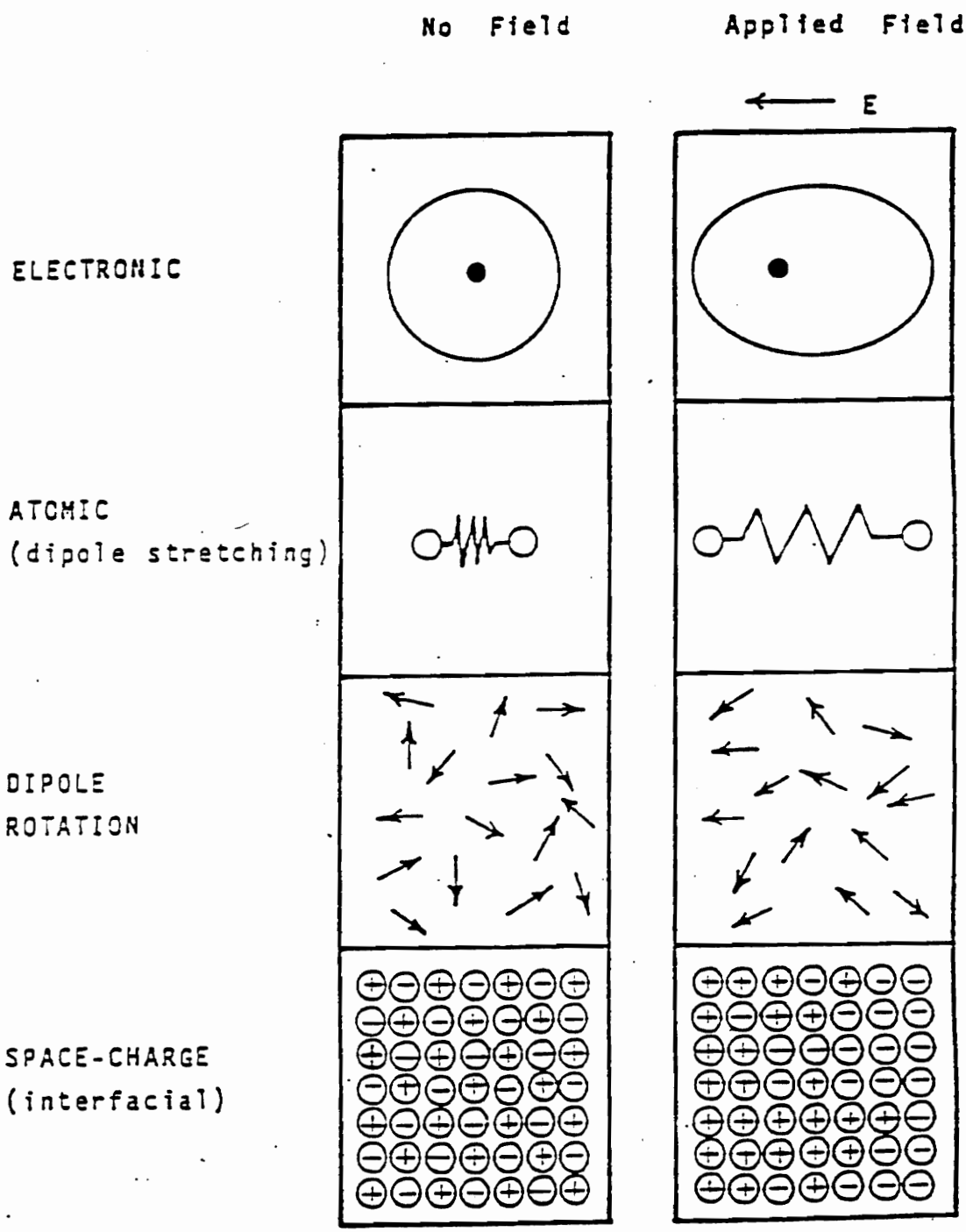

Figure 1. Mechanisms of polarization by an electric field (Von Hippel, 1954).

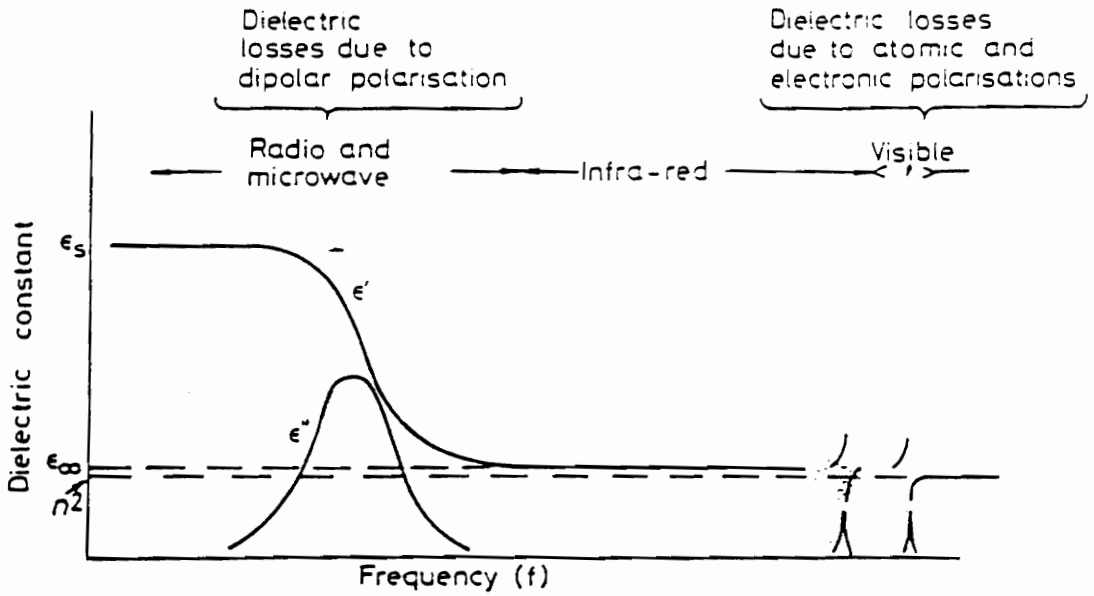

Figure 2. Dielectric properties of a typical polymer in the frequency domain (Metaxas and Meredith, 1983).

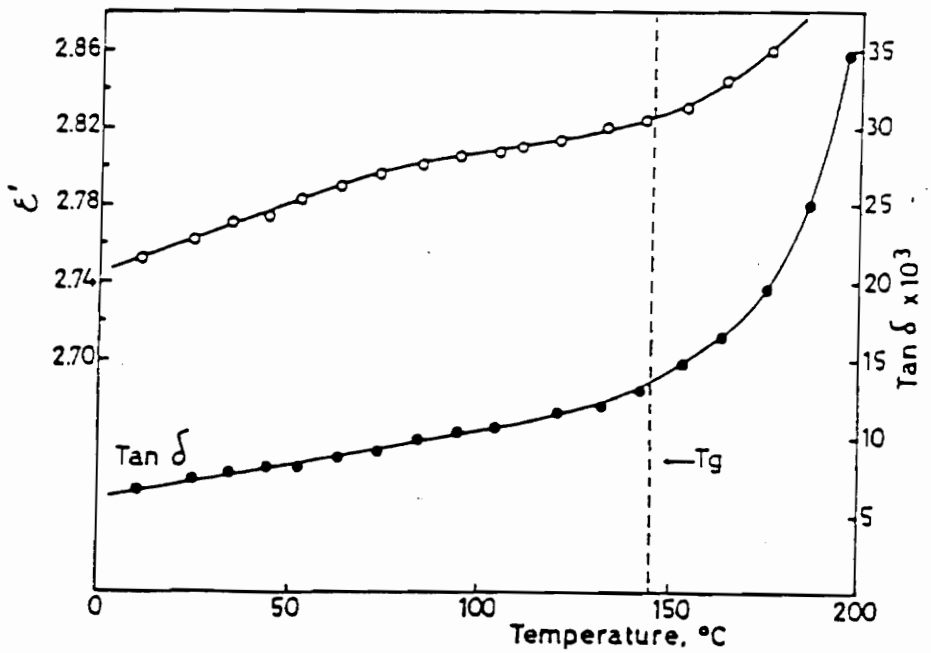

Figure 3. Dielectric properties of a typical polymer at microwave frequencies as a function of temperature (Frosini and Butta, 1967).

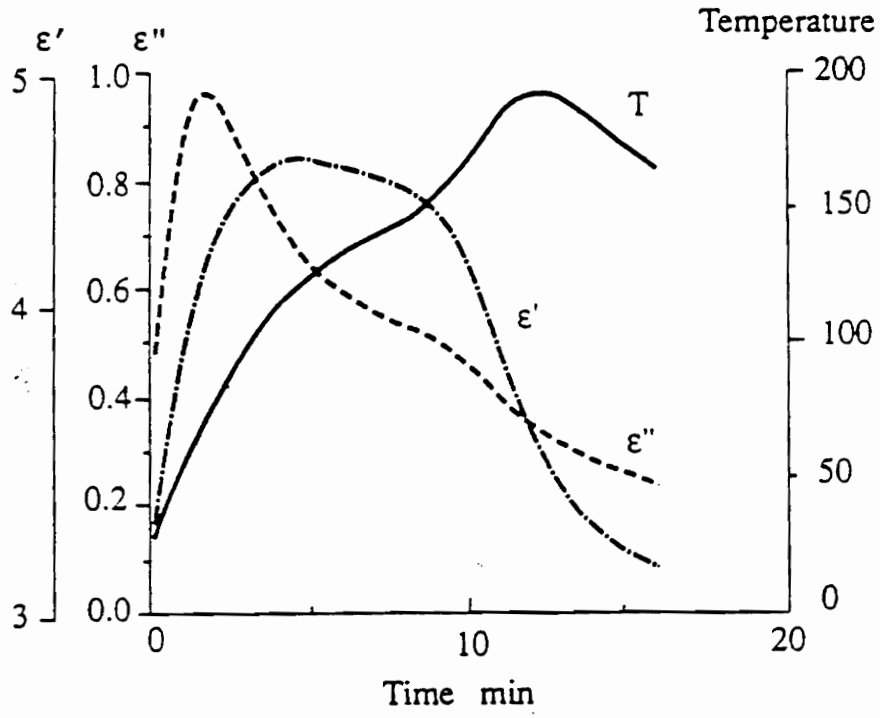

Figure 4. Variation of the dielectric properties of an epoxy system during cure (Delmotte et al., 1991).

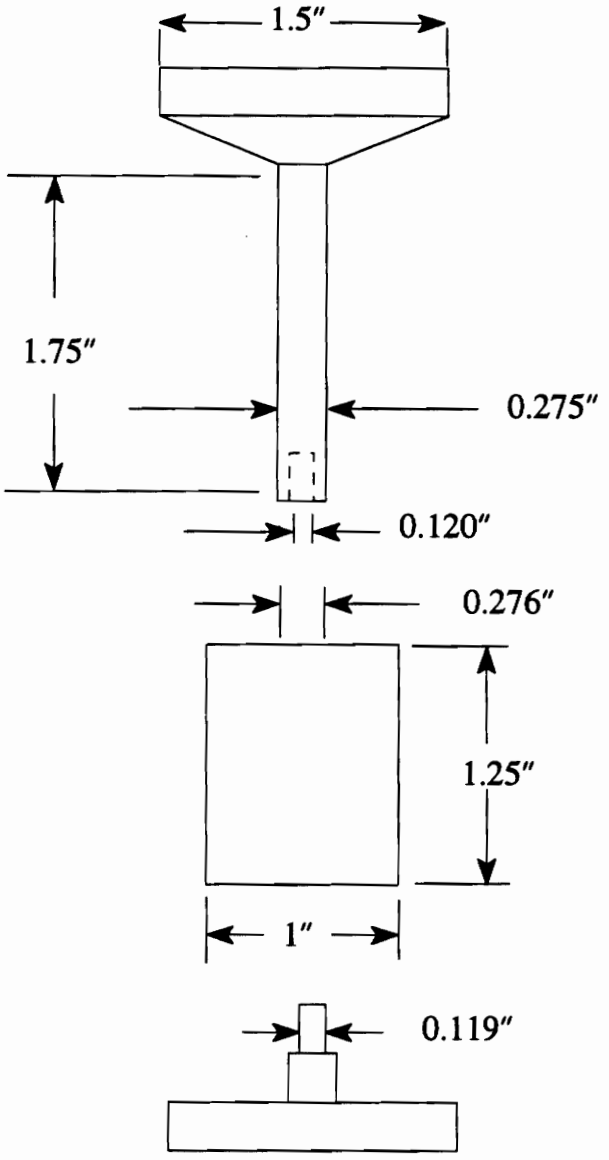

Figure 5. Steel mold used for pressing polypropylene-iron test specimens.

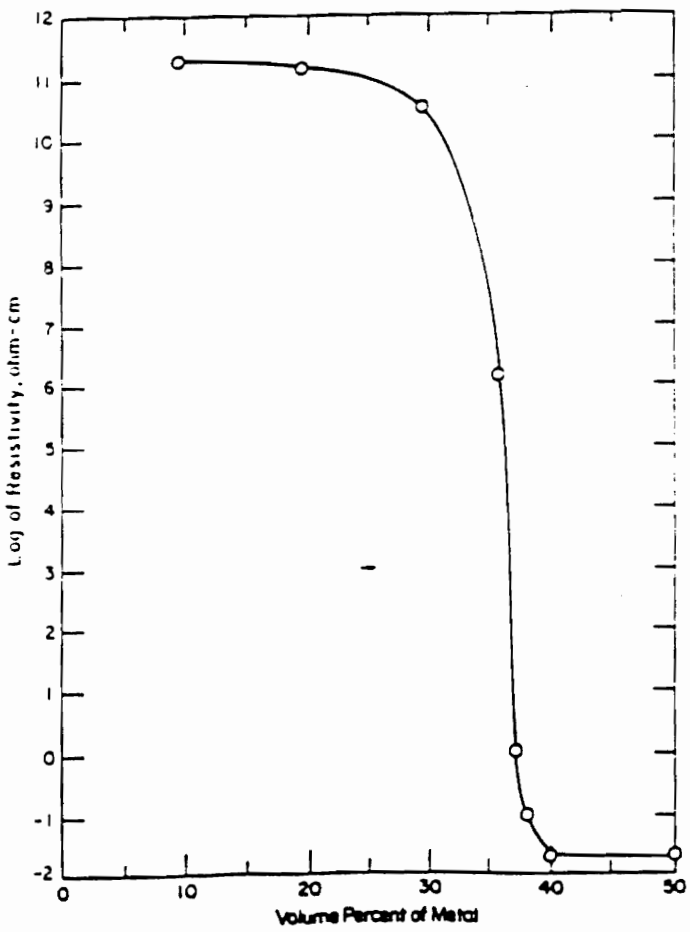

Figure 6. Percolation curve for a representative metal-filled polymer system (Gurland, 1966).

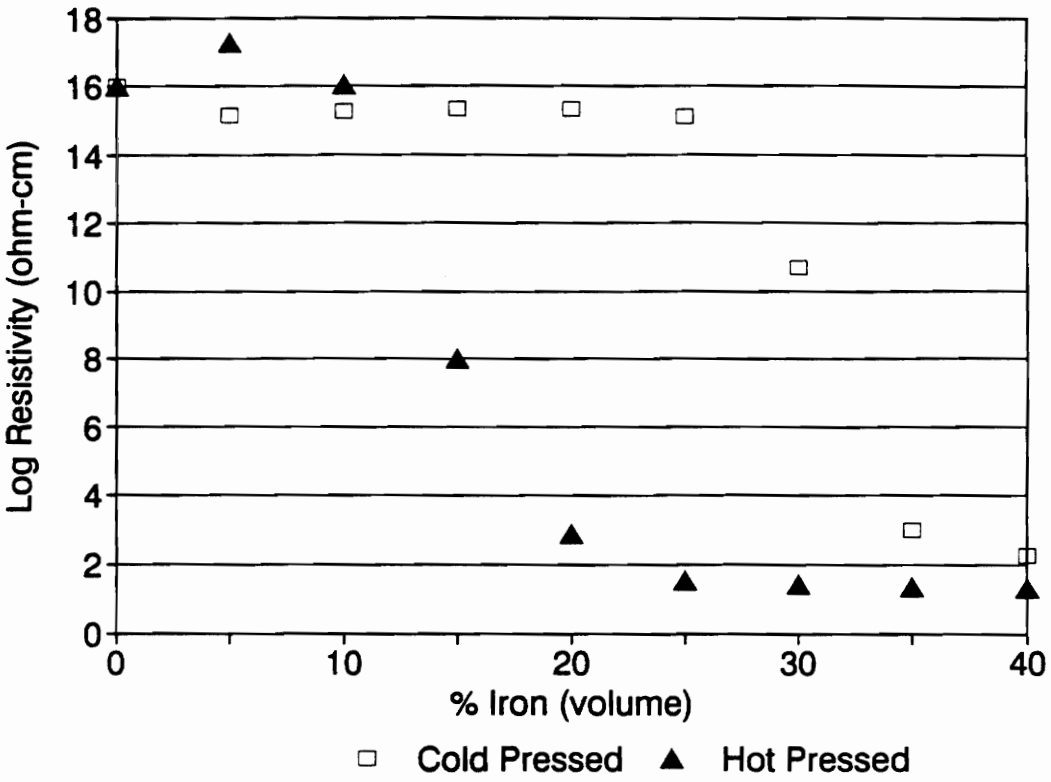

Figure 7. Resistivity of hot pressed and cold pressed polypropylene-iron composites.

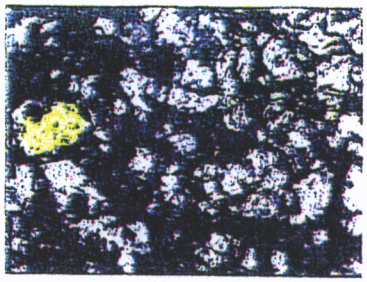

(a)

(b)

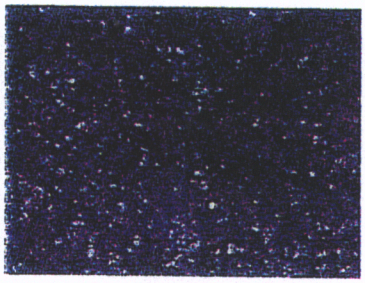

(c)

Figure 8. Photomicrographs of polypropylene-iron composites (40% iron by volume), milled for various times: (a) 2 hours; (b) 4 hours; (c) 20 hours. (Magnification x177)

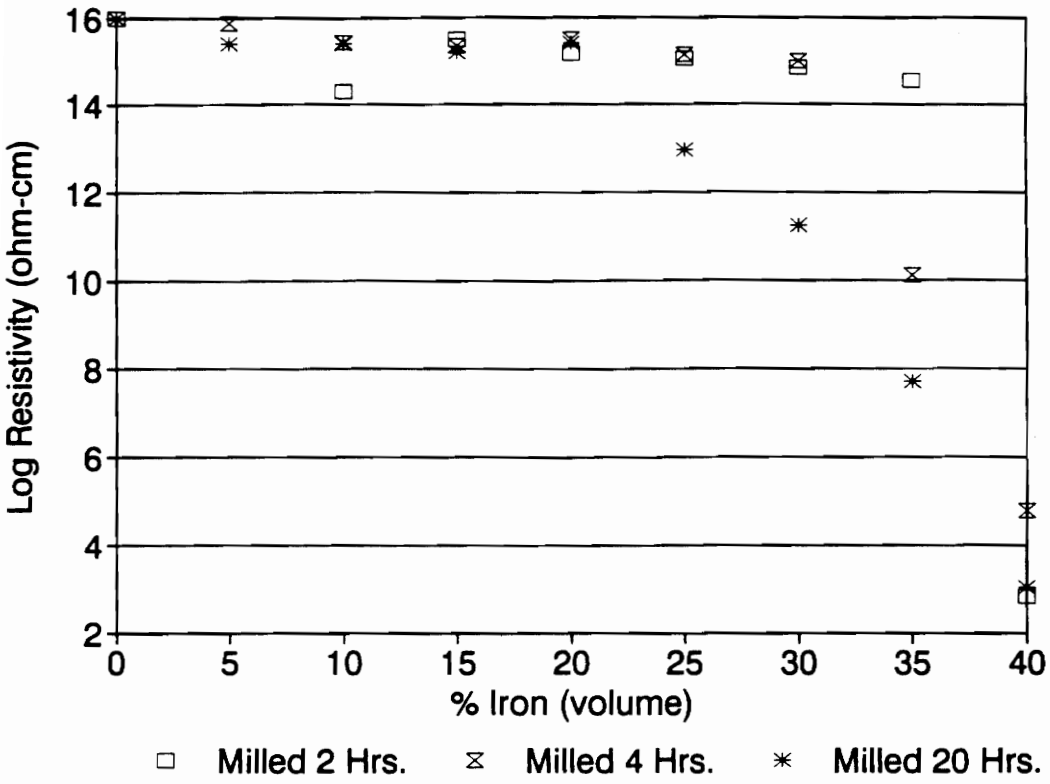

Figure 9. Resistivity measurements of polypropylene-iron composites for three milling times.

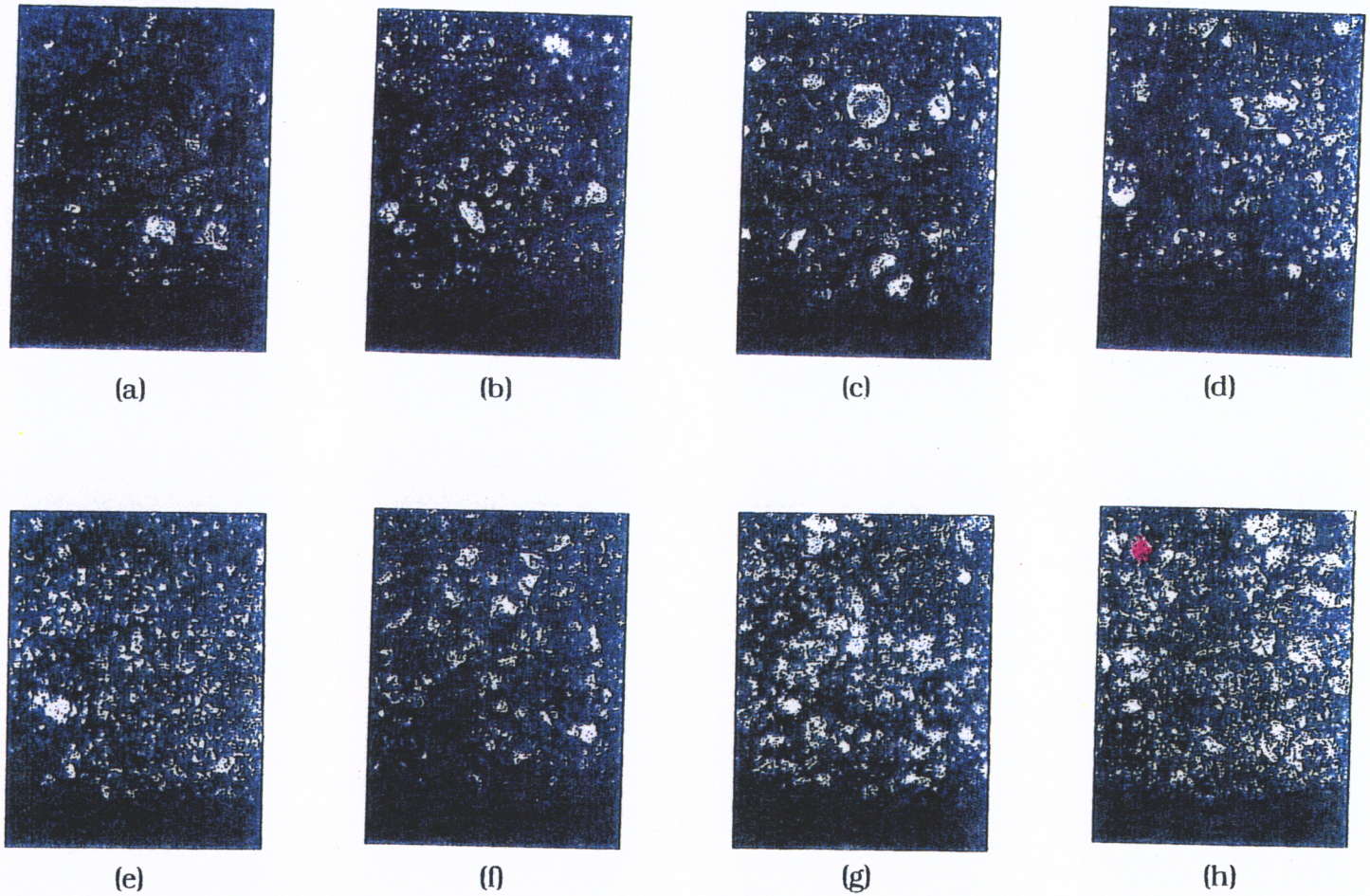

Figure 10. Photomicrographs of polypropylene-iron composites milled for 2 hours at various iron concentrations (% by volume): (a) 5; (b) 10; (c) 15; (d) 20; (e) 25; (f) 30; (g) 35; (h) 40. (Magnification x88.5)

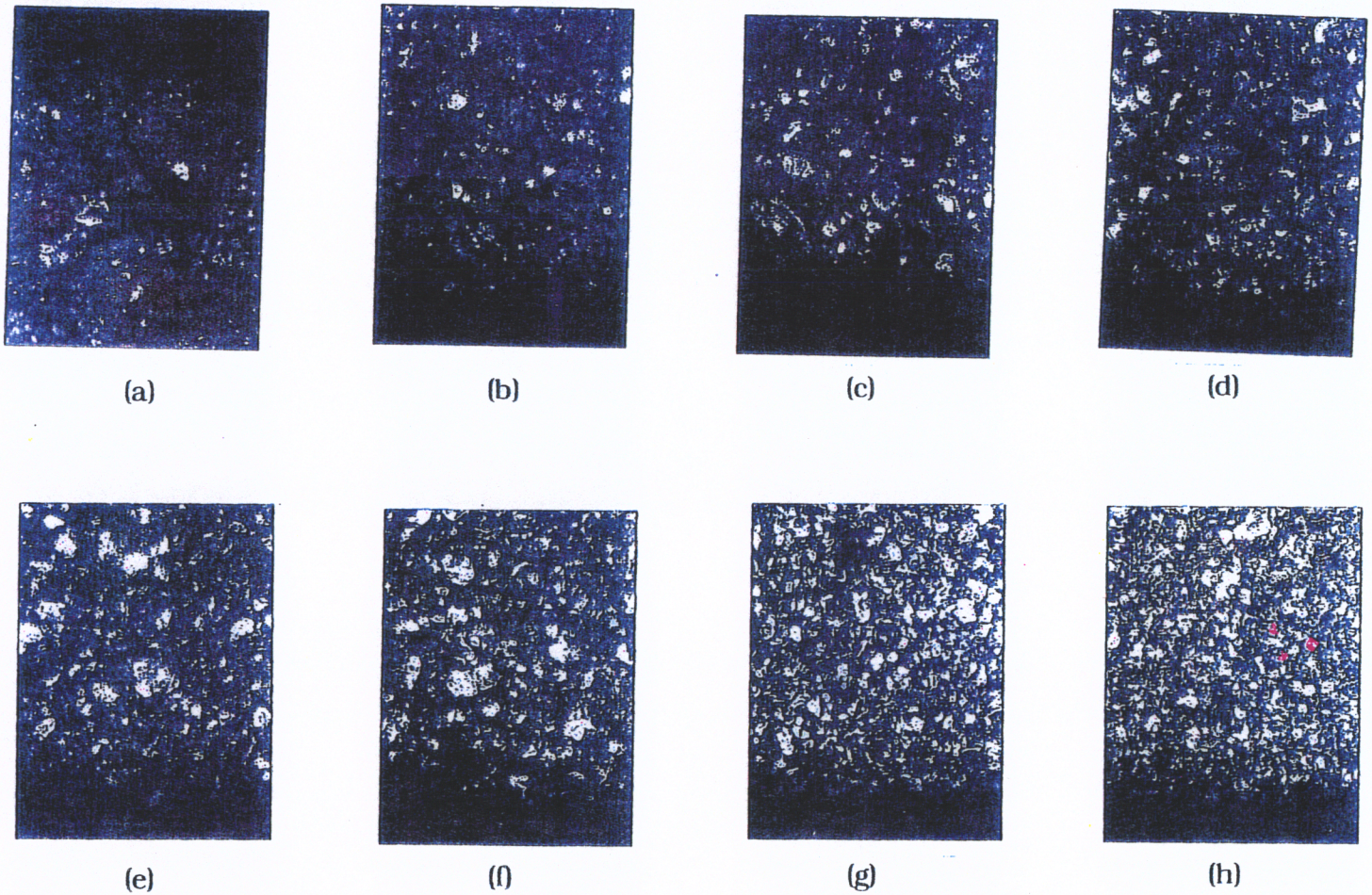

Figure 11. Photomicrographs of polypropylene-iron composites milled for 4 hours at various iron concentrations (% by volume): (a) 5; (b) 10; (c) 15; (d) 20; (e) 25; (f) 30; (g) 35; (h) 40. (Magnification x88.5)

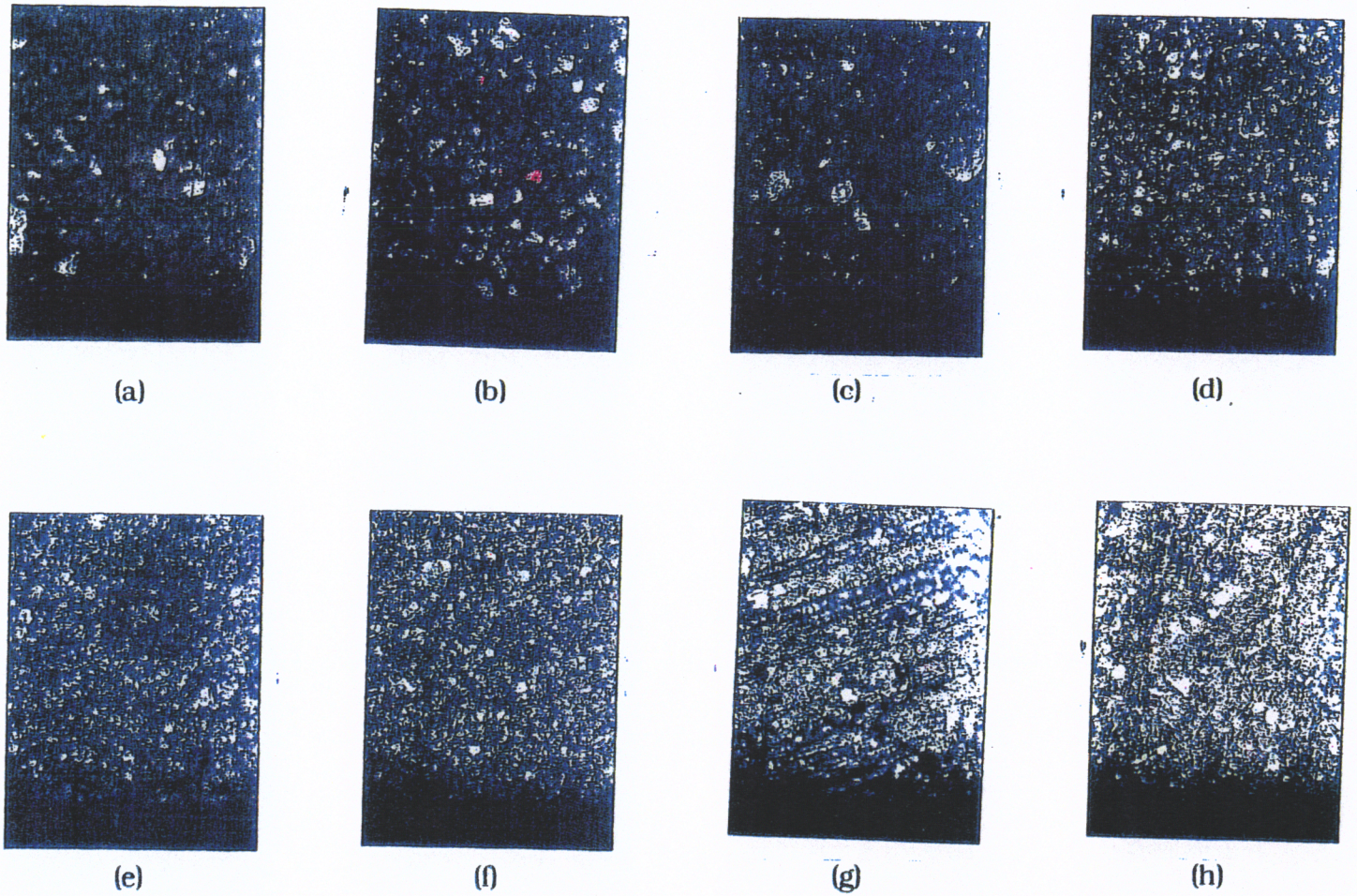

Figure 12. Photomicrographs of polypropylene-iron composites milled for 20 hours at various iron concentrations (% by volume): (a) 5; (b) 10; (c) 15; (d) 20; (e) 25; (f) 30; (g) 35; (h) 40. (Magnification x88.5)

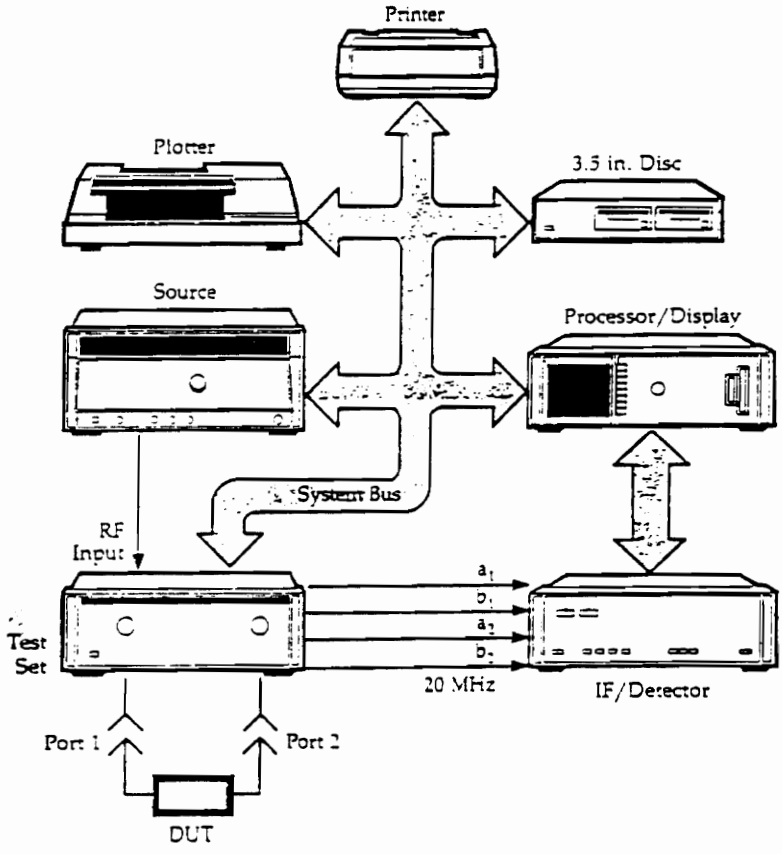

Figure 13. Schematic of the dielectric property measurement system using an HP 8510B network analyzer (HP Product Note 10).

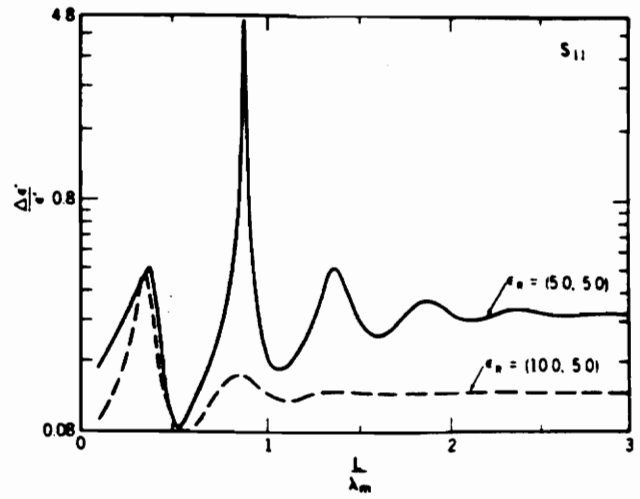

(a)

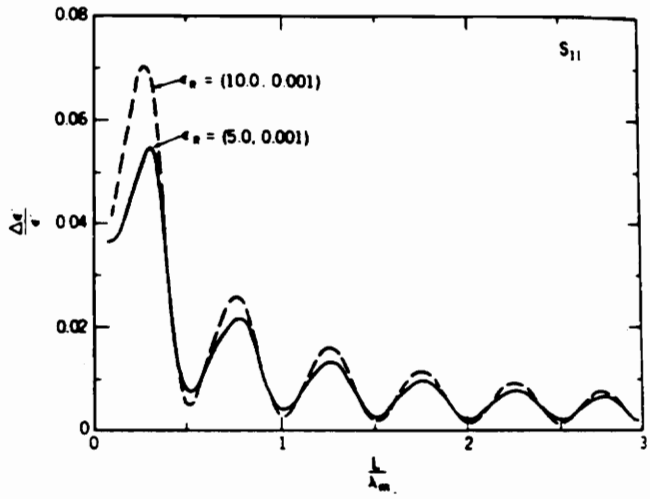

(b)

Figure 14. Uncertainty analysis for transmission/reflection technique for a) high loss (loss factor) and b) low loss (dielectric constant) materials (Jarvis, 1990).

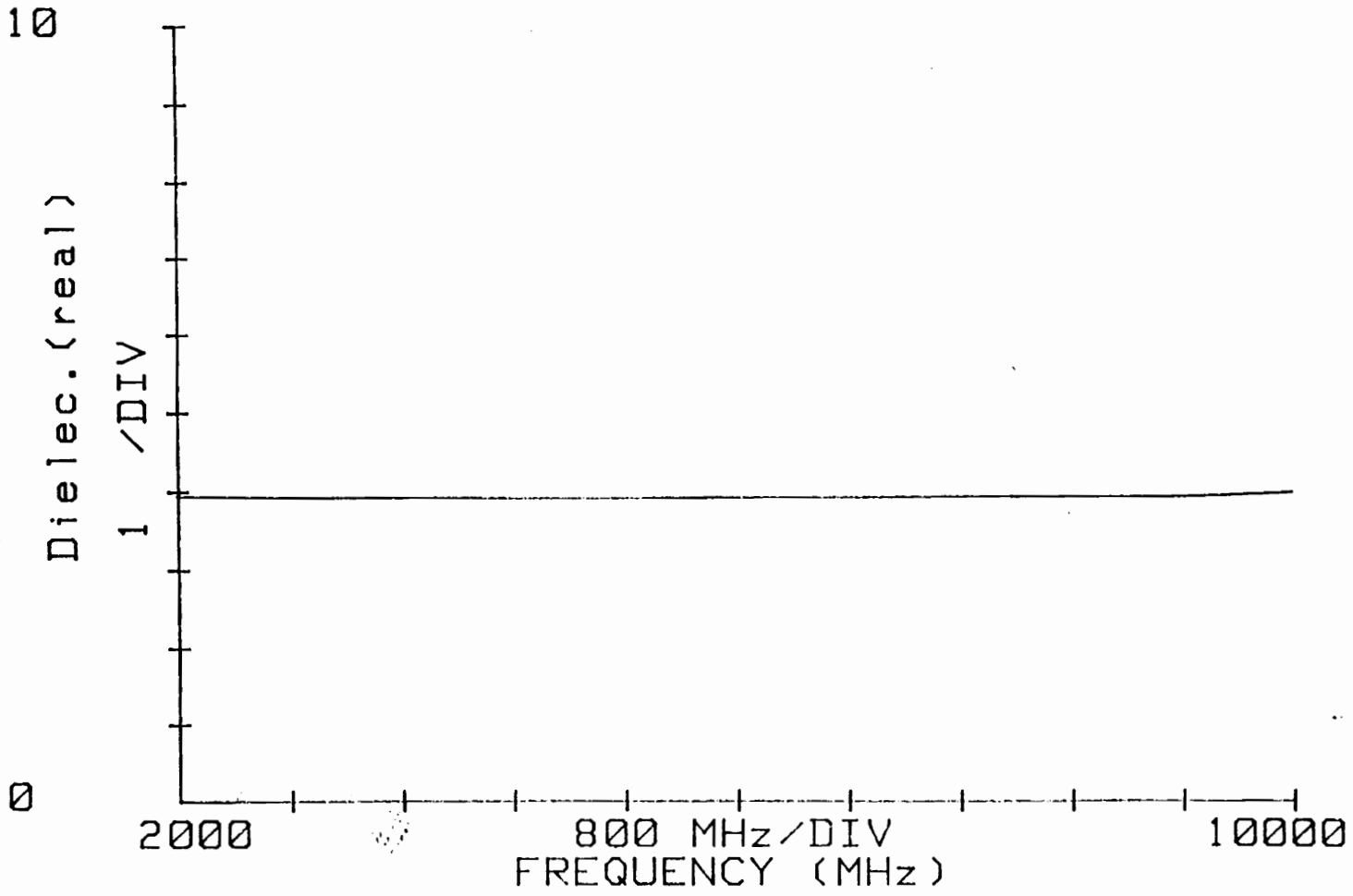

Figure 15. Dielectric constant of polypropylene-iron (10% iron by volume) composite over the frequency range 2-10 GHz.

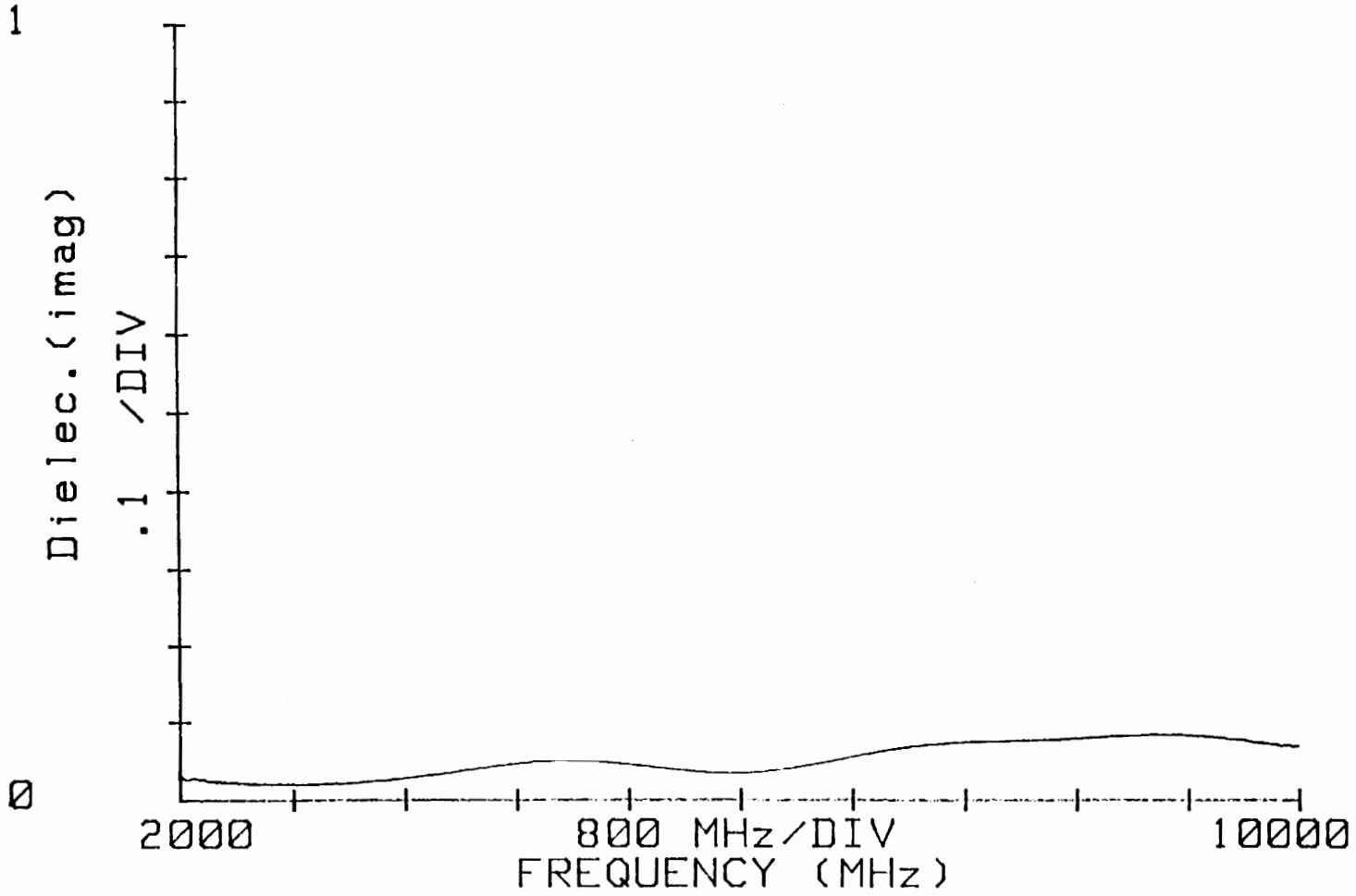

Figure 16. Electric loss factor of polypropylene-iron (10% iron by volume) composite over the frequency range 2-10 GHz.

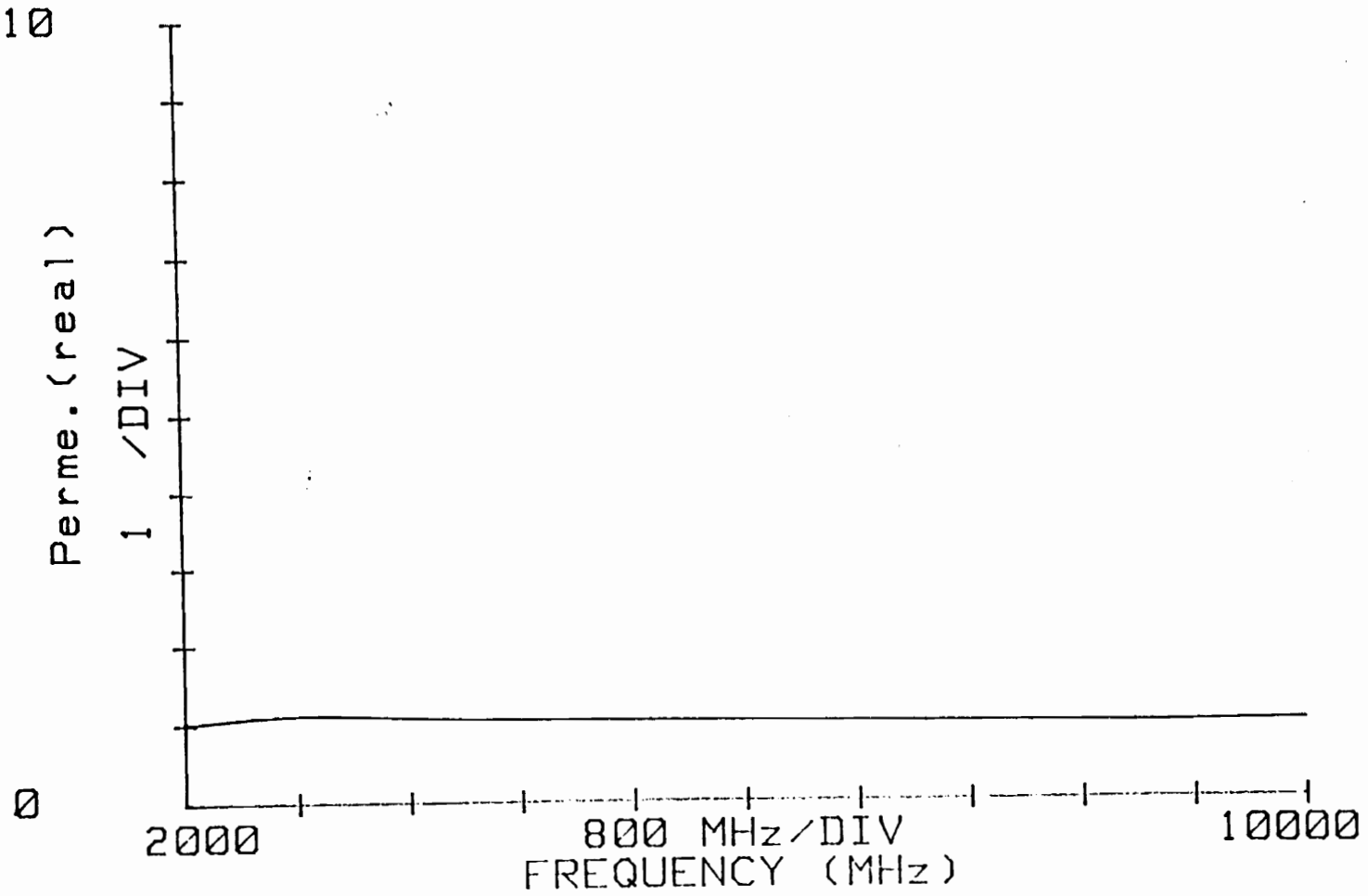

Figure 17. Permeability of polypropylene-iron (10% iron by volume) composite over the frequency range 2-10 GHz.

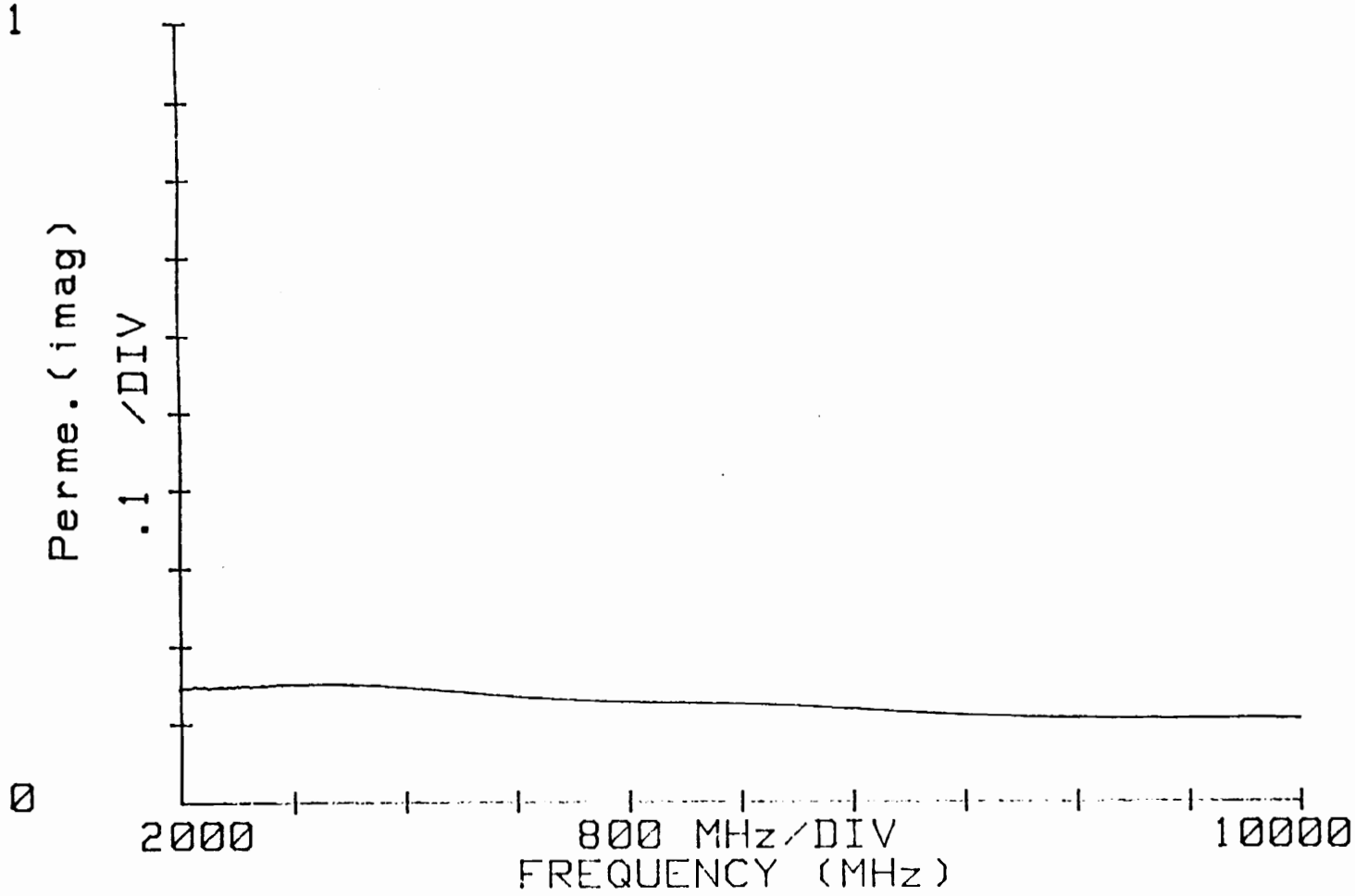

Figure 18. Magnetic loss factor of polypropylene-iron (10% iron by volume) composite over the frequency range 2-10 GHz.

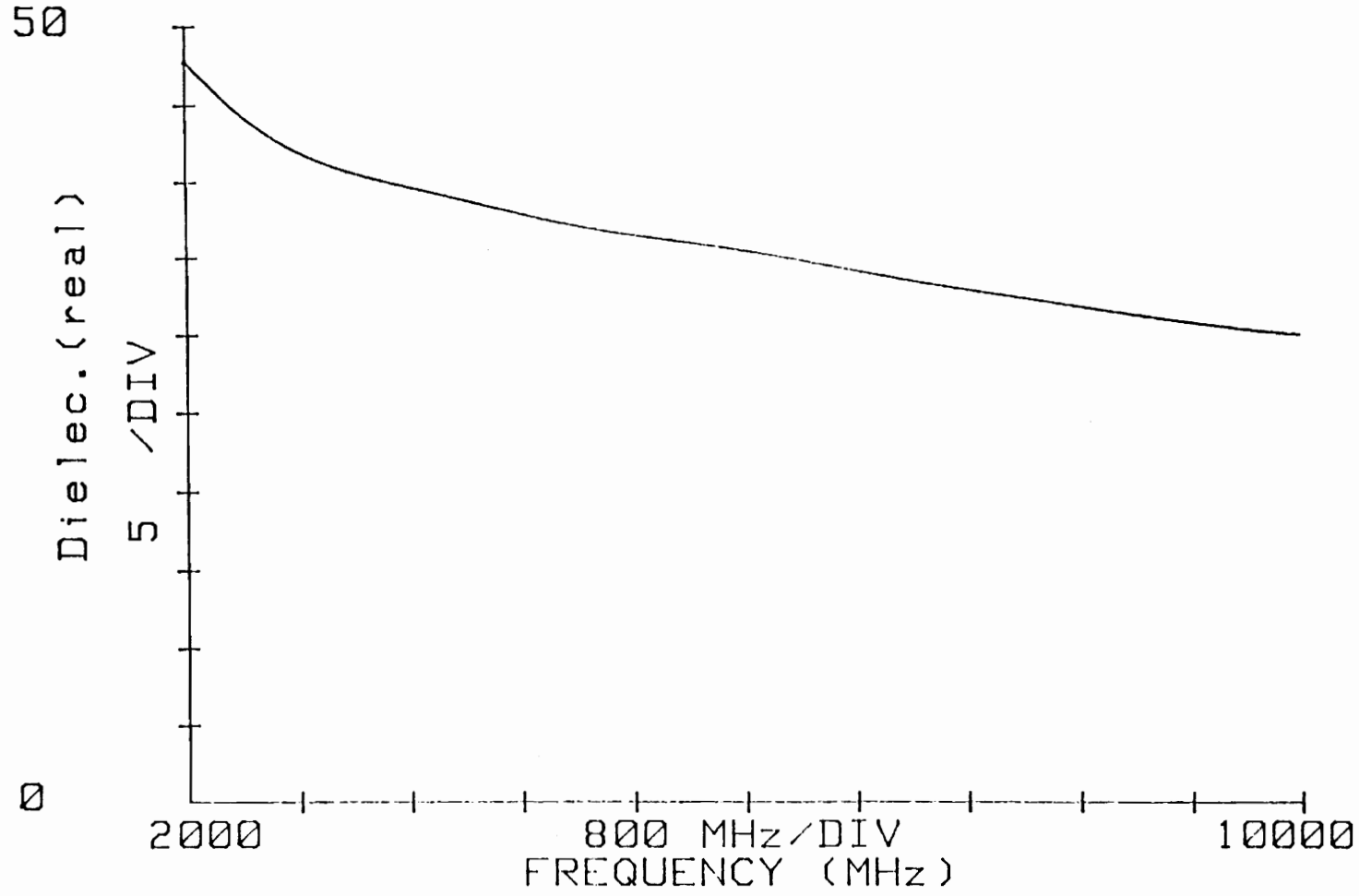

Figure 19. Dielectric constant of polypropylene-iron (30% iron by volume) composite over the frequency range 2-10 GHz.

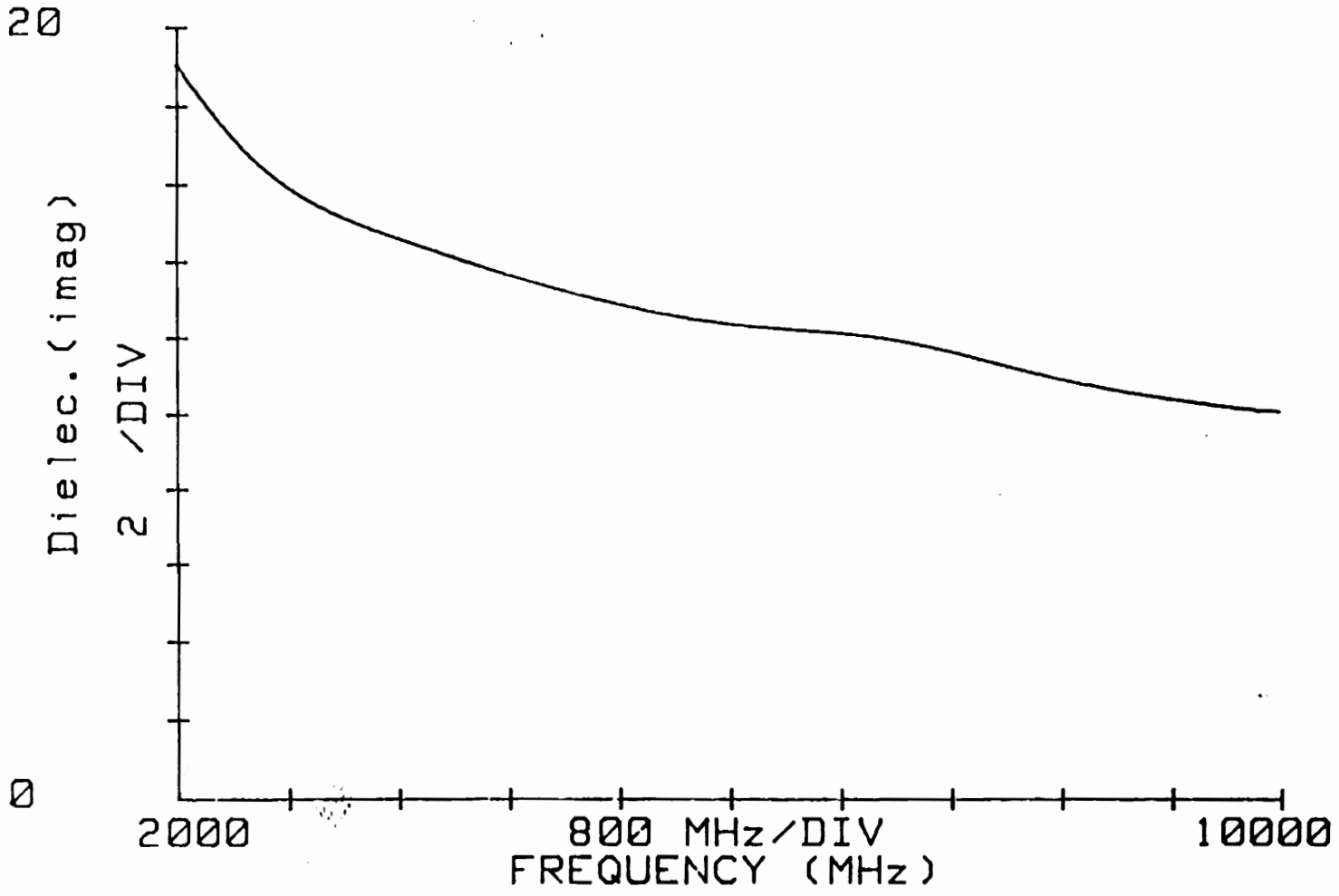

Figure 20. Electric loss factor of polypropylene-iron (30% iron by volume) composite over the frequency range 2-10 GHz.

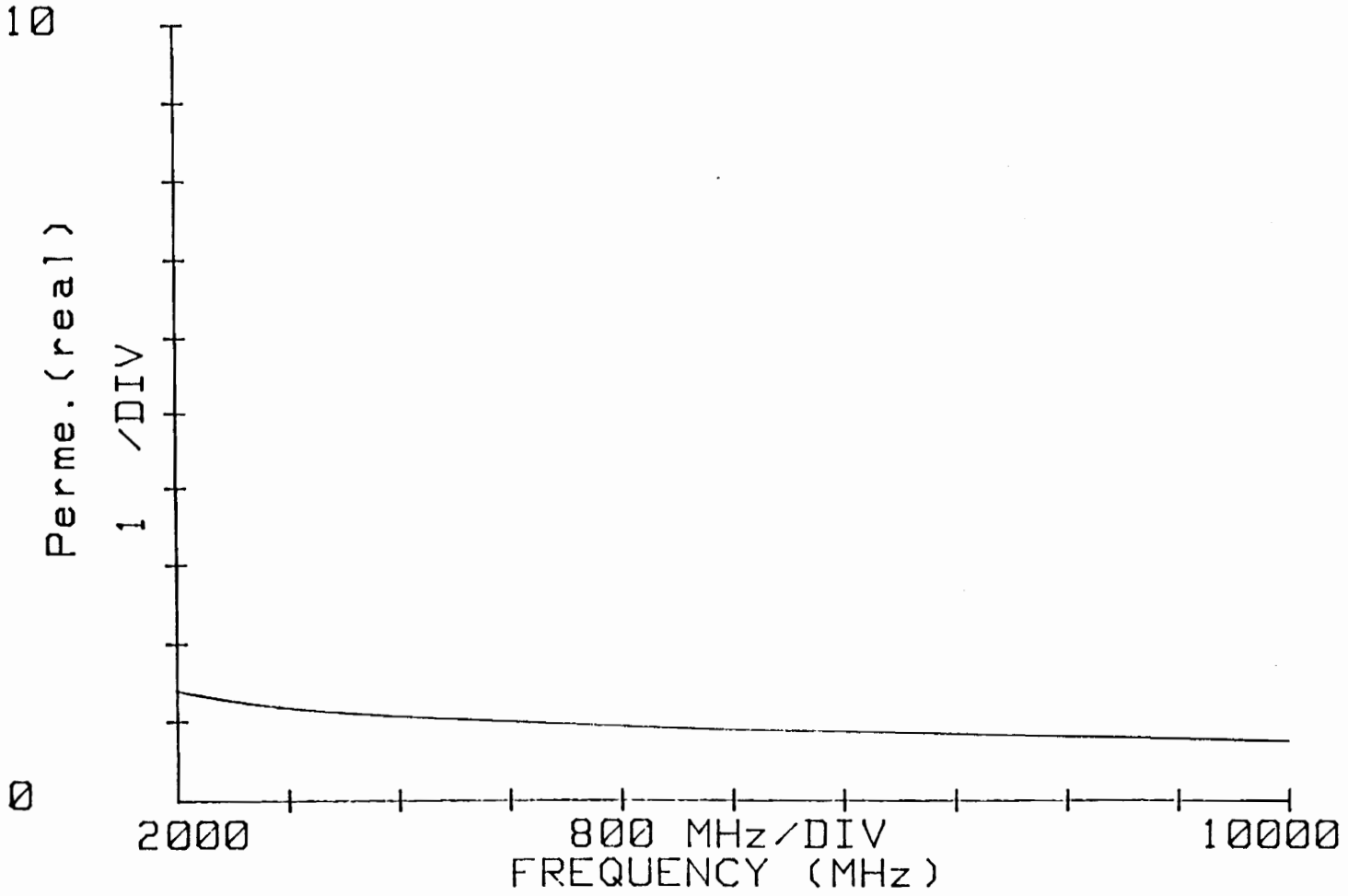

Figure 21. Permeability of polypropylene-iron (30% iron by volume) composite over the frequency range 2-10 GHz.

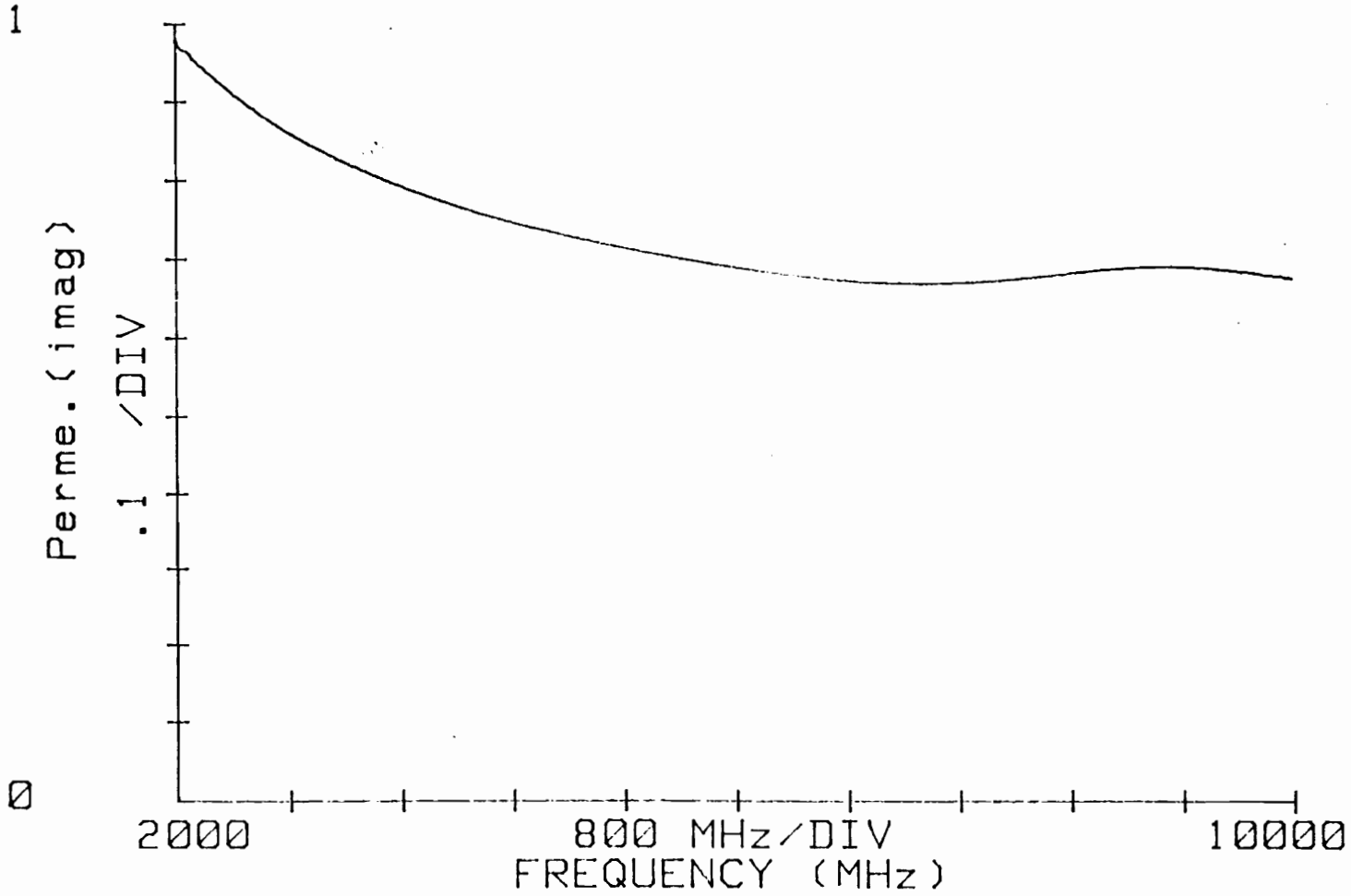

Figure 22. Magnetic loss factor of polypropylene-iron (30% iron by volume) composite over the frequency range 2-10 GHz.

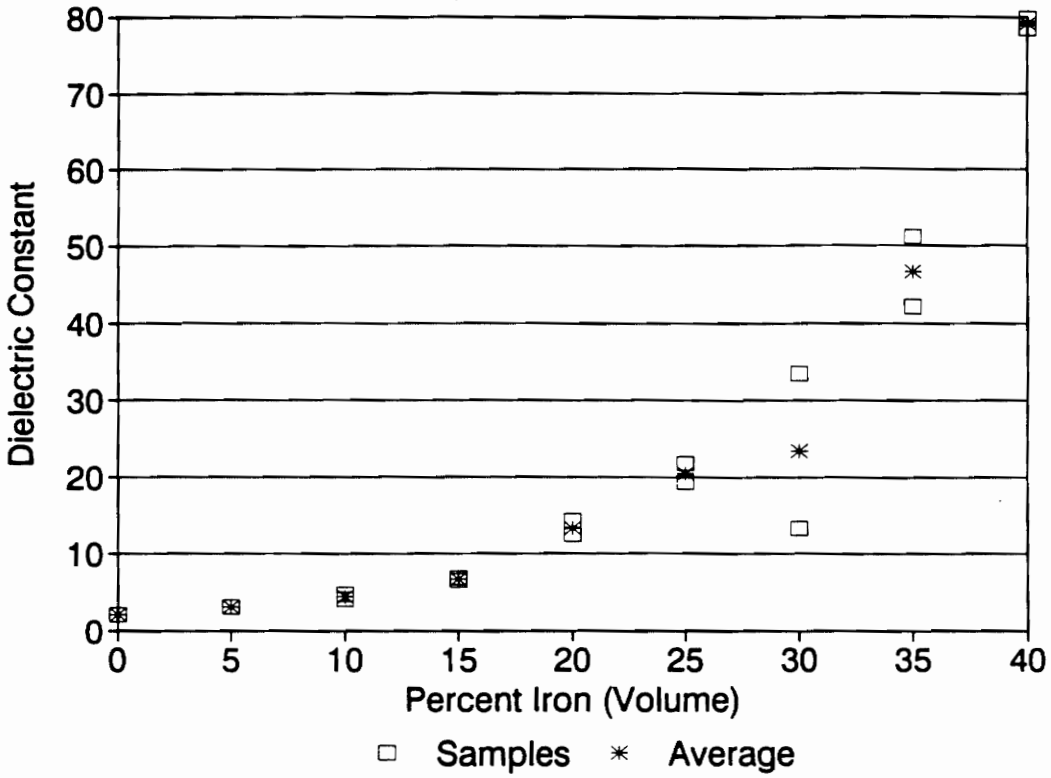

Figure 23. Dielectric constant at 2400 MHz for polypropylene-iron composites milled for 2 hours.

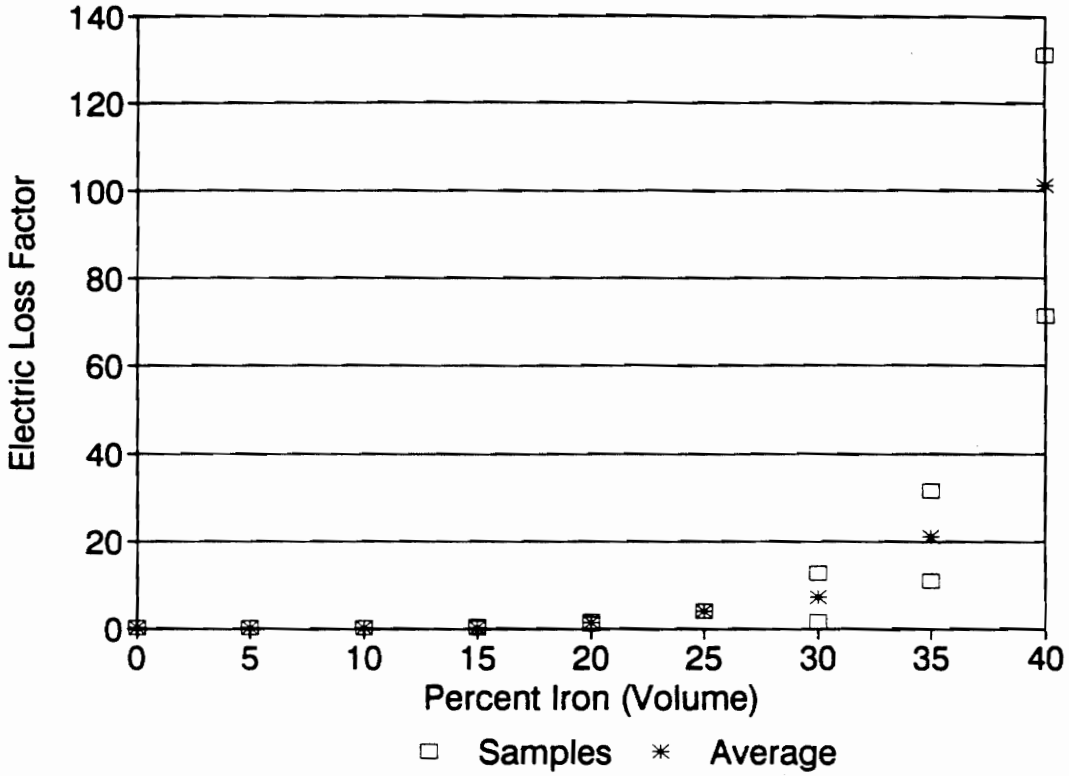

Figure 24. Electric loss factor at 2400 MHz for polypropylene-iron composites milled for 2 hours.

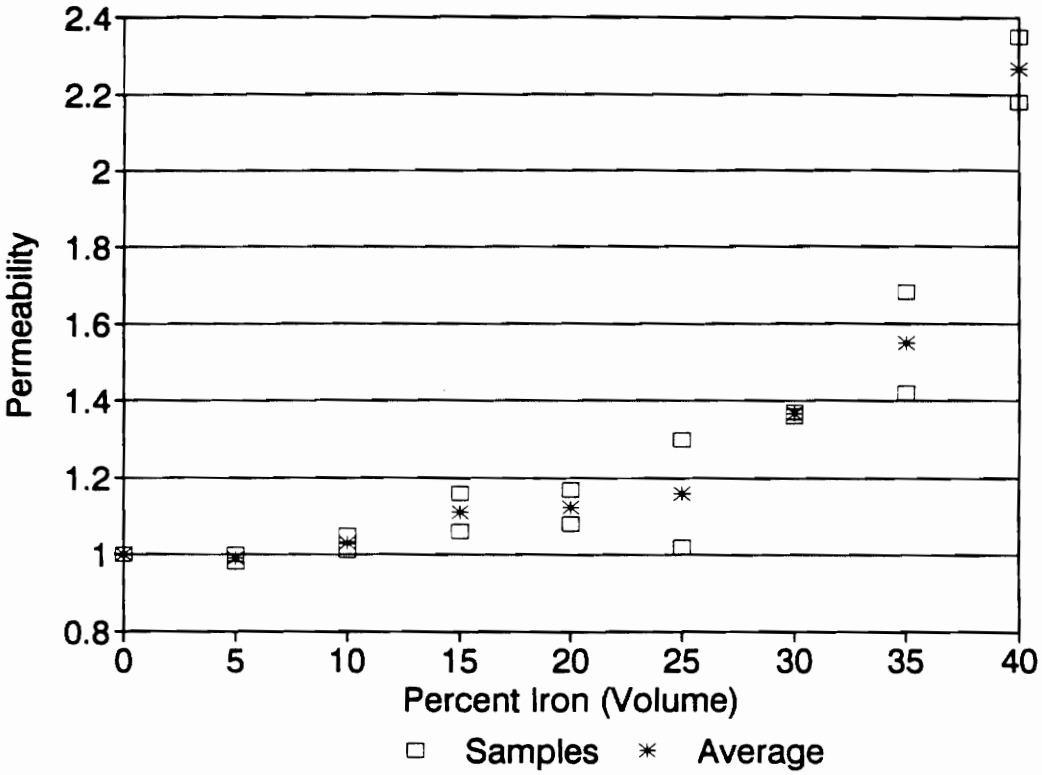

Figure 25. Permeability at 2400 MHz for polypropylene-iron composites milled for 2 hours.

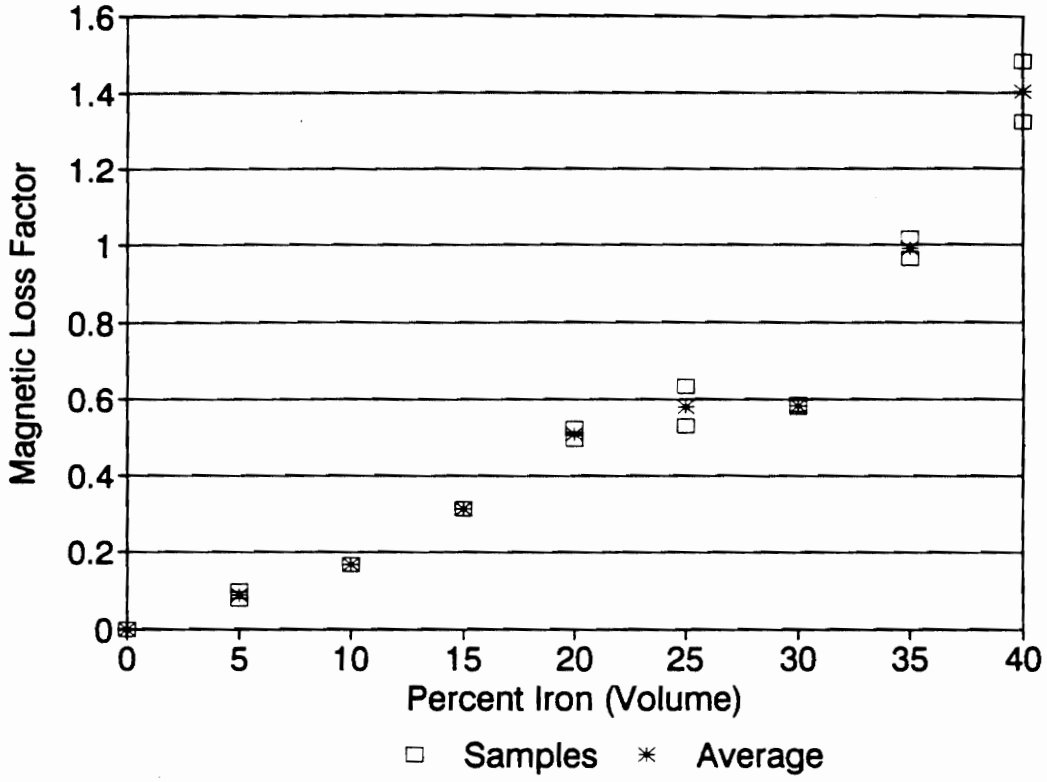

Figure 26. Magnetic loss factor at 2400 MHz for polypropylene-iron composites milled for 2 hours.

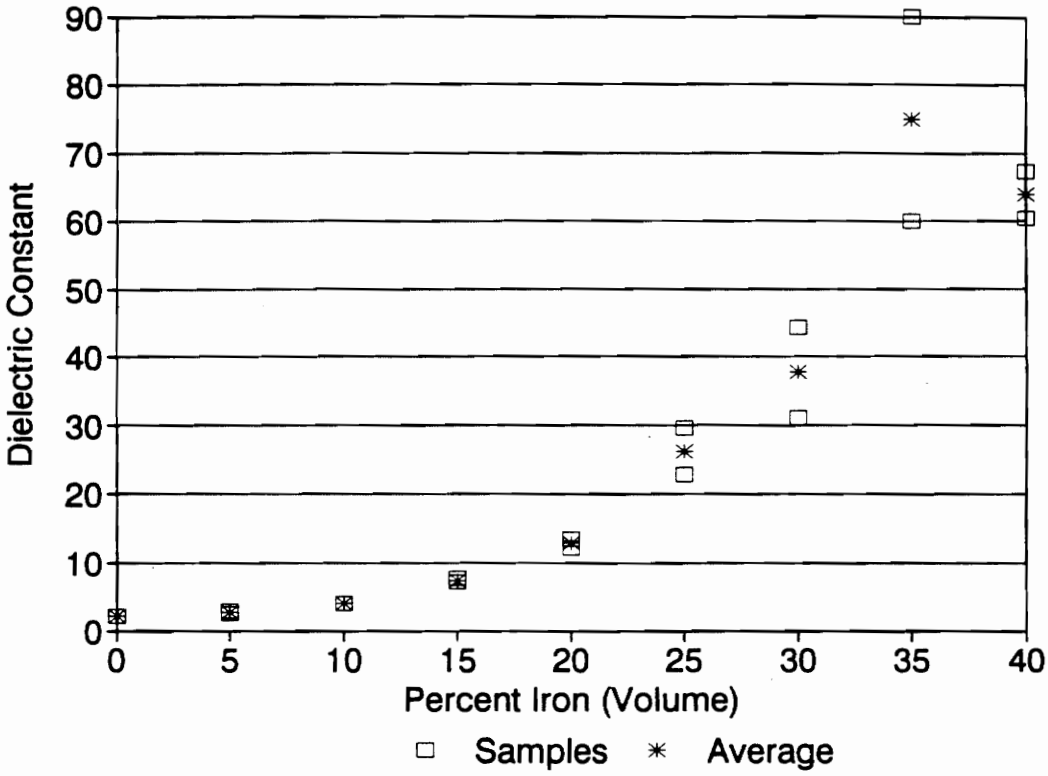

Figure 27. Dielectric constant at 2400 MHz for polypropylene-iron composites milled for 4 hours.

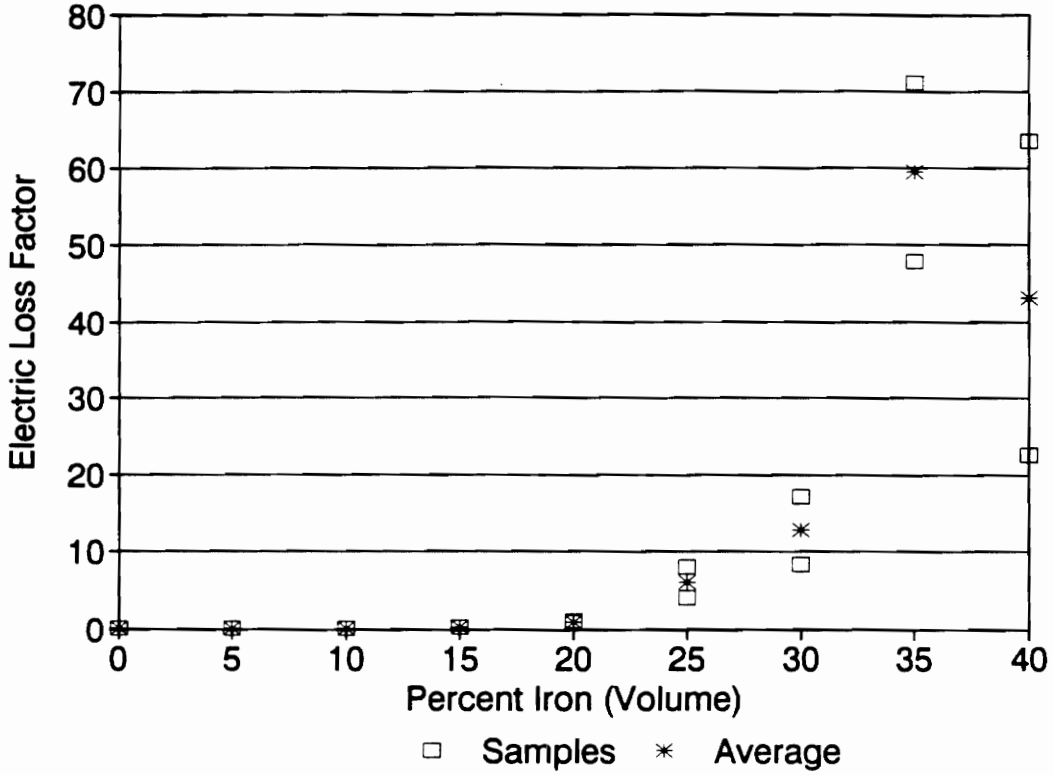

Figure 28. Electric loss factor at 2400 MHz for polypropylene-iron composites milled for 4 hours.

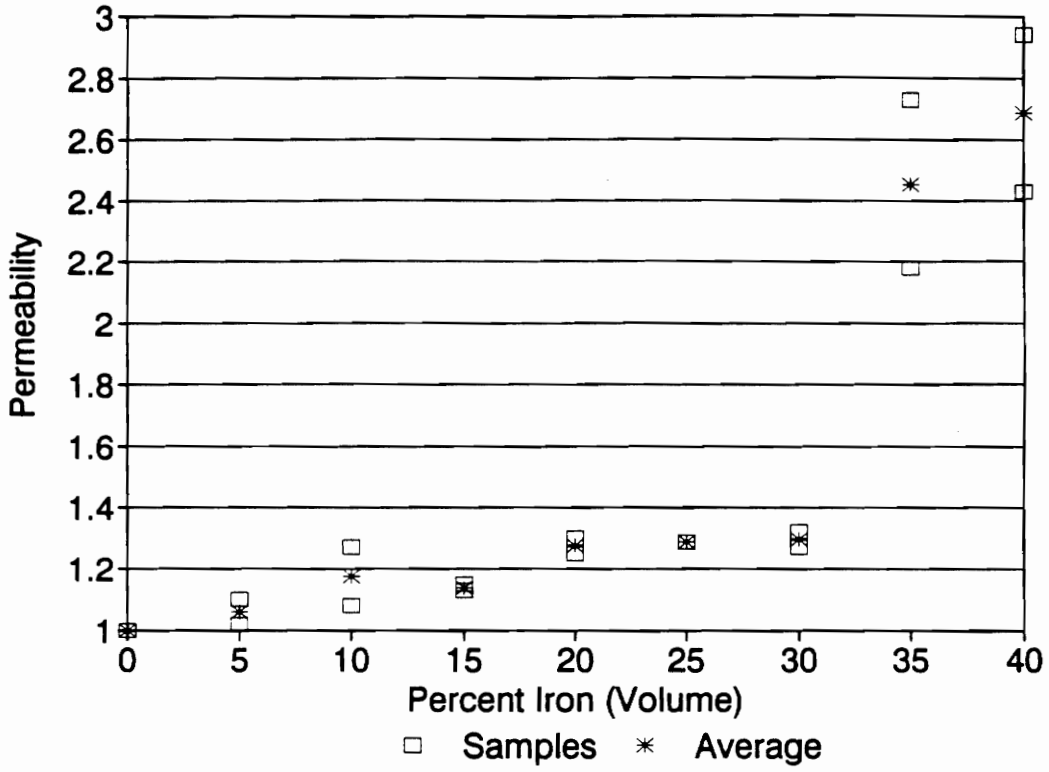

Figure 29. Permeability at 2400 MHz for polypropylene-iron composites milled for 4 hours.

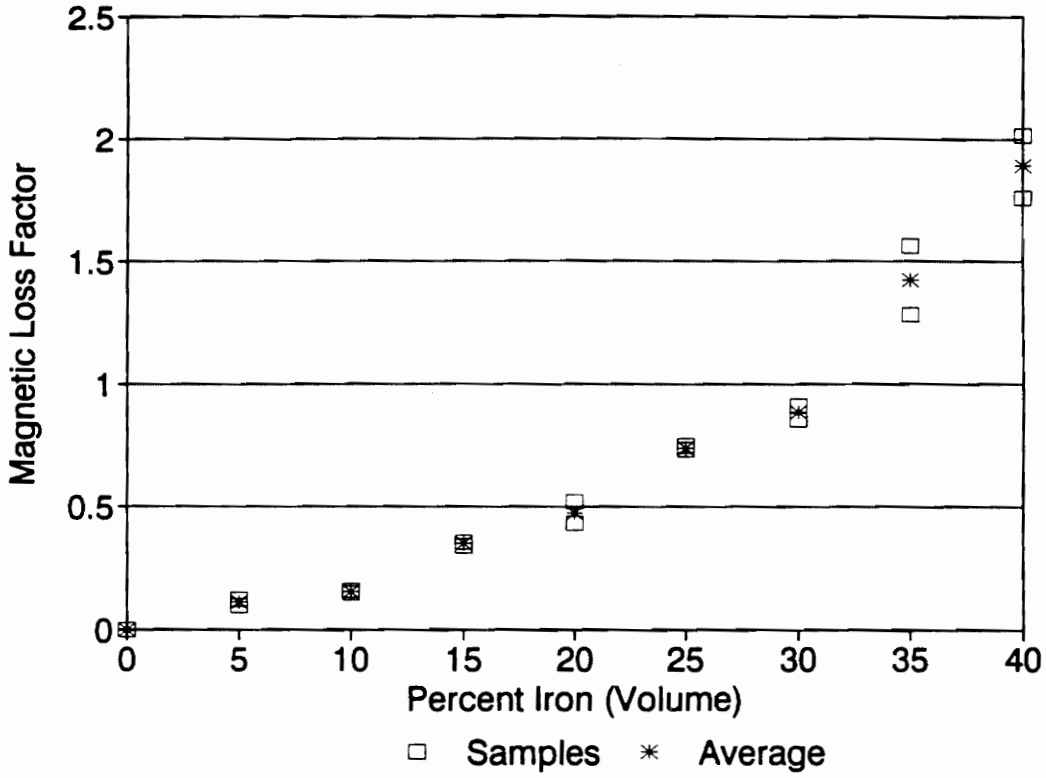

Figure 30. Magnetic loss factor at 2400 MHz for polypropylene-iron composites milled for 4 hours.

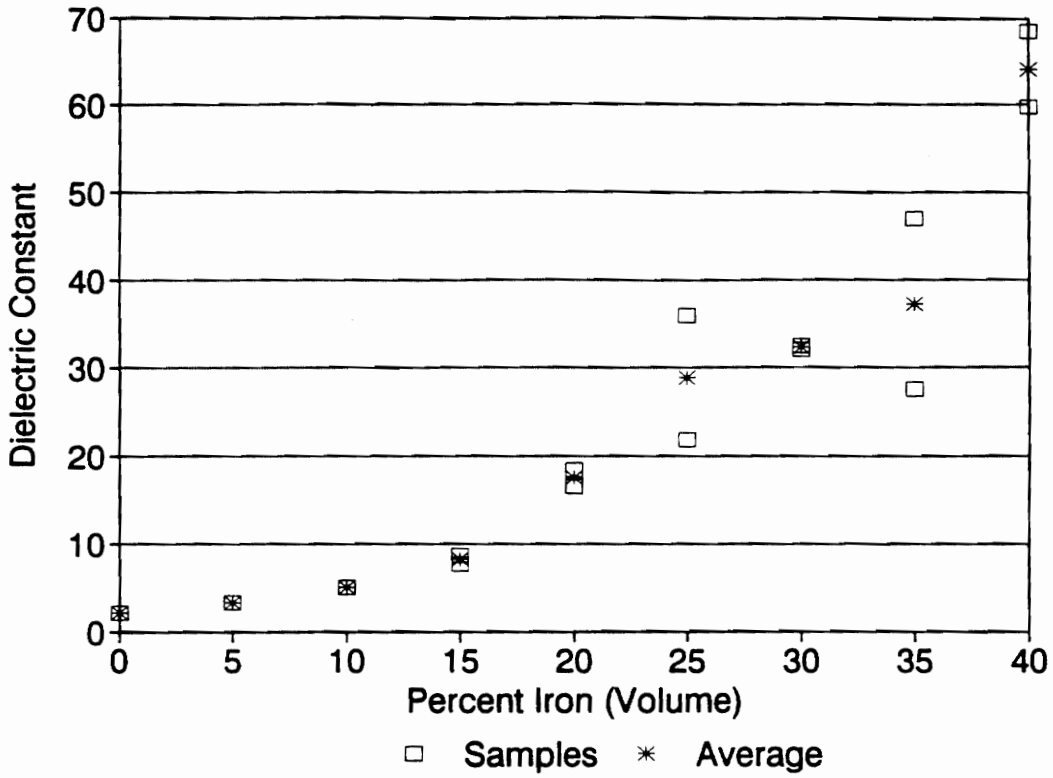

Figure 31. Dielectric constant at 2400 MHz for polypropylene-iron composites milled for 20 hours.

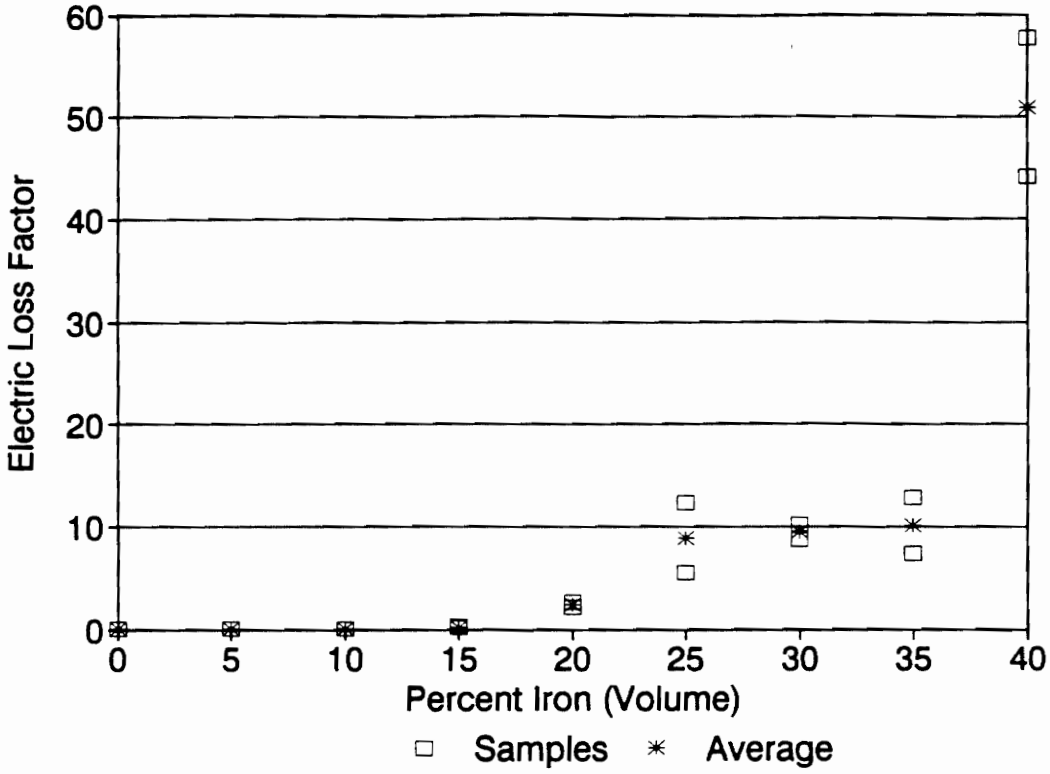

Figure 32. Electric loss factor at 2400 MHz for polypropylene-iron composites milled for 20 hours.

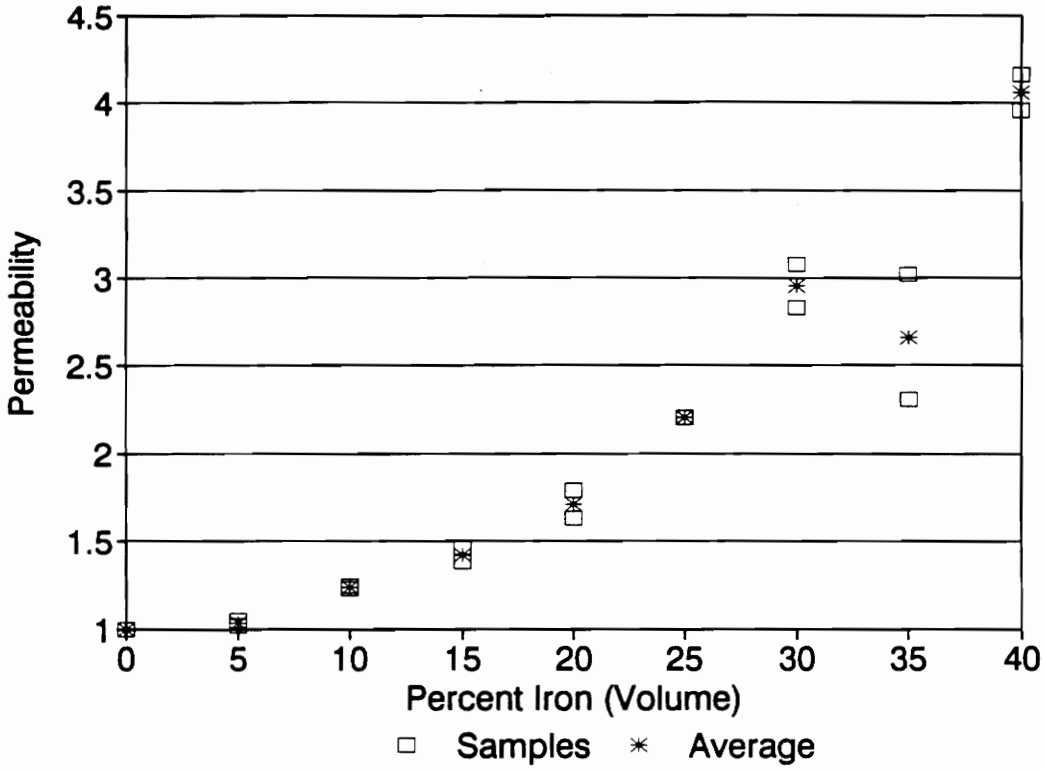

Figure 33. Permeability at 2400 MHz for polypropylene-iron composites milled for 20 hours.

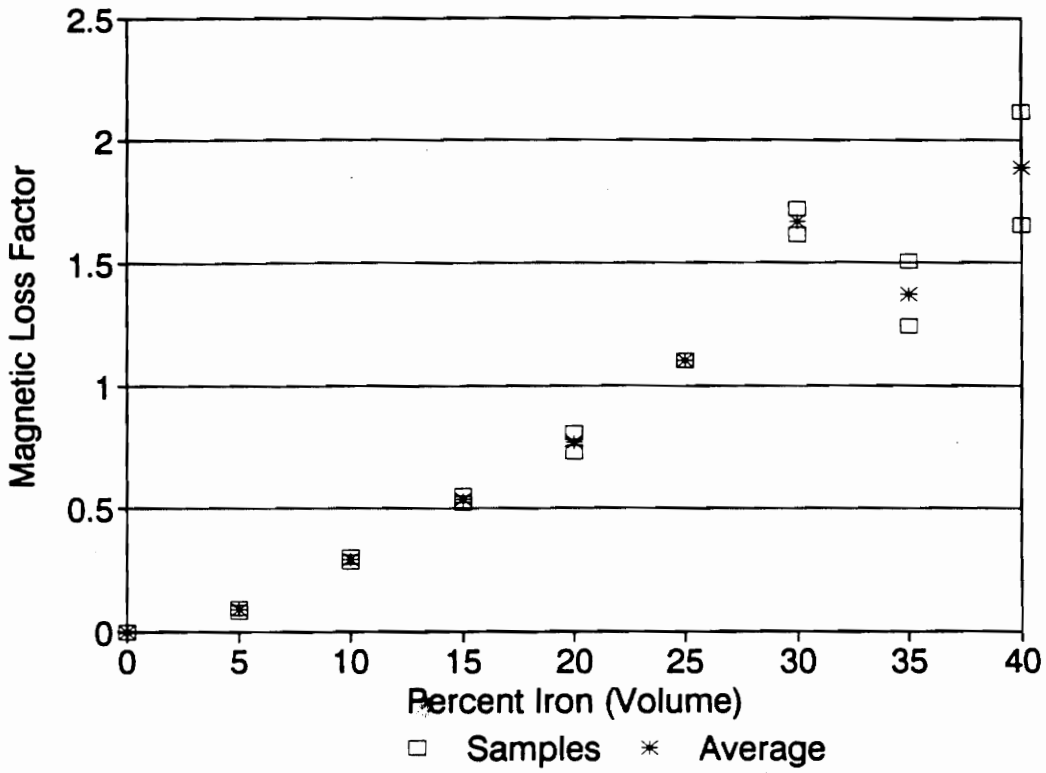

Figure 34. Magnetic loss factor at 2400 MHz for polypropylene-iron composites milled for 20 hours.

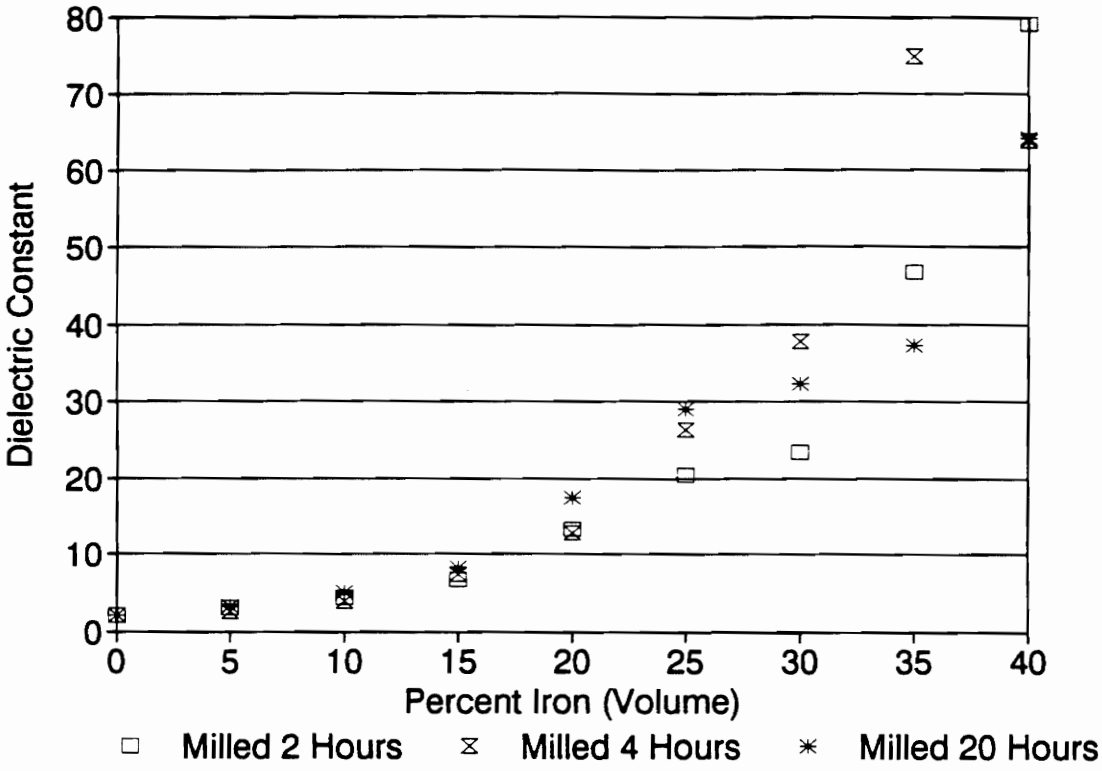

Figure 35. Dielectric constant for three milling times at 2400 MHz for polypropylene-iron composites.

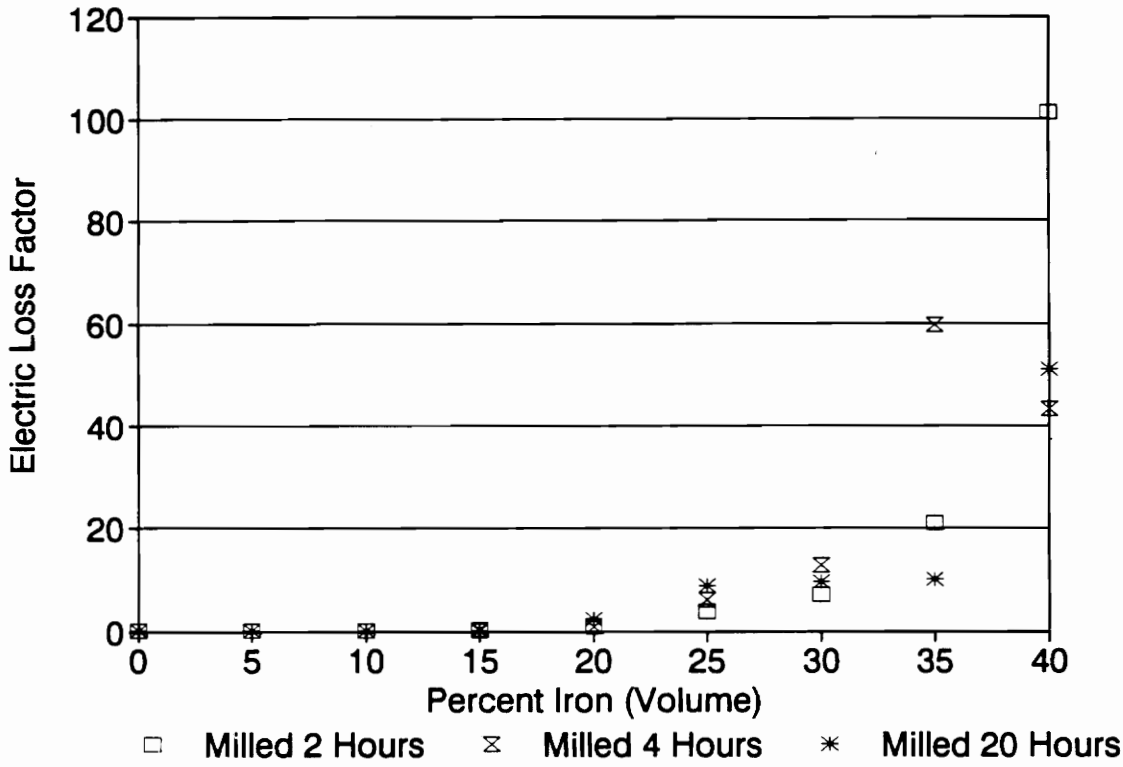

Figure 36. Electric loss factor for three milling times at 2400 MHz for polypropylene-iron composites.

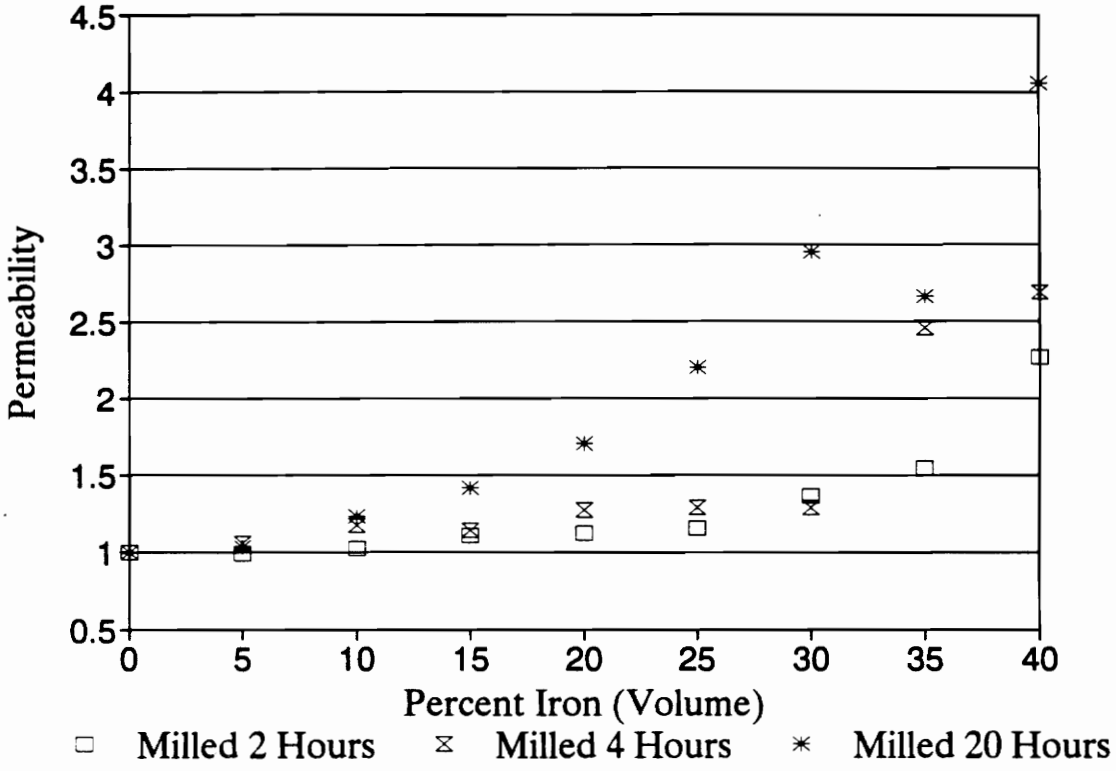

Figure 37. Permeability for three milling times at 2400 MHz for polypropylene-iron composites.

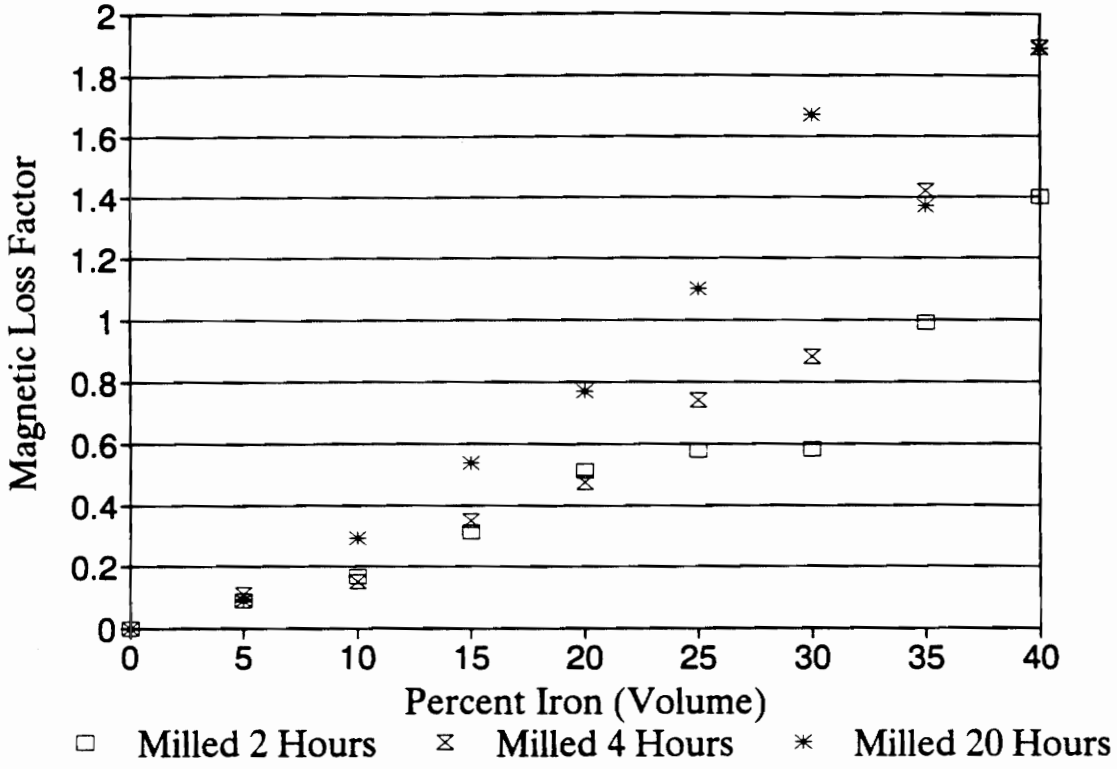

Figure 38. Magnetic loss factor for three milling times at 2400 MHz for polypropylene-iron composites.

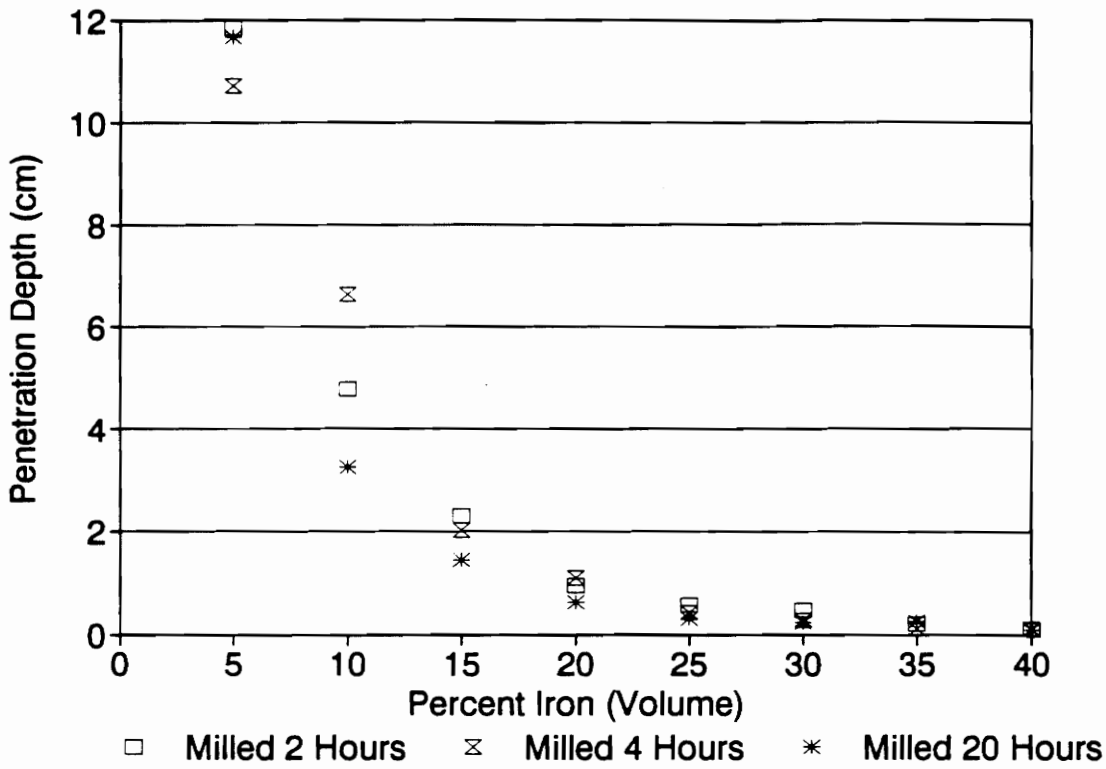

Figure 39. Penetration depth for three milling times at 2400 MHz for polypropylene-iron composites.

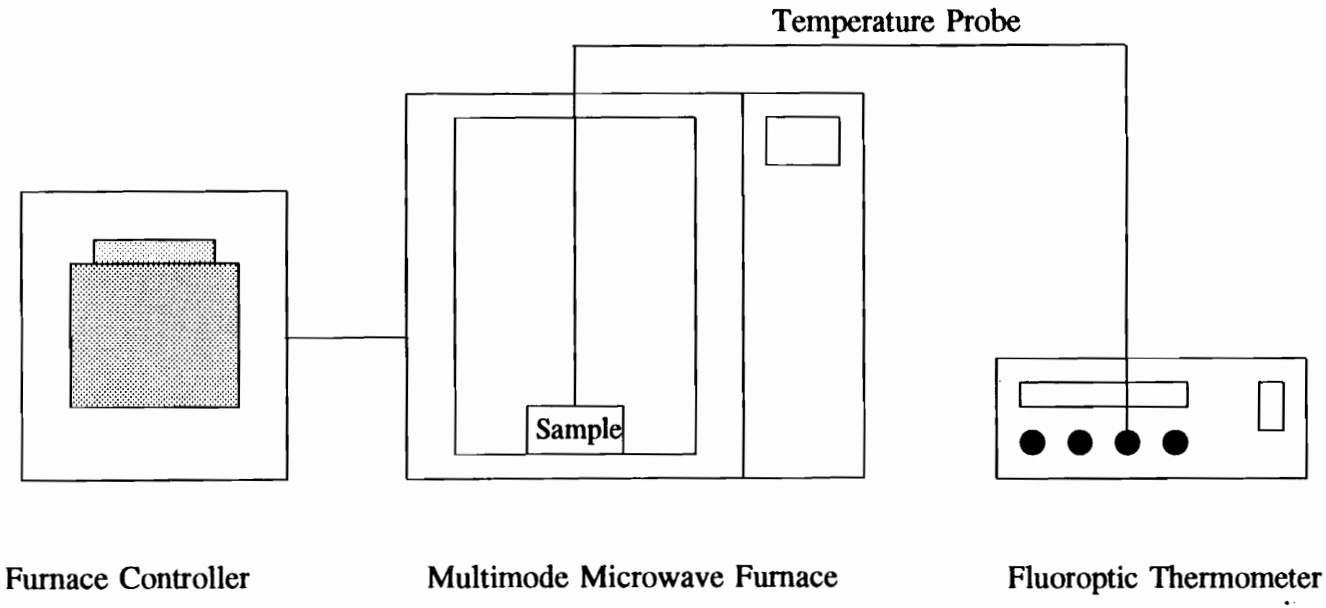

Figure 40. Schematic of microwave processing set-up.

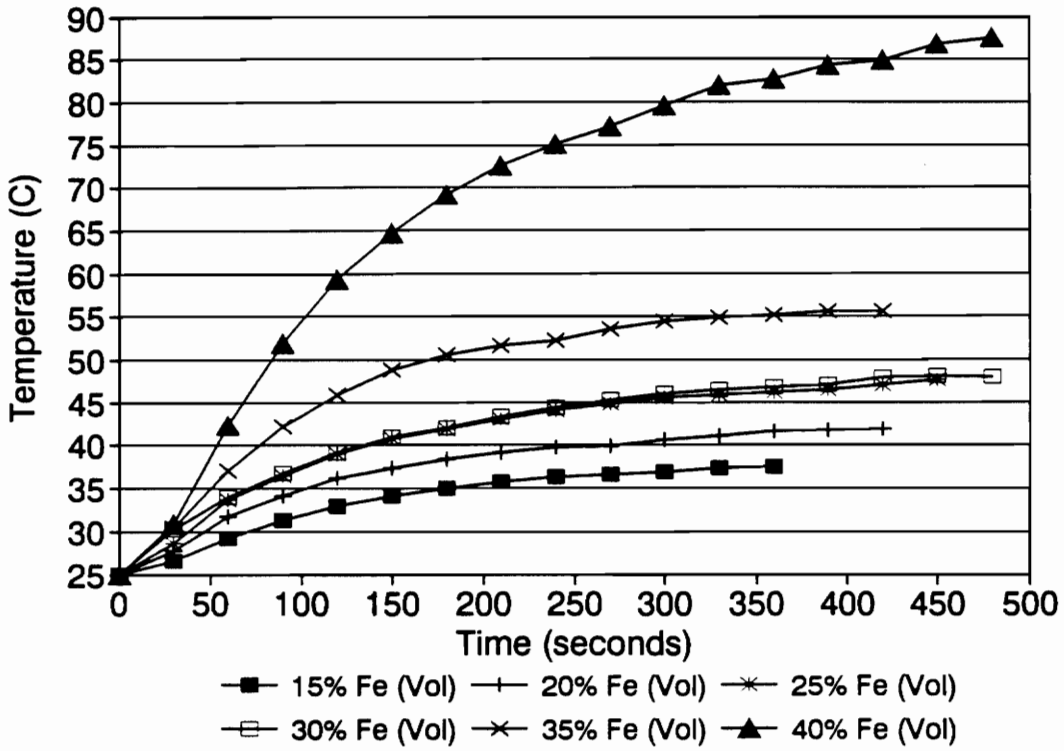

Figure 41. Microwave heating of cold pressed polypropylene-iron composites (milled 2 hours) in a multimode oven with a nominal power of 58 watts.

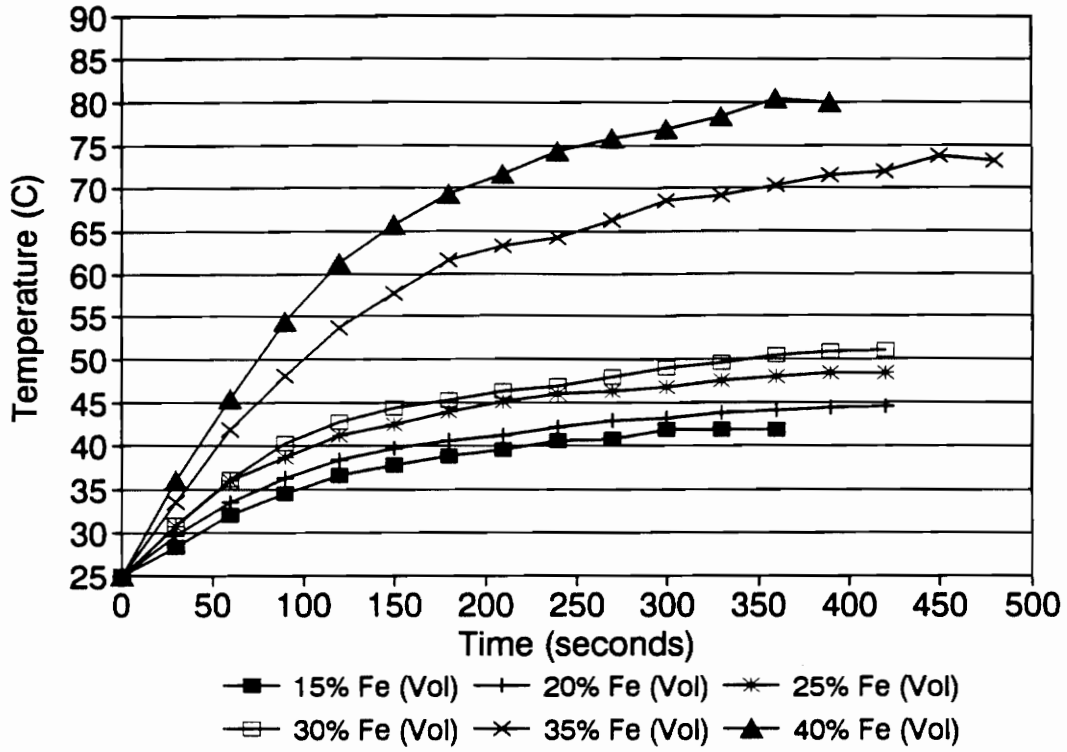

Figure 42. Microwave heating of cold pressed polypropylene-iron composites (milled 4 hours) in a multimode oven with a nominal power of 58 watts.

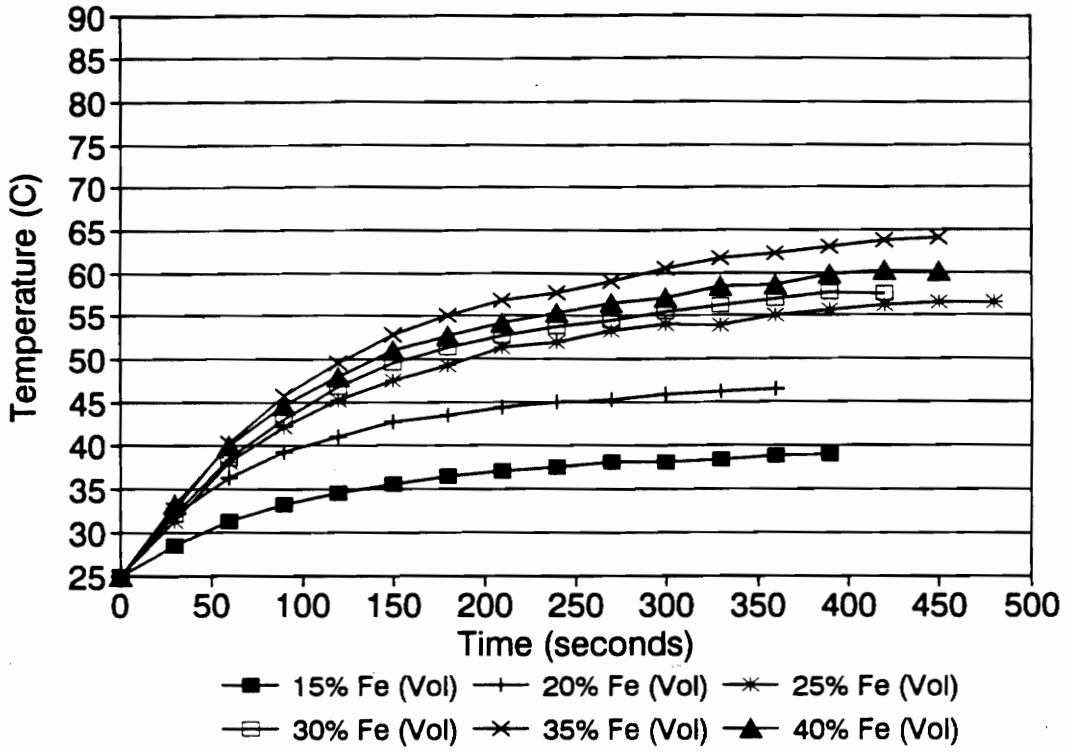

Figure 43. Microwave heating of cold pressed polypropylene-iron composites (milled 20 hours) in a multimode oven with a nominal power of 58 watts.

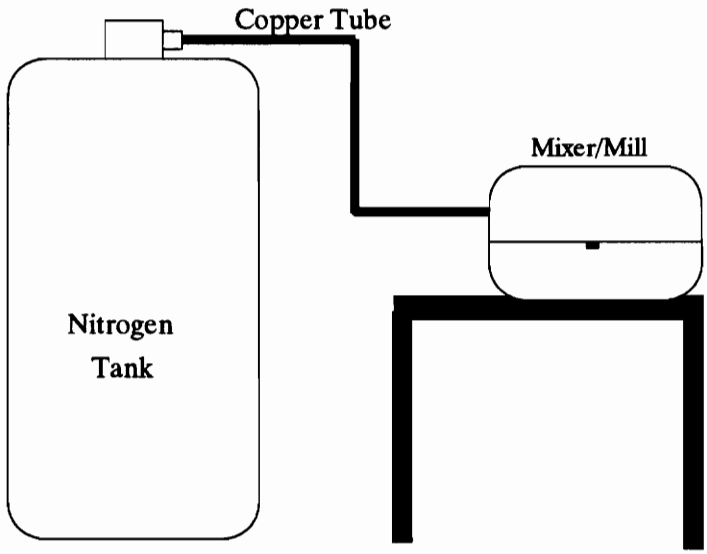

Figure 44. Schematic of cryogenic milling set-up.

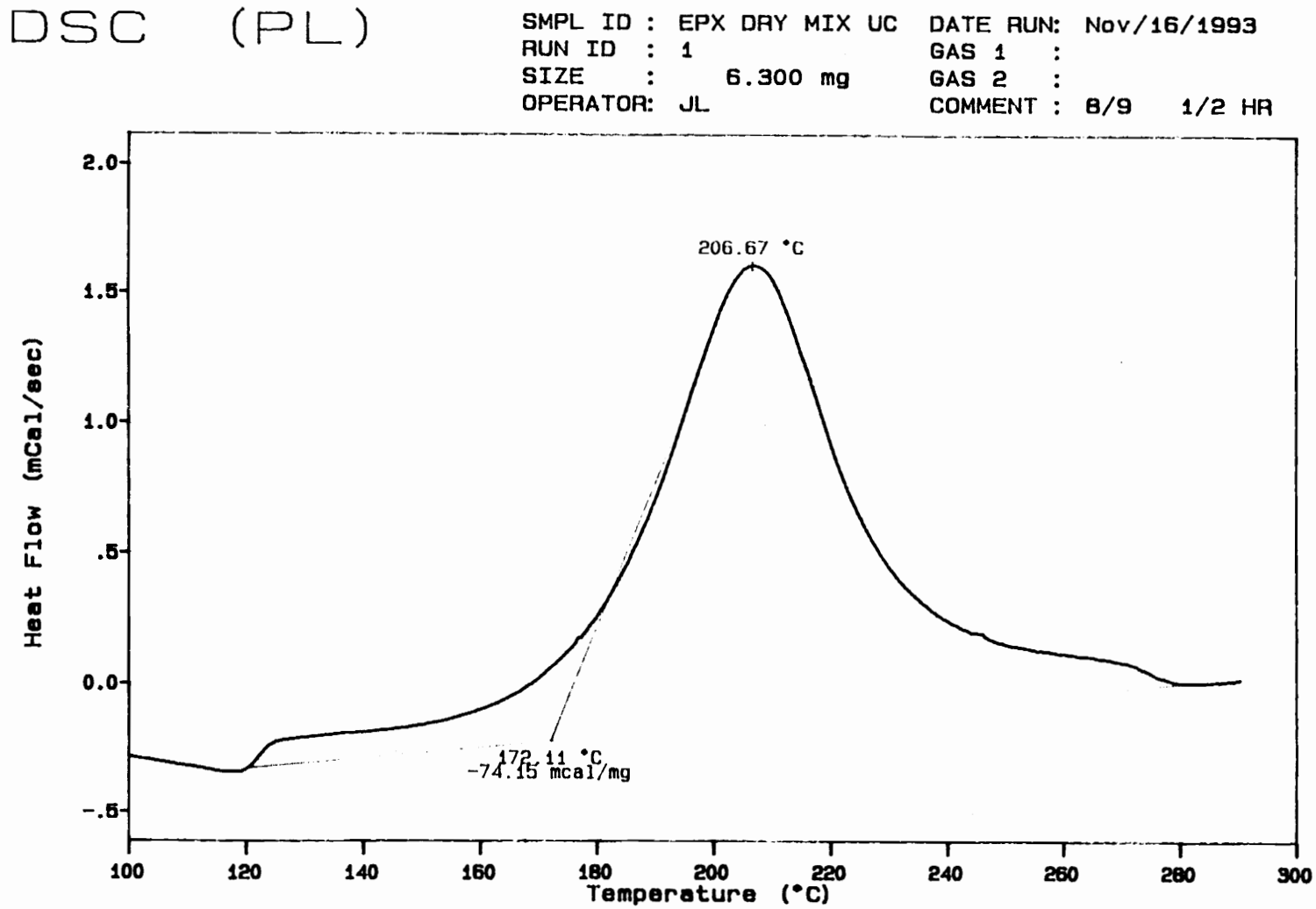

Figure 45. DSC plot of 1071/1061M epoxy cryogenically milled for 1/2 hour.

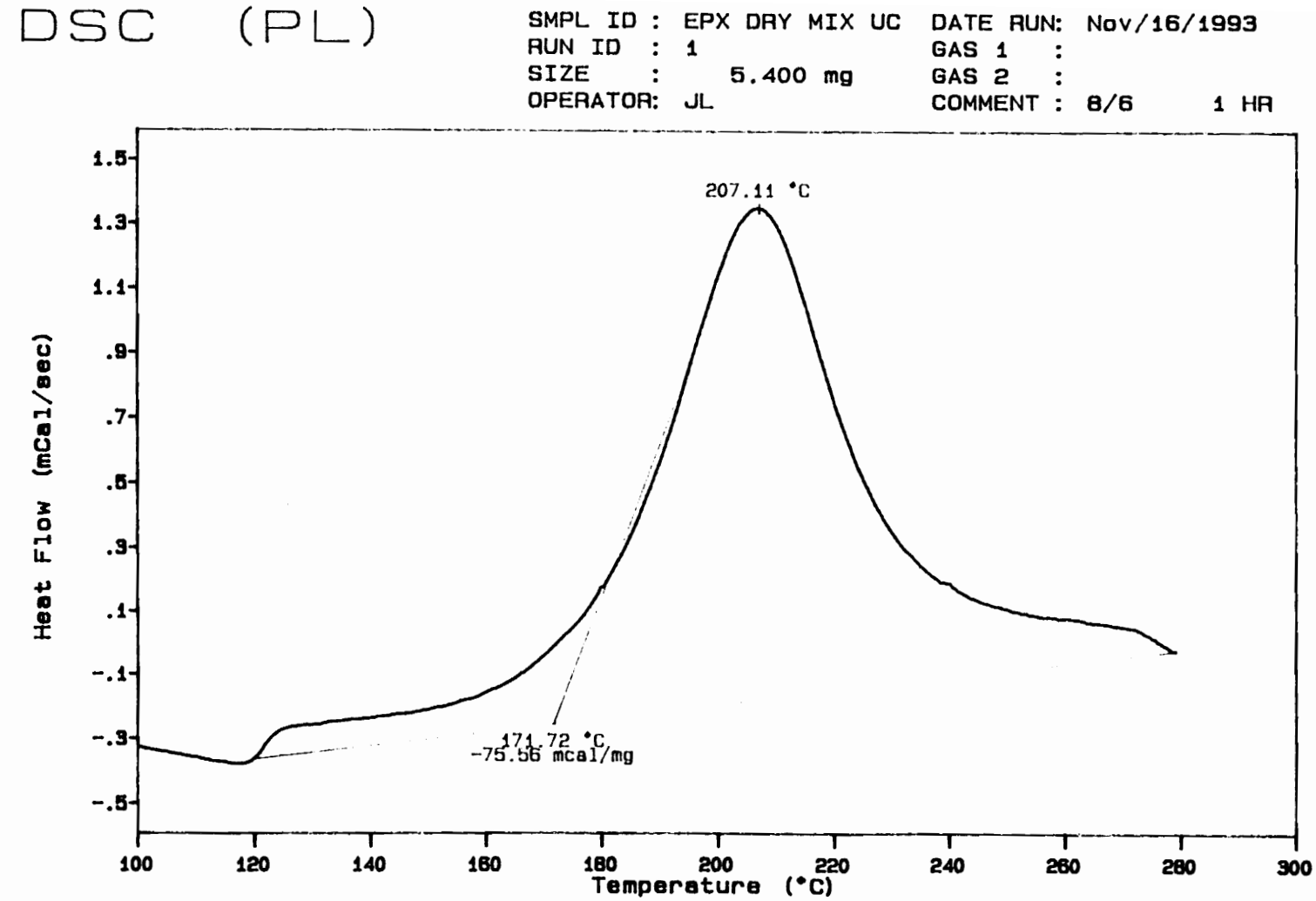

Figure 46. DSC plot of 1071/1061M epoxy cryogenically milled for 1 hour.

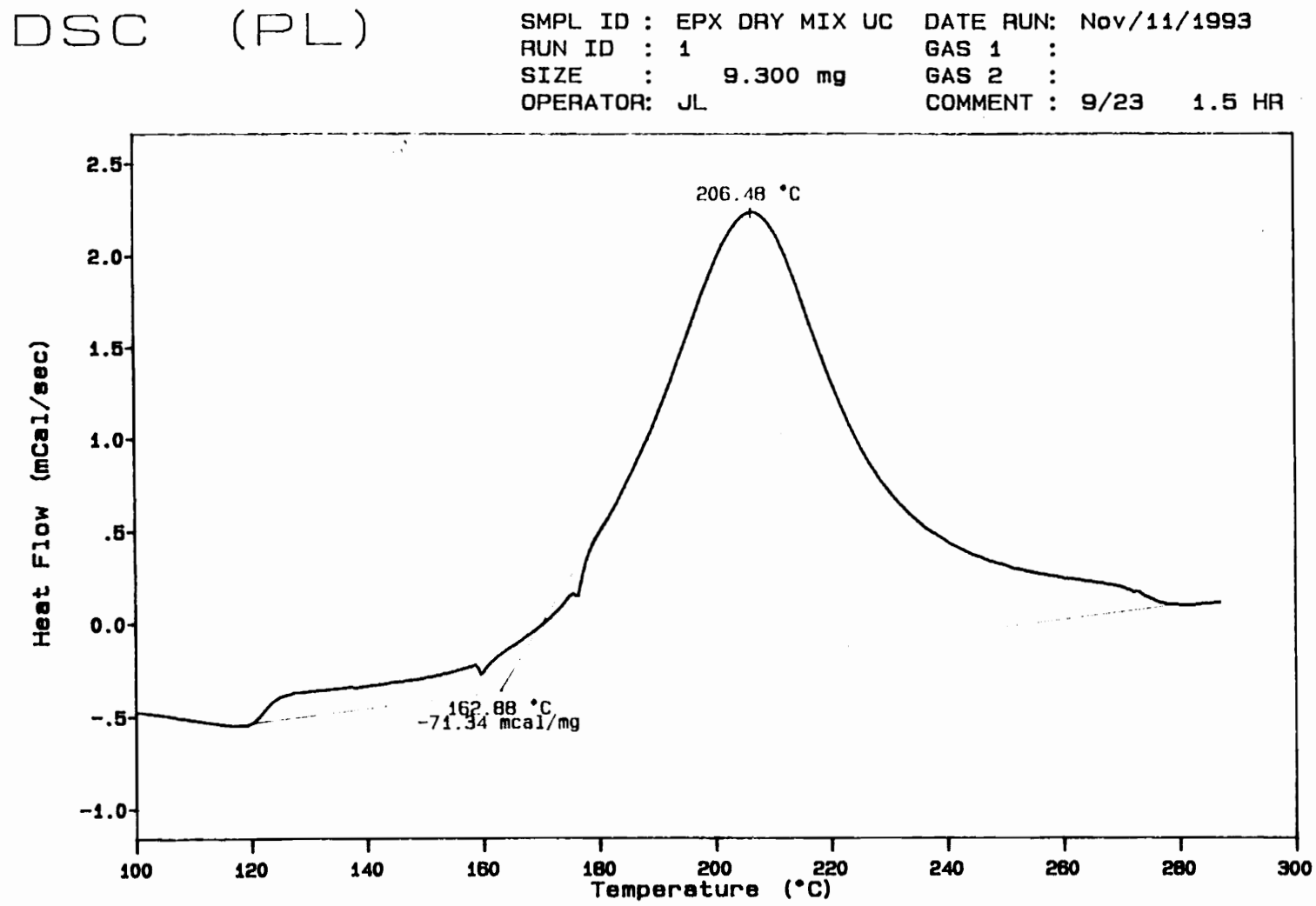

Figure 47. DSC plot of 1071/1061M epoxy cryogenically milled for 1-1/2 hours.

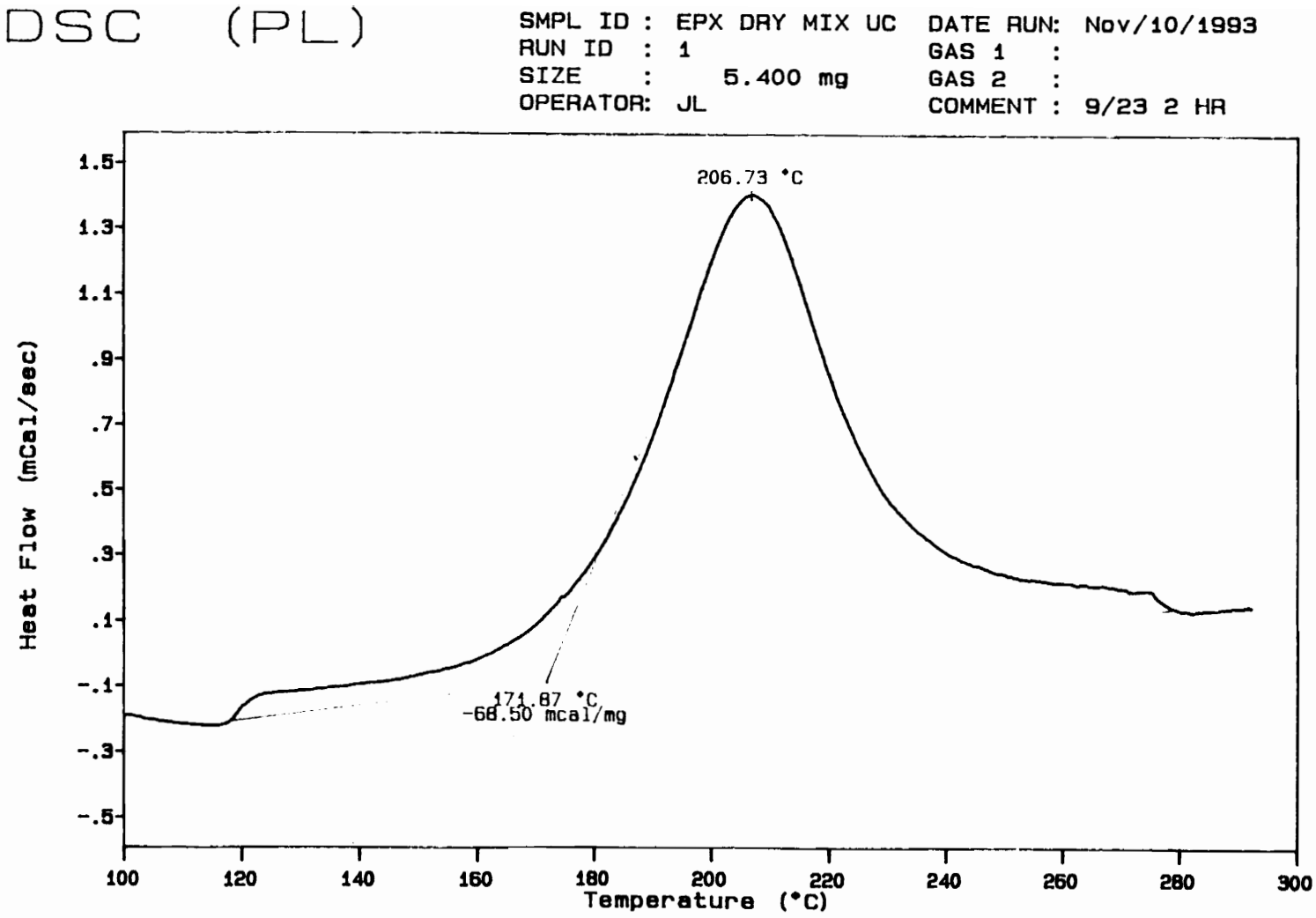

Figure 48. DSC plot of 1071/1061M epoxy cryogenically milled for 2 hours.

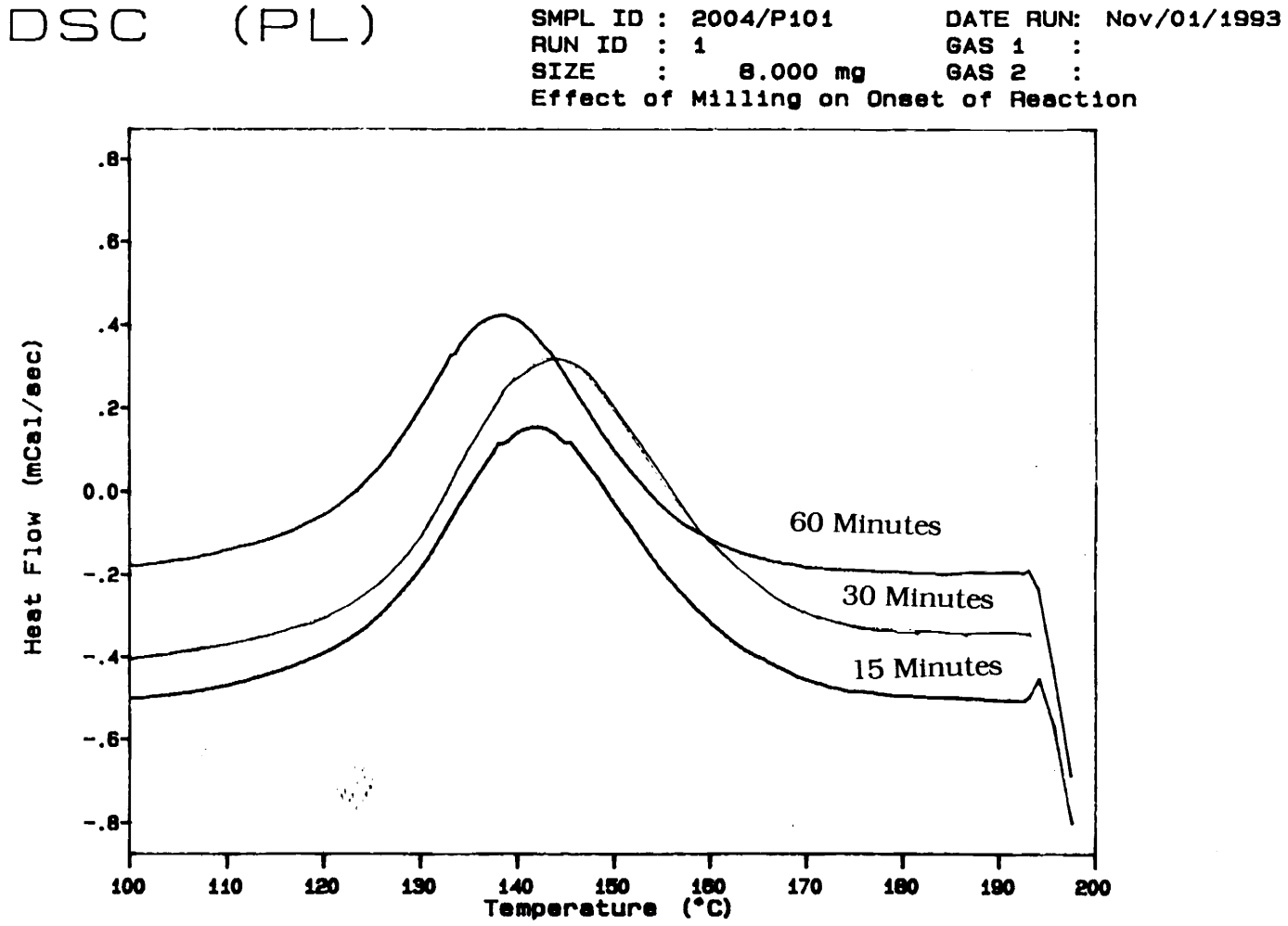

Figure 49. DSC plot of 2004/P101 epoxy milled for 15, 30, and 60 minutes.

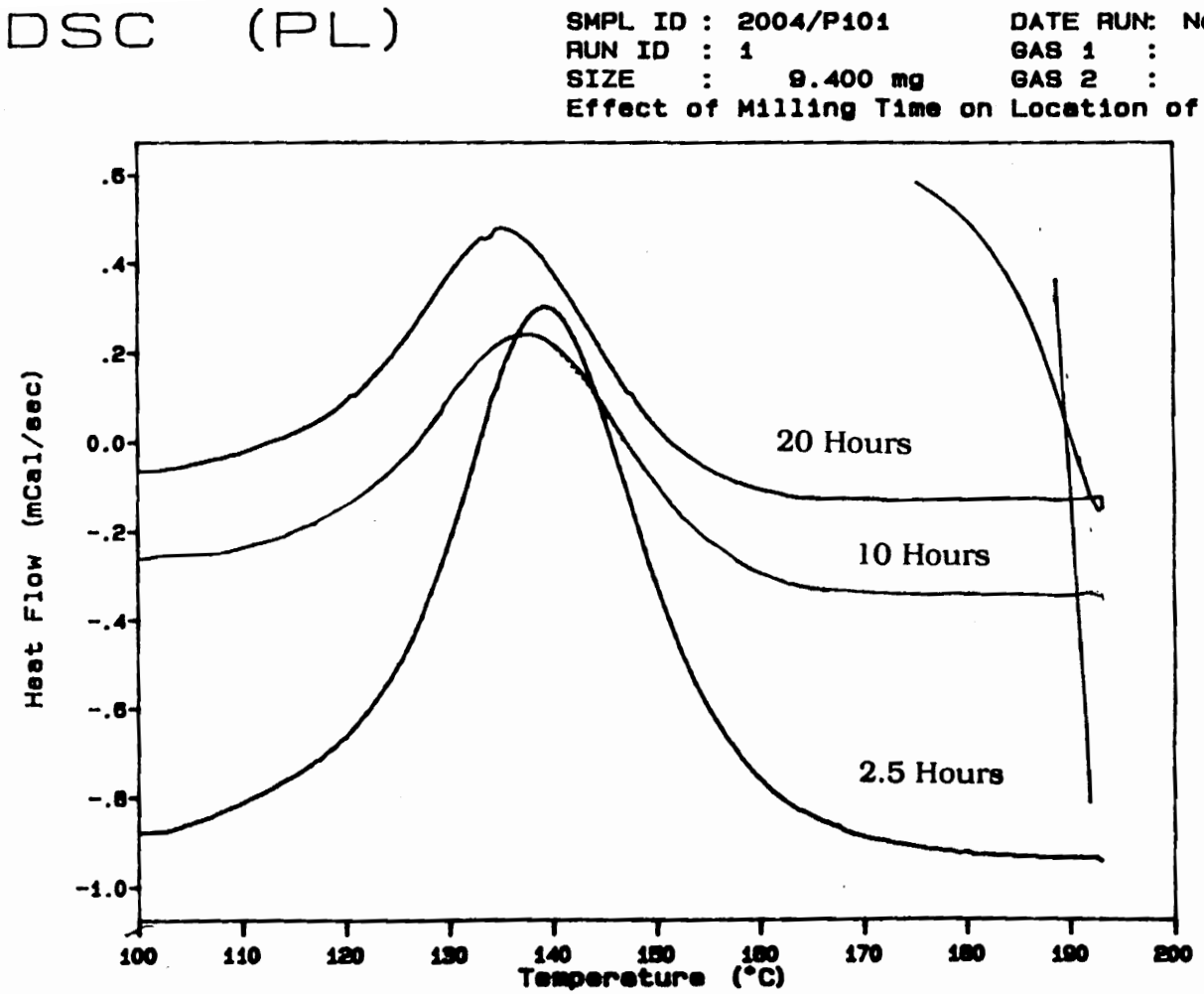

Figure 50. DSC plot of 2004/P101 epoxy milled for 2.5, 10, and 20 hours.

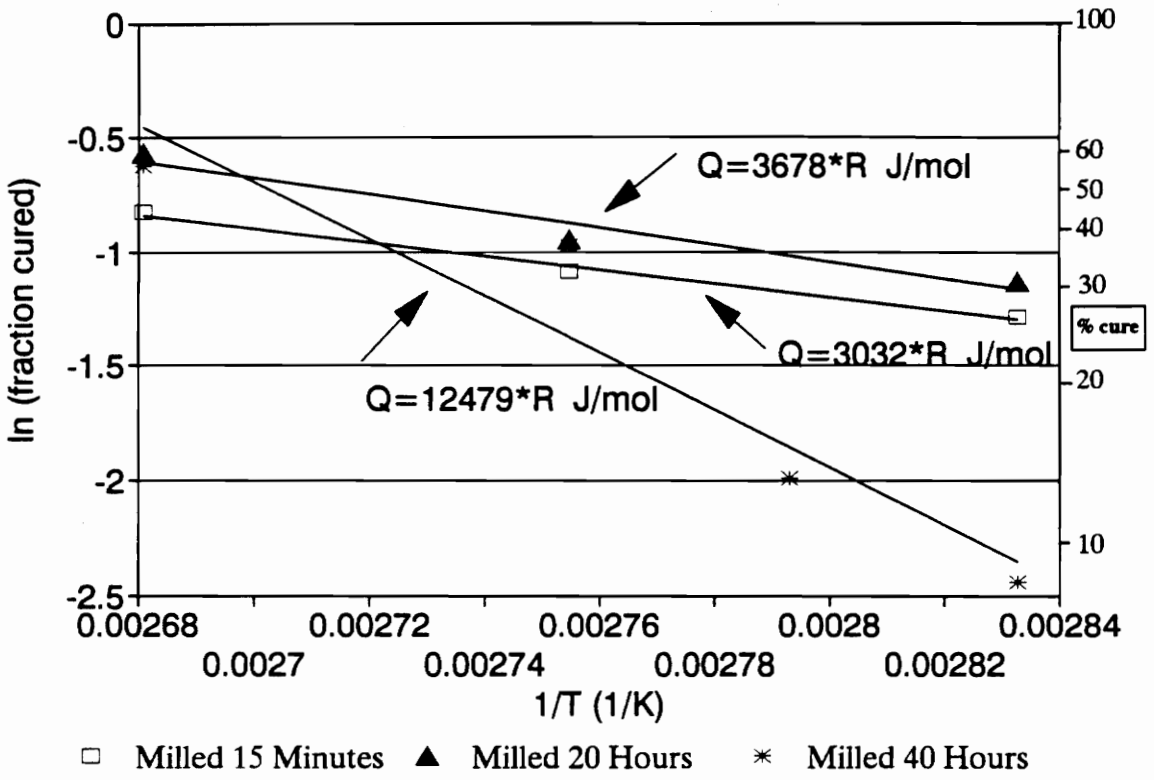

Figure 51. Activation energies of 2004/P101 epoxy system milled for 15 minutes, 20 hours, and 40 hours where R=8.314 J/molK.

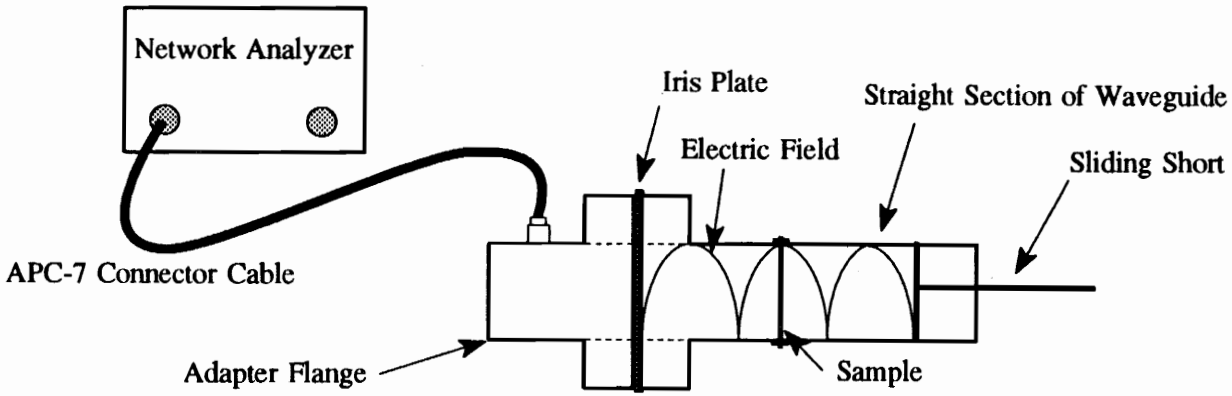

Figure 52. Experimental set-up for Perturbation Technique.

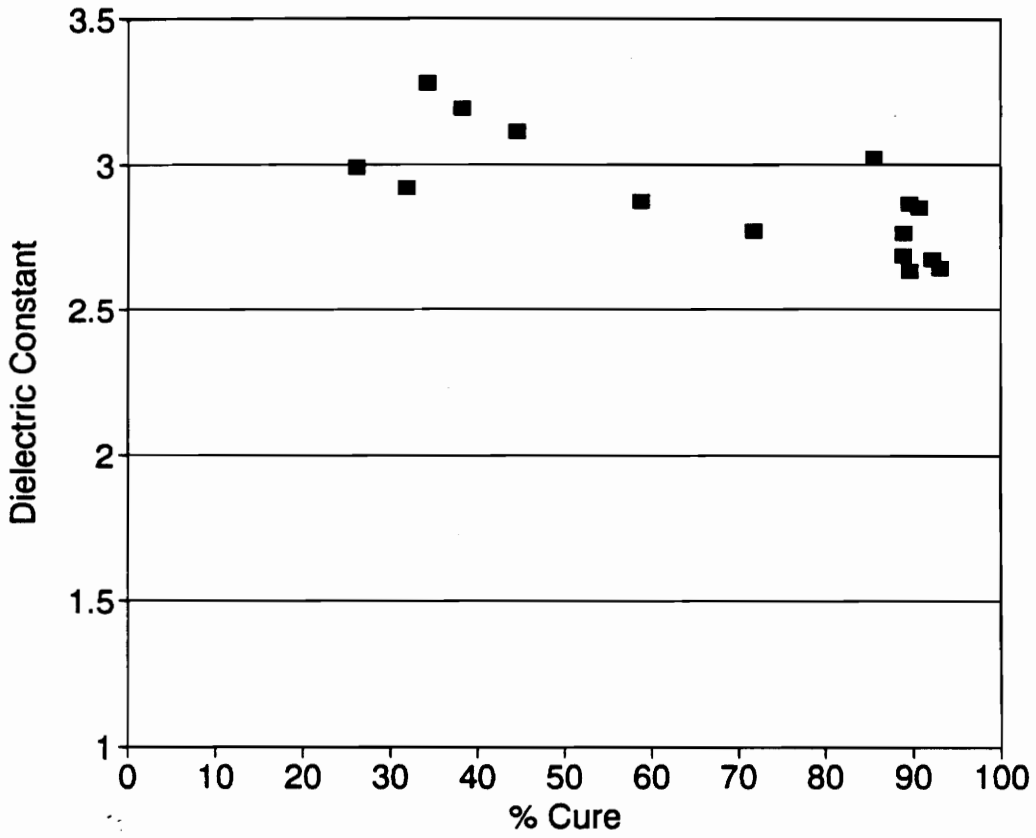

Figure 53. Dielectric constant of 1071-1061-M epoxy system at 2.5 GHz as a function of degree of cure.

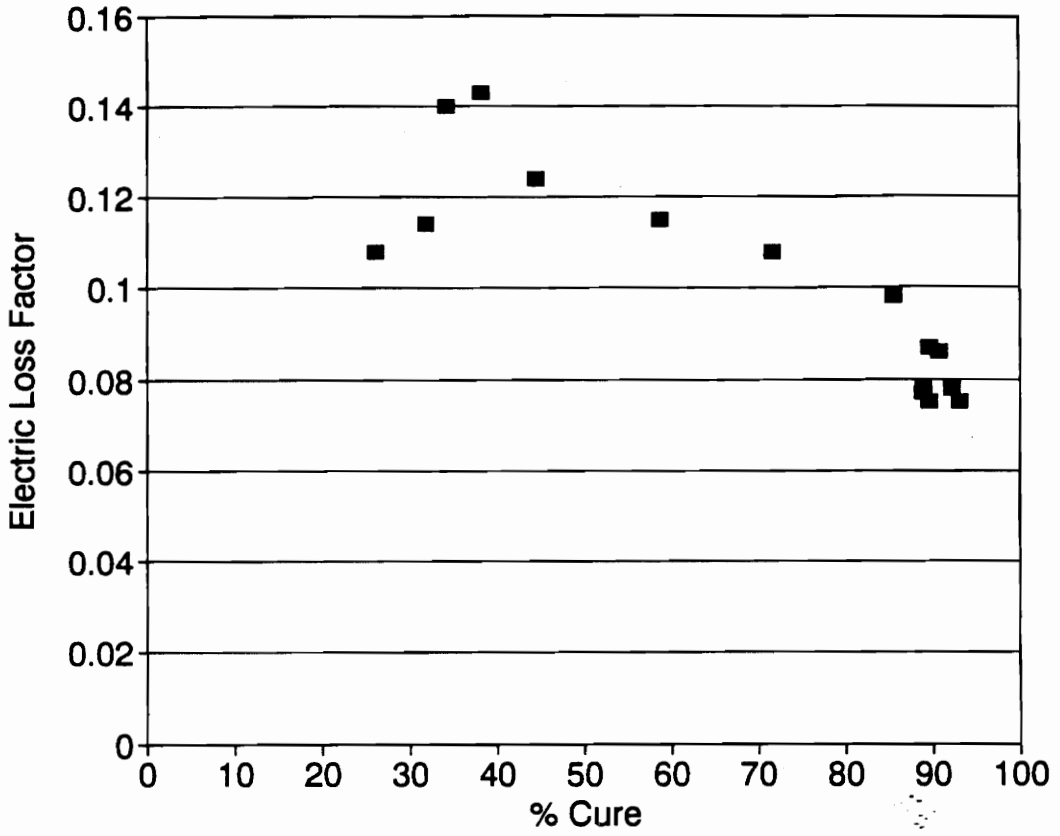

Figure 54. Electric loss factor of 1071-1061-M epoxy system at 2.5 GHz as a function of degree of cure.

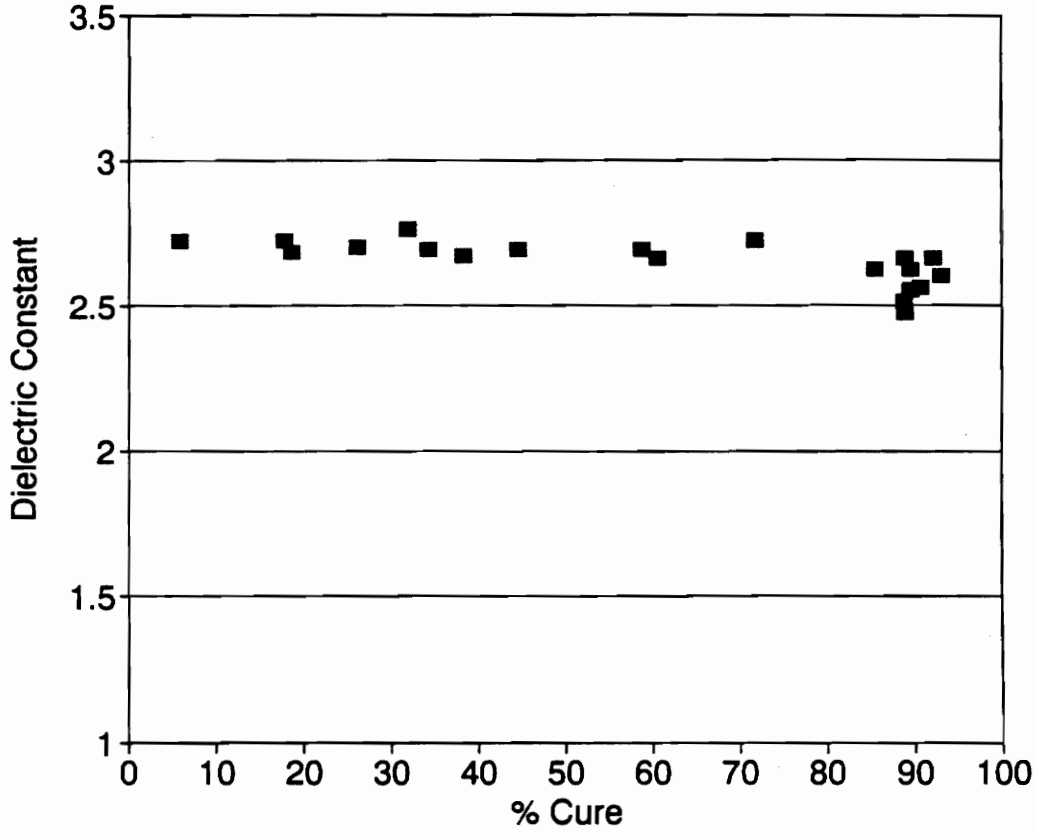

Figure 55. Dielectric constant of 1071-1061-M epoxy system at 9 GHz as a function of degree of cure.

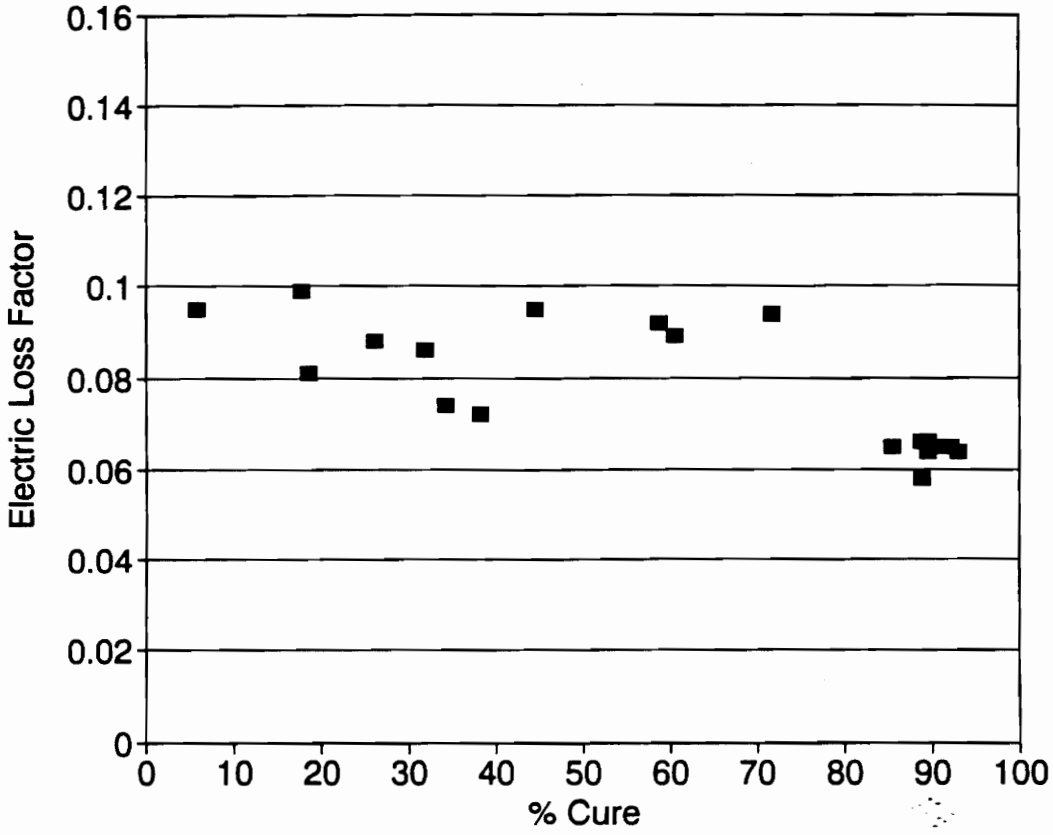

Figure 56. Electric loss factor of 1071-1061-M epoxy system at 9 GHz as a function of degree of cure.

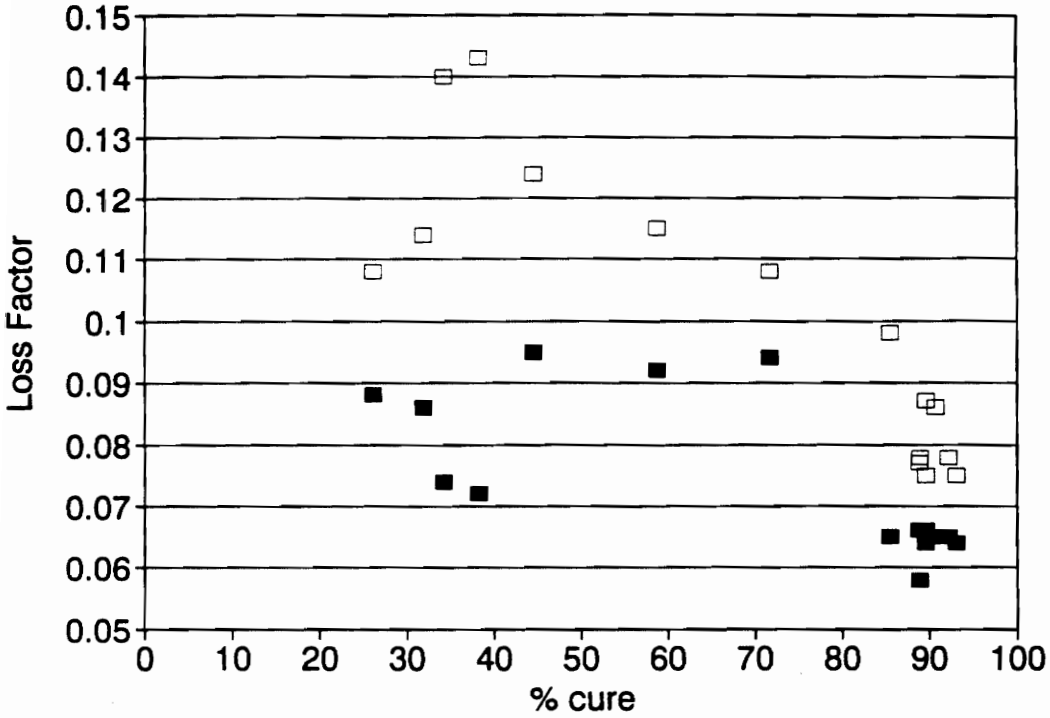

Figure 57. Electric loss factor of 1071-1061M epoxy system at 2.5 GHz and 9 GHz as a function of degree of cure.

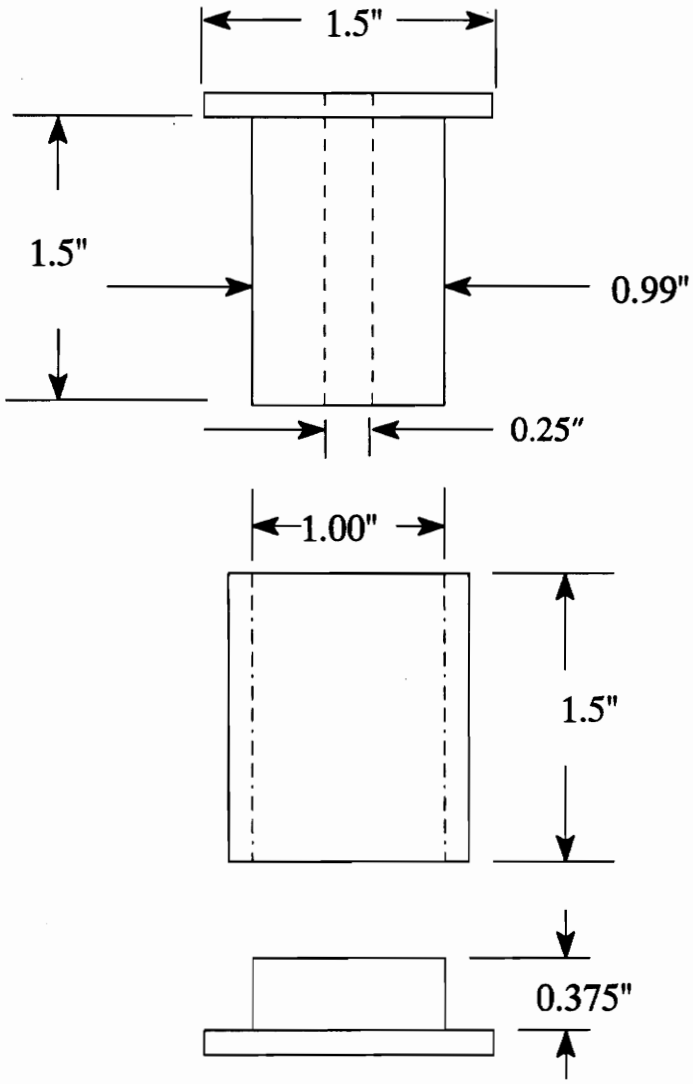

Figure 58. Teflon mold used for microwave heating of epoxy.

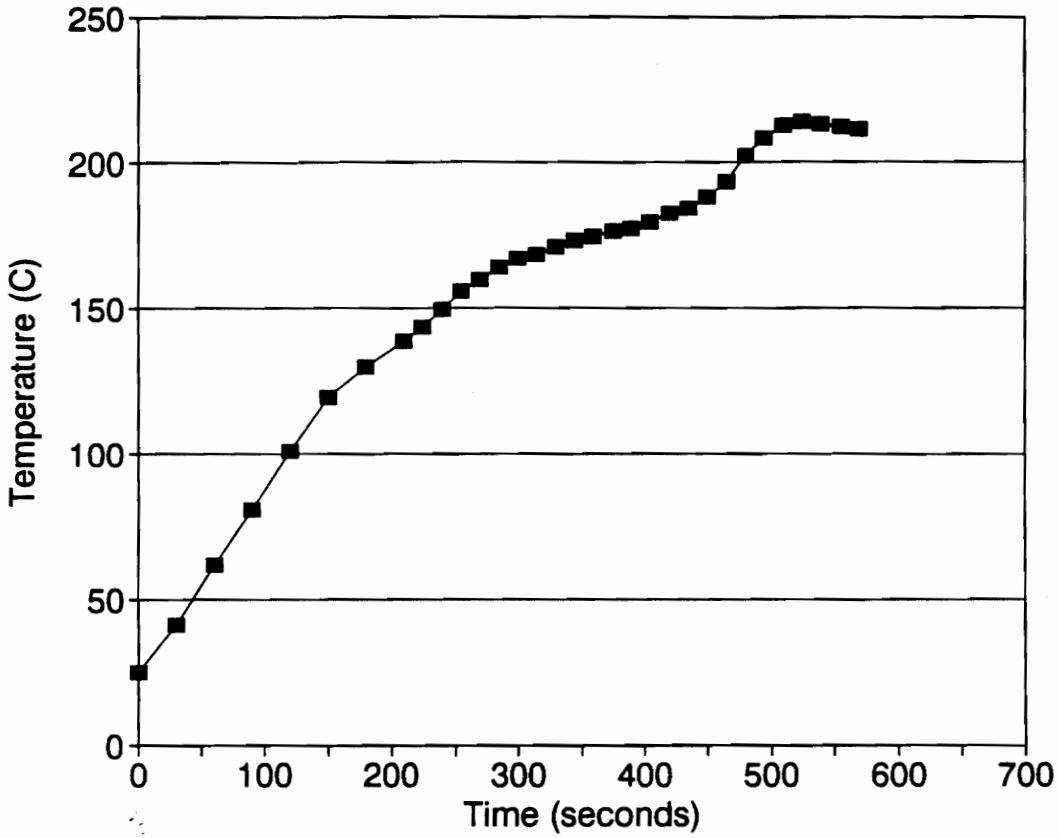

Figure 59. Microwave heating of 1071-1061M epoxy system in a multimode oven at a nominal power of 385 watts.

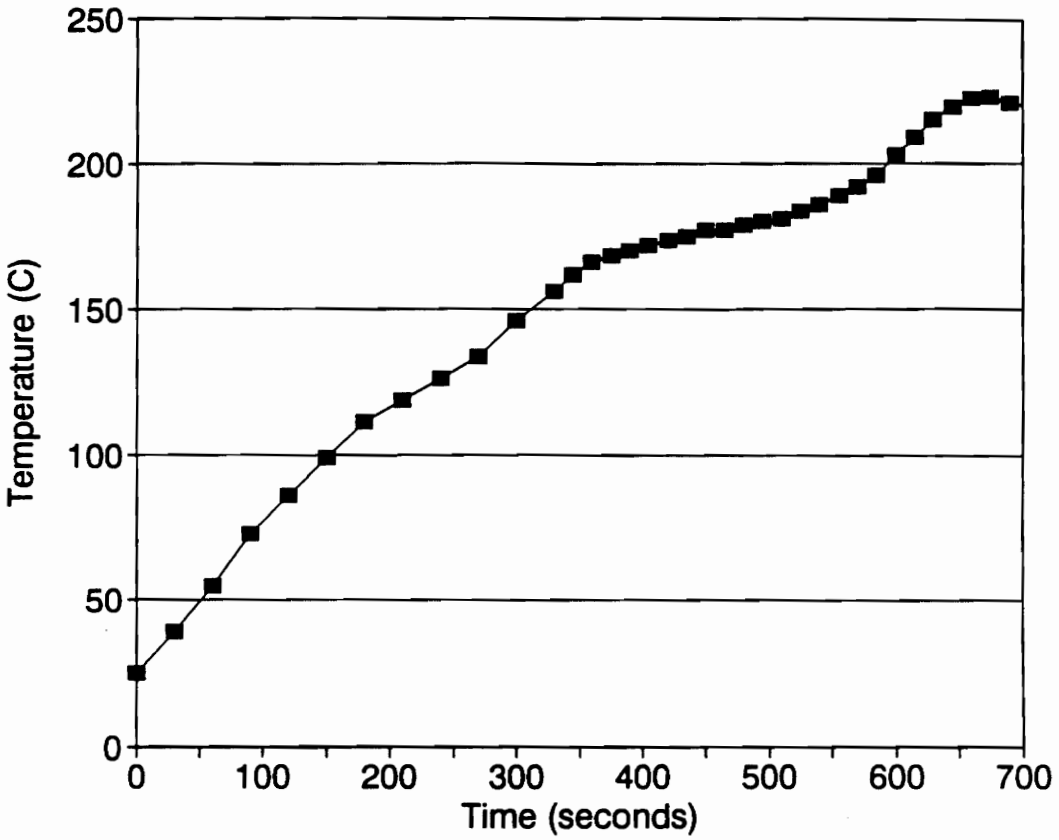

Figure 60. Microwave Heating of 1071-1061M epoxy system in a multimode oven at a nominal power of 320 watts.

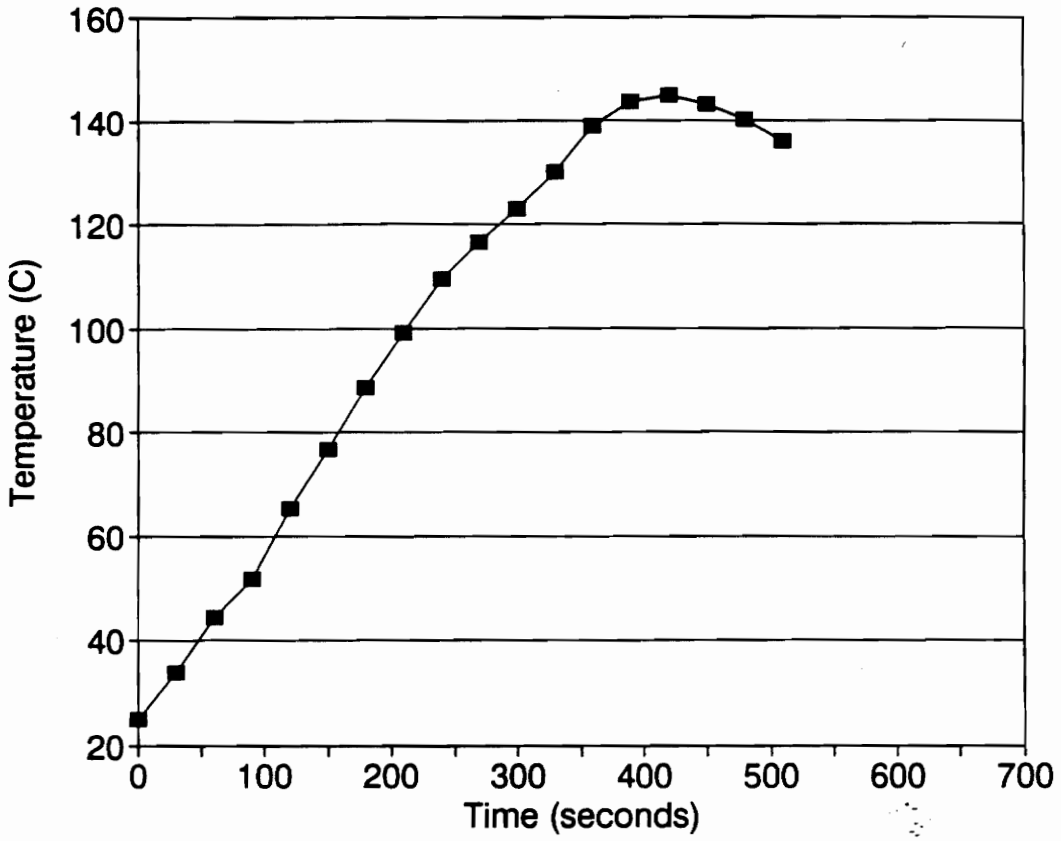

Figure 61. Microwave heating of 1071-1061M epoxy sytem in a multimode oven at a nominal power of 255 watts.

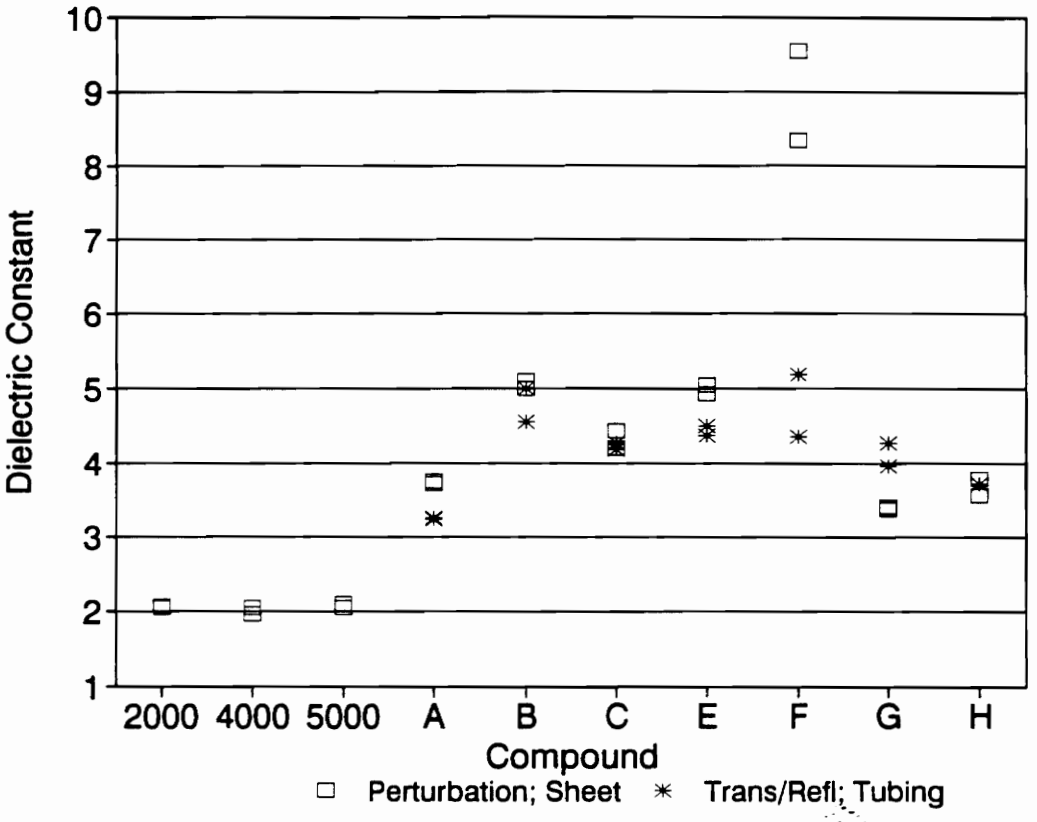

Figure 62. Dielectric constant of perfluoroelastomer compounds at room temperature using the transmission/reflection and perturbation technique.

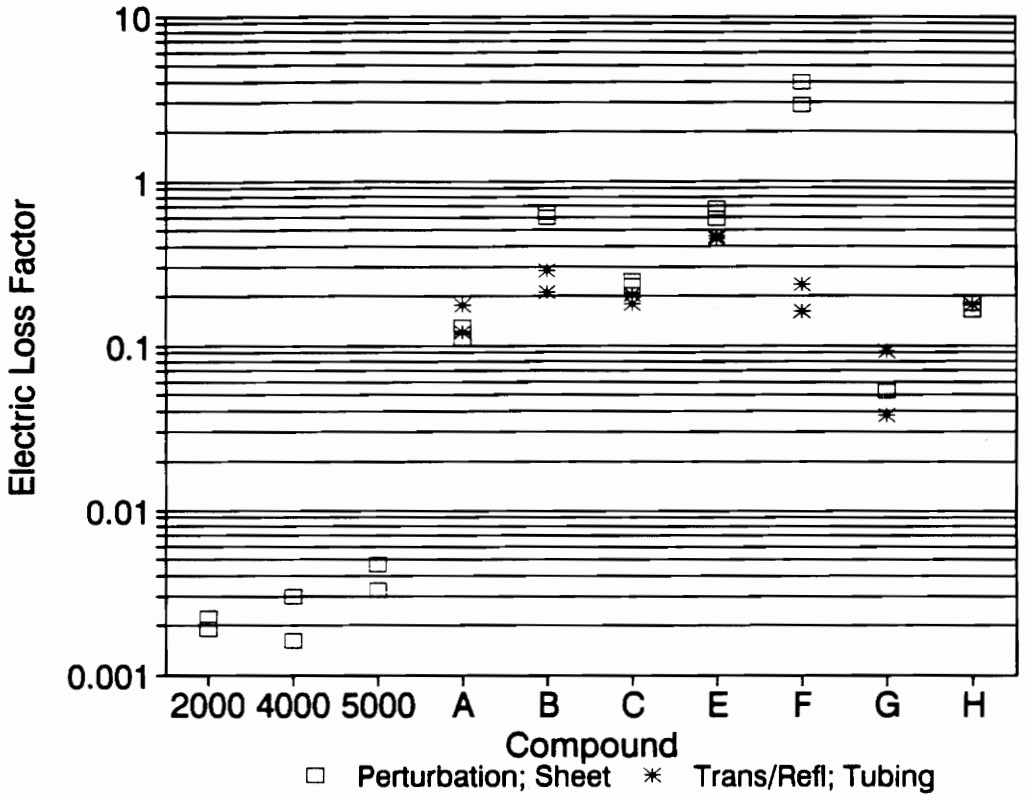

Figure 63. Electric loss factor of perfluoroelastomer compounds at room temperature using the transmission/reflection and perturbation technique.

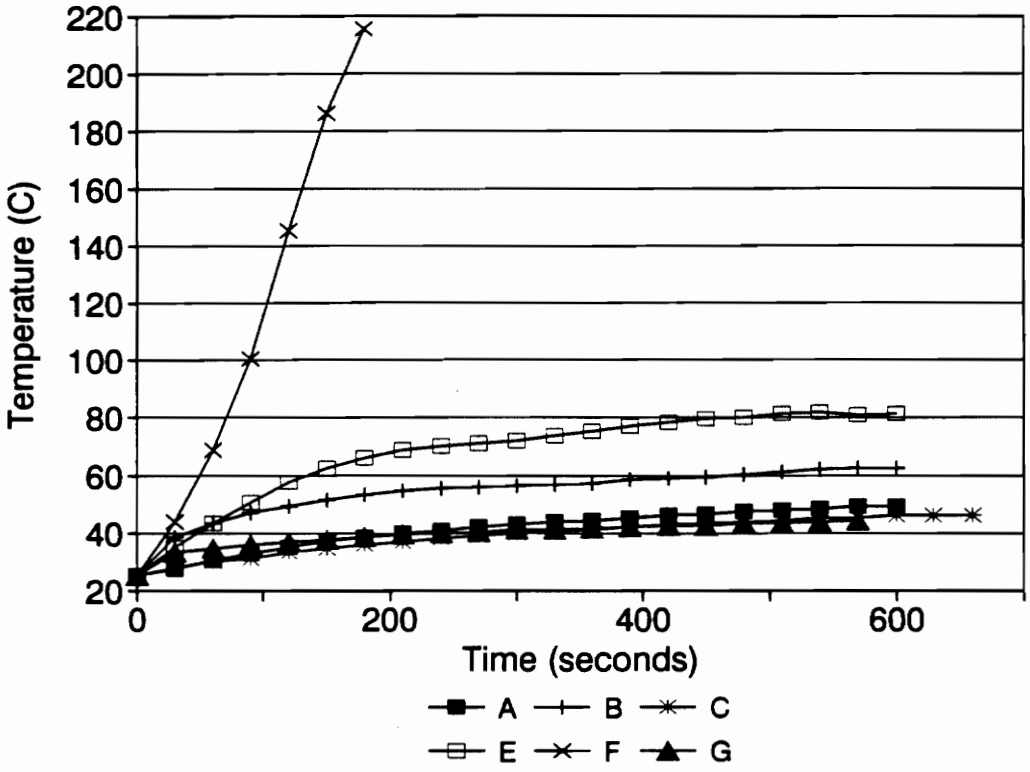

Figure 64. Microwave heating of carbon-black-filled perfluoroelastomer sheet in a multimode oven at a nominal power of 125 watts.

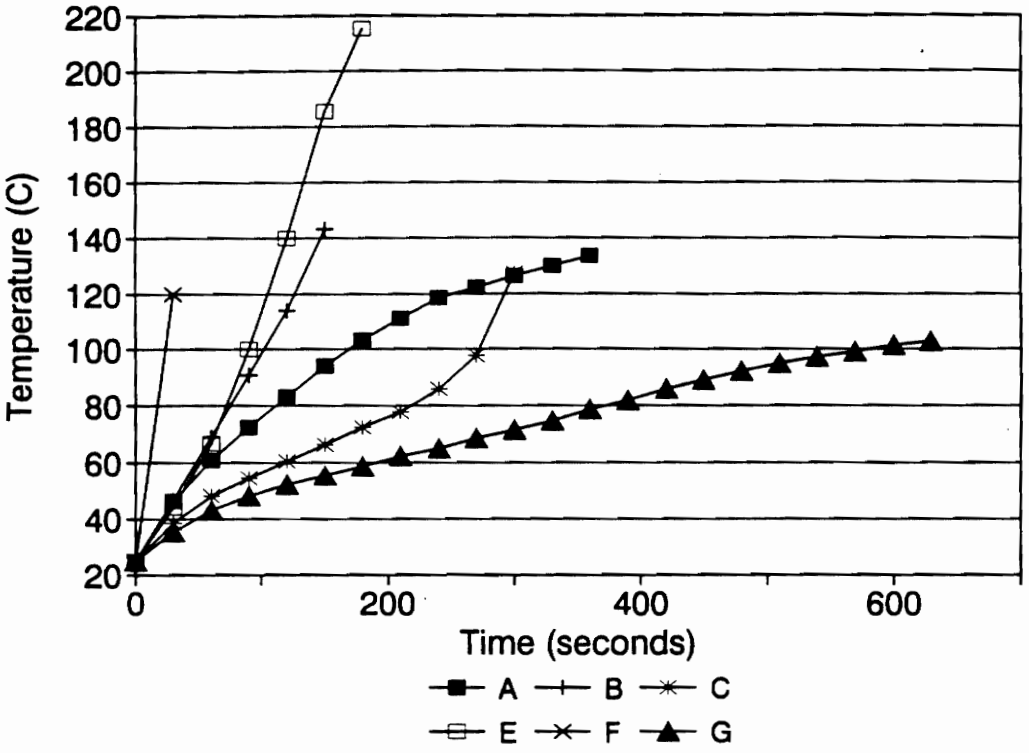

Figure 65. Microwave heating of carbon-black-filled perfluoroelastomer sheet in a multimode oven at a nominal power of 650 watts.

Appendix A

This section describes the equations used to solve for the complex permittivity and complex permeability from S-parameters determined experimentally using the HP vector network analyzer. An S-parameter is the ratio of the signal transmitted or reflected from the device under test (DUT) to the incident signal. The S-parameters are complex values expressed as a linear magnitude ratio, and a relative phase angle. The notation S_{11} stands for the ratio of the reflected signal to the incident signal, while S_{21} stands for the ratio of the transmitted signal to the incident signal.

Nicolson and Ross (1970) first showed that the S-parameter data could be related to the complex permittivity and complex permeability. This solution technique is often referred to as the transmission/reflection technique because the S-parameters are first related to the reflection and transmission coefficients, and then are related to the complex permittivity and permeability. The following solution technique is for a coaxial sample holder, and is outlined in HP Product Note 8510-3.

1) Given - Two measured S-parameters: S_{11} and S_{21}.

2) First calculate K, which will be used to determine the reflection coefficient:

$$K=\frac{S_{11}^2-S_{21}^2+1}{2S_{11}} \tag{A.1}$$

3) Solve for the reflection coefficient Γ using K:

$$\Gamma = K \pm \sqrt{K^2 - 1} \tag{A.2}$$

4) Note that the correct sign is determined by applying the restriction that the absolute value of Γ is less than 1.

5) Solve for the transmission coefficient:

$$T = \frac{S_{11} + S_{21} - \Gamma}{1 - (S_{11} + S_{21})\Gamma} \tag{A.3}$$

6) Take the reciprocal of the transmission coefficient.

7) Take the natural log of the magnitude of (1/T), and add $2\pi n$ to the phase, where n is the integer of L/λ_m. L is the thickness of the sample, and λ_m is the wavelength of the signal in the sample.

8) Next, calculate the following intermediate value:

$$\frac{1}{\Lambda^2} = -\left[\frac{1}{2\pi L}\ln\left(\frac{1}{T}\right)\right]^2 \tag{A.4}$$

9) Calculate (1/Λ), where the correct sign is determined by applying the restriction that the real part of (1/Λ) is always greater than or equal to zero.

10) Now the relative complex permeability can be determined from

$$\mu_r = \lambda_0 \frac{1 + \Gamma}{\Lambda(1 - \Gamma)} \tag{A.5}$$

where λ_0 is the wavelength of the signal in free space.

11) Finally, the relative complex permittivity can be determined from

$$\varepsilon_r = \frac{1}{\mu_r \Lambda^2} \tag{A.6}$$

Appendix B

Calibration Procedure

Calibration of the network analyzer is necessary to remove systematic errors caused by frequency response, leakages, and mismatches. The HP 8510B comes with eight calibration methods that address these errors to varying degrees. In general, calibration is performed by measuring the response of known standards with the network analyzer. The measured response is then compared with the expected response, and any differences are used to determine error correction factors. The quality of the error correction depends on which calibration routine is chosen. The TRL (Thru-Reflect-Line) 2-PORT method used in this work is the most accurate calibration that can be made for a 2-port DUT (HP Product Note 10). The accuracy of the error correction depends on the standards used for calibration. Since the calibration kits provided by HP are very precise, very good error correction is achieved (HP Product Note 10). This appendix will go through a step by step procedure of how the HP network analyzer is calibrated using the TRL 2-PORT method, and how it is integrated with the general measurement sequence.

The TRL 2-PORT calibration routine is part of a calibration set. The calibration set consists of the error correction terms generated during calibration, and a set of measurement parameters over which the calibration is good. If a different set of parameters is desired for a measurement, the calibration must be

redone with these new parameters. Therefore the first step of the calibration sequence is to define the measurement parameters. The following steps should be performed to define the measurement parameters before starting the calibration routine. Note that words in bold are buttons that actually appear on the network analyzer, while underlined words represent soft buttons, or buttons next to the words that appear on the CRT.

1) Hit the green **PRESET** button to return the system to a predefined state.

2) Set the measurement frequency range. The beginning and end of the range are set by pressing the **START** and **STOP** buttons under the STIMULUS menu, and entering the appropriate frequencies on the numeric keypad.

3) Next, enter the number of measurement points in this frequency range. This is done by hitting the **MENU** button under STIMULUS, pressing the Number of Points soft key, and then pressing the soft key next to the appropriate number. Measurements can be taken at either 51, 101, 201, 401, or 801 points. Note that 801 points will provide the most accuracy, but it decreases the measurement speed. The sweep mode is also selected in the STIMULUS menu. Either a RAMP or STEP mode can be selected. The STEP mode provides more accuracy than the RAMP mode.

4) Finally averaging and smoothing of the data can be performed automatically by hitting the **MENU** button in the RESPONSE menu, and then hitting the softkey that says AVERAGING ON, and SMOOTHING ON.

It is important to remember that the error correction will be turned off if the frequency range or number of points is changed from the values at which the network analyzer was calibrated. Although changing other parameters may not cause the correction to turn off, it may invalidate the error correction. Therefore it is imperative to calibrate the network analyzer using the parameters you wish to make measurements with.

The eight calibration methods internal to the network analyzer are composed of a series of calibration standards. A group of these standards comprise a calibration method. The TRL 2-PORT calibration method is comprised of 2 delay standards, and a reflection standard. The following procedure can be used to define the standards, and associate the standards with the TRL calibration.

1) Define the standards. Go into the calibration menu by pressing **CAL**. Note that the screen will say correction is off. Press the soft button More. Press Modify Cal 1 to create a new calibration. Now push the soft button Define Standards. First enter the number of the standard to be defined. Next, enter the standard type by pushing the appropriate soft key. OPEN, SHORT, LOAD, DELAY/THRU, and ARBITRARY IMPEDANCE are the choices. After selecting a standard type,

specific information about the standard type needs to be given including the DELAY, IMPEDANCE, MIN FREQUENCY, MAX FREQUENCY, and type of transmission line (COAX or WAVEGUIDE). For the OPEN and DELAY/THRU standards this information is dependent on the length and type of transmission line available, and the location of the reference plane. For the TRL 2-PORT method this reference plane can either be defined by the THRU or the REFLECT/OPEN standard. For the measurements in this work, the REFLECT standard was used to define the reference plane. The reference plane coincides with the measurement plane in the transmission/reflection technique. If the test specimen is not placed at the reference plane, then it must be phase corrected. For the TRL 2-PORT method, three standards need to be defined: two DELAY/THRU standards, and a REFLECT/OPEN standard.

2) After defining the necessary standards, the standards need to be associated with the appropriate class. For the TRL 2-PORT measurement the classes are TRL THRU, TRL REFLECT, TRL LINE. This is done by pressing the SPECIFY CLASS soft button, and pressing MORE until TRL THRU, TRL REFLECT, and TRL LINE appear. Press each soft button and assign one of the standards just defined to each of the classes. After assigning the standards to the each class you can label each class by pressing the LABEL CLASS soft key. This makes the calibration more user friendly, since information about the standard can be put in the label. After all classes have been defined and labeled, the entire calibration kit can be labeled by pressing LABEL KIT. Finally, by pressing the KIT DONE soft key the

calibration routine is saved. Now that the calibration has been defined, calibration can be performed. Calibration is performed with the following steps:

1) Go into the calibration menu by hitting **CAL**. Note that the calibration is off. Hit the soft key that says CAL 1. This soft key will also have a label which was defined earlier using the LABEL KIT key. Then press TRL 2-PORT. A list of standards now appear on the screen. They include: THRU, S11 REFLECT, S22 REFLECT, and LINE. These standards also have the label assigned to them earlier using the LABEL CLASS soft key. Two other standards ISOLATION and LOWBAND REFLECTION are also listed, but not needed for the TRL 2-PORT CALIBRATION. The words "connect standard" will also appear on the screen. This is the next step.

2) To perform the calibration, each standard needs to be connected and analyzed by the network analyzer. The set-up for each standard has been defined in the DEFINE STANDARDS menu. In this study three slightly different TRL calibrations needed to be performed, since three different types of transmission line were used (WR-430 waveguide, WR-90 waveguide, and 7 mm coaxial line).

For the two waveguide the THRU was performed by placing the coaxial to waveguide transition flanges directly together. The S11 REFLECT and S22 REFLECT standards were performed by placing highly reflective shorting plates at the end of each transition flange. Finally, the LINE was performed by placing a straight section of waveguide of known length between the two coax-to-waveguide

adapter flanges. The THRU for the 7 mm coaxial line measurements were made by simply connecting the APC-7 connectors directly together since no transition was needed for the 7 mm coaxial line. The S11 REFLECT and S22 REFLECT standards were performed by placing a 7 mm reflection standard to each of the APC-7 connectors. The reflection standard was included with the 7 mm calibration kit. Finally the LINE was performed by placing a 5 cm line of coax between the APC-7 connectors.

After connecting the standards described above, the soft key coinciding with the standard should be pressed. Note that the message on the screen will change from "connect standard" to "measuring coefficients". After some time the standard becomes underlined, and you can go on to the next standard. After all four standards have been connected and measured, the calibration is saved by pressing the SAVE TRL 2-PORT key. The calibration is saved to a user specified location. The network analyzer is now ready to make measurements.

The calibration procedure only corrects for repeatable or systematic errors inherent to the network analyzer. Although this increases the accuracy of the network analyzer measurements, many other sources of experimental error exist including uncertainties in the composition and location of the test sample.

VITA

The author, John Paul Ludman, was born on December 25, 1969 in Parkersburg, West Virginia. He lived in Newark, Delaware and graduated from Newark High School in 1988. He attended the University of Delaware and received a Bachelor of Science degree in Mechanical Engineering in June, 1992. In March, 1994 he completed the requirements for a Master of Science degree in Mechanical Engineering at Virginia Tech. Currently, he is working as a consulting engineer in Washington D.C..